AN INVESTIGATION INTO THE VIBRATION CHARACTERISTICS OF A PASSENGER CAR, WITH AND WITHOUT HYDRAULIC ENGINE/TRANSMISSION SUSPENSION DAMPING.

Girling Limited - Suspension Products Group

and the University of Aston in Birmingham -

Faculty of Engineering.

*

Submitted in fulfilment of the requirements of the degree of Ph.D. - University of Aston in Birmingham

by

Cyril George Watson, B.Tech. (Hons.) Loughborough.

*

Head of the Faculty of Engineering: Professor A.J. Ede.

Supervisors:

Professor E. Downham (Research Professor, Department of Mechanical Engineering, University of Aston in Birmingham).

Mr. R.T. Burton, B.Sc. (Chief Engineer, Suspension Products Group, Girling Limited).

MAY 1970.

SUMMARY.

In this thesis a theoretical and experimental study into the vibration characteristics and 'riding comfort' of a passenger car, with and without hydraulic engine/transmission suspension damping, is described.

The phenomenon of vehicle 'shake' is defined. In order to assess the problem objectively the physical quantity, 'transfer mobility' (the acceleration response ratioed to the force input at a given frequency) for various parts of the vehicle, is determined.

A study of the experimental techniques available for assessing vehicle riding comfort in the 'field' and laboratory is made. The various 'vehicle ride comfort' criteria are reviewed. These reviews have established that a measurement of vehicle body mass acceleration will give a correct indication of riding comfort, and best show the effect of system damping upon riding comfort.

The theoretical study is carried out, in the frequency domain, by looking at mathematical models of the vehicle, and computing the 'transfer mobilities' for various parts of a six degree of freedom model. Theoretical and experimental results show that the longitudinal bending of the body structure of the vehicle should be included in the theoretical model, if 'shake'

is to be fully assessed.

For the experimental investigation, the 'transfer mobilities', in the frequency domain, are digitally computed from the transiently recorded force input and acceleration responses, in the time domain, using Fourier Transformation Analysis. Results show that hydraulically damping the engine/transmission mass, on its mounts, is effective in reducing the acceleration amplitudes at the engine/transmission mass natural frequency and the body structure 'shake' natural frequency. This increased damping gives an improvement in passenger riding comfort.

A theoretical vibration study, of a two degree of freedom spring/mass/damped system representing one corner of the vehicle is made, to arrive at the optimum values of the suspension damping factor to give best riding comfort and best vehicle riding safety.

An experimental assessment of the small amplitude performance of a velocity conscious hydraulic engine damper, with various grades of rubber and fittings, has been carried out using a 'Dowty' Vibrator.

The theoretical study of the mathematical models, as carried out in this work, will be useful as design aids. The experimental analysis technique opens a new field for the

study of the vibration behaviour of the motor vehicle, using relatively inexpensive and readily available vibration measuring and analysis equipment, in the Laboratory.

All theoretical work is carried out assuming that all spring rates are linear with displacement, and all damping rates linear with velocity.

The theoretical, frequency domain, analysis uses frequency as the independent variable. This approach is limited to linear representation of the system parameters and steady state analysis. The economy of this approach makes it most useful for the study of vehicle vibration performance, provided its limitations are observed. The experimental investigations, in the time domain, account for non-linearities of the system parameters and permit investigation of both transient and steady state motion.

In situations where time and cost are at a premium and the system non-linearities have little or no effect, the theoretical frequency domain analysis presents the best method of investigation. On the other hand, when system parameters are non linear to a large degree, then the experimental time domain investigations should be used for more accurate results.

ACKNOWLEDGEMENTS.

The work reported in this thesis was carried out by the author, on a part-time basis, at the premises of his employers - Girling Limited (Birmingham). The author wishes to express his appreciation to the Company, for making facilities available to enable this project to be carried out.

The author is grateful for the encouragement given by his supervisors - Mr. R.T. Burton (Girling Limited) and Professor E. Downham (Department of Mechanical Engineering, Aston University).

Finally, the author wishes to thank Dr. R. Woods (Department of Mechanical Engineering, Aston University) and colleagues at Girling Limited for advice given during the project, and Miss J. Ivins of Girling Limited, who typed the draft copy of this thesis.

C O N T E N T S.

INTRODUCTION.

1. An Outline of the Problem.

For many years, the problem of vehicle 'shake' has concerned the mechanical engineer in the Motor Industry. Confusion has arisen through misuse of the word. A survey of literature on the subject, and experimental investigations in the thesis, have enabled 'shake' to be defined.

'Shake' is simply 'the beam like vibrations of the motor vehicle body structure, excited by front road wheel imbalance, road irregularities or engine/transmission mass vibration'. (Reference Chapter 1.2.)

It has been the opinion of vibration specialists in the Motor Industry that a high value of damping, in parallel with the engine/transmission mounting springs, will reduce the vehicle 'shake' and improve 'riding' comfort.

The object of this project is to physically assess the effect that this damping has on the 'riding comfort' of the vehicle.

2. Approach to Solution of the Problem.

From a study of literature, which has been published, dealing with the subject of vehicle riding comfort, it is clear

that, to assess the comfort level of the motor vehicle, it is necessary to obtain the acceleration amplitude/frequency response for the vehicle body mass. (It is assumed that, because of the high frequency filtering effect of the vehicle seat, it is more desirable to measure the acceleration level on the vehicle body, rather than taking the measurements on the vehicle seat.) Reduced acceleration levels at resonant frequencies are assumed to produce increased 'riding comfort' in the motor vehicle.

In this thesis, theoretical and experimental analyses of the vehicle vibration behaviour are made, for various conditions of system damping.

For the theoretical work, the natural frequencies of the vibration modes, for single degree of freedom, decoupled spring-mass-systems representing the motor vehicle, are determined. A more comprehensive, six degree of freedom, coupled, spring-mass system is also analysed. An iterative matrix method is used to obtain the six coupled natural frequencies. To assess the effect of the hydraulic damping upon the vibration behaviour of the vehicle, the six degree of freedom system, with damping, is studied. The acceleration amplitude ratioed to the force input, at a given forcing frequency, is digitally computed, in the frequency domain,

from the equations of motion for each mass, for different conditions of system damping.

For the experimental investigations, the acceleration response ratioed to the force input, at a given forcing frequency, is determined for various parts of the motor vehicle. The vibration measurements are carried out in the time domain. From the recorded force input and acceleration response transients, the response in the frequency domain is computed digitally using a method of Fourier analysis. The effect of damping upon vehicle riding comfort can be assessed, by looking at the acceleration response/force input spectrum, for the vehicle body mass on which the passenger rides.

3. Transfer mobility.

In this thesis, the ratio of the acceleration response (for any part of the motor vehicle) to the force input to the vehicle, at the tyre/road interface (at a given forcing frequency) will be referred to as the 'transfer mobility' for the particular mass. In the case of the vehicle body mass, this ratio will be more specifically referred to as the 'vehicle ride transfer characteristic'.

4. A description of the thesis layout.

A summary of the thesis layout is included below.

CHAPTER 1.

This chapter reviews literature that has been published dealing with the suspension of the automobile engine/transmission mass, its free vibrations and the associated analysis. The phenomenon of 'vehicle shake' is reviewed, together with work that has been carried out to design engine mounting systems to reduce this resonant condition.

This chapter also reviews literature that has been published dealing with 'vehicle ride', passenger comfort, comfort criteria and the effect of changing the main vehicle parameters on 'ride comfort' and 'vehicle safety'.

Finally a study of the various techniques, that have been used for investigating vibrations and the 'riding comfort' in the motor vehicle, is made.

CHAPTER 2.

This chapter outlines the general problem of motor vehicle 'secondary mass' vibration, its effect on passenger comfort, and the selection of the methods for analysis.

CHAPTER 3.

This chapter describes the theoretical investigations that have been carried out. Vibration models of the vehicle

are described. The equations of motion are evolved, and then solved to yield decoupled and coupled natural frequencies for the models. The theory for calculating the damping factors, associated with the decoupled and coupled vibrations, is also given.

The Fourier transformation theory, used in the experimental investigations to transform a function from the time domain to the frequency domain, is described. The system ccnstants for the theoretical mathematical model, together with all the theoretical results, are given in this chapter. The theoretical 'transfer mobilities', for the vehicle, are presented in graphical form. The chapter is completed with a discussion and conclusions for the theoretical work.

CHAPTER 4.

The experimental investigations carried out are reported in this chapter. A description of the experimental equipment and procedure used, to obtain the 'transfer mobilities' for the test vehicle, is given. The choice of instruments and test procedure used is justified. Information is given on the method used to determine the various vehicle damping characteristics. All the experimental results are presented in graphical form. The chapter is concluded with a discussion and conclusions for the experimental work.

CHAPTER 5.

A comparison and discussion of the theoretical and experimental work.

CHAPTER 6.

General conclusions derived from the research.

CHAPTER 7.

Vehicle design recommendations.

CHAPTER 8.

Proposals for further work are included in this chapter.

APPENDICES.

To avoid confusion in the main body of the thesis, all the supporting theoretical and empirical work, together with the bibliography, is given in the appendices.

Appendix 1 shows how the equations, for the six degree of freedom mathematical model, were solved to give the vehicle 'transfer mobilities' and the coupled, undamped natural frequencies.

Appendix 2 contains all the ancillary calculations incurred in the project, i.e. the calculation of the linear damping rates, decoupled natural frequencies and damping factors.

Included in this appendix is the calculation of the effective mass of the non-rigid body structure which supports the engine/transmission mass.

Appendix 3 gives the theory and calculations for the determination of the optimum vehicle suspension damping factor, which results in the best 'riding comfort' and best 'riding safety'.

Appendix 4 gives the calculations of the engine/transmission mass suspension spring stiffness and damping rate, which results in the optimum dynamic absorption of the vehicle 'shake' resonance.

Appendix 5 describes the experiments carried out to assess the performance of a velocity conscious hydraulic engine/transmission mass damper, subjected to small amplitude vibrations.

Appendix 6 contains all the references used in the work. These will be valuable for most vibration investigations.

NOMENCLATURE.

a (in. or m.)	The horizontal distance of the front engine/transmission mounts to the c. of g. of the engine/transmission mass.
A (lbf. or N.)	Amplitude of a step function.
b (in. or m.)	The horizontal distance of the rear engine/transmission mounts to the c. of g. of the engine/transmission mass.
c (in. or m.)	The horizontal distance from the "front axle" to the vehicle body mass c. of g.
d (in. or m.)	The horizontal distance from the rear axle to the vehicle body mass c. of g.
E (lbf./in.^{2} or N/m.^{2})	Elastic modulus.
F_3 (lbf. or N.)	The total friction, in a vertical direction, measured in the front suspension of the vehicle (effectively in parallel with the front road springs and referred to the plane of the wheel).

F_4 (lbf. or N.)	The total friction, in a vertical direction, measured in the rear suspension of the vehicle (effectively in parallel with the rear road springs referred to the plane of the wheel).
g (in./sec.^{2} or m/sec.^{2})	Acceleration due to gravity.
j_1 (lbf. in.sec.^{2} or N.m.sec.^{2})	The pitch inertia of the engine/transmission mass (m_1), about the y axis through its c. of g.
j_2 (lbf. in.sec.^{2} or N.m.sec.^{2})	The pitch inertia of the vehicle body mass (m_2), about the y axis through its c. of g.
k_x (lbf./in. or N/m.)	The rate of a spring in a single degree of freedom system.
k_1 (lbf./in. or N/m.)	The total rate of the front engine/ transmission mounts, in the z direction.
k_2 (lbf./in. or N/m.)	The total rate of the rear engine/ transmission mount, in the z direction.

k_3 (lbf./in. or N/m.)	The total rate of the front road springs, referred to the plane of the road wheels, in the z direction.
k_4 (lbf./in. or N./m.)	The total rate of the rear road springs, referred to the plane of the road wheels, in the z direction.
k_5 (lbf./in. or N./m.)	The total rate of the front tyres, in the z direction.
k_6 (lbf./in. or N./m.)	The total rate of the rear tyres, in the z direction.
K (in./sec. or m./sec.)	Hydraulic damper piston velocity.
l (in. or m.)	The horizontal distance from the engine/transmission rear mount to the vehicle body mass c. of g.
m_1 (lb./in./sec.^{2} or kg./m./sec.^{2})	The mass of the engine/transmission unit (mass includes engine, gearbox and half the propeller shaft).

m_2 (lb./in./sec.^{2} or kg./m./sec.^{2})	The mass of the trimmed body shell (not including the engine/transmission mass or axle masses).
m_3 (lb./in./sec.^{2} or kg./m./sec.^{2})	The front 'unsprung' axle mass.
m_4 (lb./in./sec.^{2} or kg./m./sec.^{2})	The rear 'unsprung' axle mass.
m_7 (lb./in./sec.^{2} or kg./m./sec.^{2})	The effective mass of the front end of the vehicle (less m_1), assumed to be subjected to front end "body shake".
m_{10} (lb./in./sec.^{2} or kg./m./sec.^{2})	The sum of the masses m_1, m_2, m_3 and m_4.
m_x (lb./in./sec.^{2} or kg./m./sec.^{2})	The mass supported by the spring k_x for a single degree of freedom system.
P_3 (lbf. or N.)	The amplitude of the sinusoidal forcing function input (theoretical analysis) at the tyre/road interface, in the plane of the front axle. Force input in the z direction.

R (lbf. or N.)	Hydraulic damping resistance, at K in./sec. piston velocity.
v_1 (lbf./in./sec. or N./m./sec.)	The rate of an equivalent linear viscous damper, in parallel with the front engine/transmission mount springs. (Includes hydraulic and hysteretic components.)
v_2 (lbf./in./sec. or N./m./sec.)	The rate of an equivalent linear viscous damper in parallel with the rear engine/transmission mounting spring. (Includes hydraulic and hysteretic components.)
v_3 (lbf./in./sec. or N./m./sec.)	The rate of an equivalent linear viscous damper in parallel with k_3. (Includes hydraulic and hysteretic components.)
v_4 (lbf./in./sec. or N./m./sec.)	The rate of an equivalent linear viscous damper in parallel with k_4. (Includes hydraulic and hysteretic components.)
v_5 (lbf./in./sec. or N./m./sec.)	The linear viscous damping rate of the front tyres. (In parallel with k_5.)

v_6 (lbf./in./sec. or N./m./sec.)	The linear viscous damping rate of the rear tyres (in parallel with k_6.)
v_x (lbf./in./sec. or N./m./sec.)	The equivalent linear viscous damping rate referred to a single degree of freedom system.
v_h (1, 2, 3 or 4) (lbf./in./sec. or N./m./sec.)	The equivalent linear viscous hydraulic damping rate component of $v_{1,\ 2,\ 3}$ or $_4$ respectively.
v_i (1, 2, 3 or 4) (lbf./in./sec. or N./m./sec.)	The equivalent linear inherent or hysteretic damping rate component of $v_{1,\ 2,\ 3}$ or $_4$ respectively.
v_{crit} (lbf./in./sec. or N./m./sec.)	The critical linear viscous damping rate.
v^1_{hn} (lbf./in./sec. or N./m./sec.)	The damping rate associated with a non-linear viscous damper, of damping index γ
$W_e = A_e$ (lbf./in./sec. or J.)	The work done by a hydraulic damper during extension.

$W_c = A_c$ (lbf./in./ sec. or J.)	The work done by a hydraulic damper during compression.
z_1, z_2, z_3, z_4 (in. or m.)	The vertical displacement of centroids of the m_1 to m_4 respectively.
θ_5 or z_5 & θ_6 or z_6 (radians)	The angular displacement of masses m_1 and m_2 respectively, about the y axis through their c.'s of g.
$\dot{z}_1$, $\dot{z}_2$, $\dot{z}_3$, $\dot{z}_4$ (in./sec. or m./sec.)	The vertical velocity of the centroids of masses m_1 to m_4 respectively.
$\dot{\theta}_5$ or $\dot{z}_5$ & $\dot{\theta}_6$ or $\dot{z}_6$ (radians/s.)	The angular velocity of masses m_1 and m_2 respectively, about the y axis through their c.'s of g.
$\ddot{z}_1$, $\ddot{z}_2$, $\ddot{z}_3$, $\ddot{z}_4$ (in./sec.^{2} or m./ sec.^{2})	The vertical acceleration of the centroids of masses m_1 to m_4 respectively.
$\ddot{\theta}_5$ or $\ddot{z}_5$ & $\ddot{\theta}_6$ or $\ddot{z}_6$ (rads./sec)	The angular acceleration of the masses m_1 and m_2 respectively, about the y axis through their c. of g's.

δ	(non dimensional)	The inherent damping factor for rubber.
$\overline{\delta}$	(non dimensional)	The inherent damping ratio for rubber (refers to the complete mounting system).
ξ	(lbf.in.^{2}/sec. or N.m.^{2}/sec.)	The viscosity coefficient for rubber.
η	(1, 2 ... n)	The damping factors associated with the masses 1 to n vibrating with decoupled modes.
w	(radians/sec.)	The frequency of the theoretical sinusoidal forcing function P_3.
w_1	(Hz.)	The theoretical decoupled natural frequency of the engine/transmission mass in pure bounce (constrained to move only in the z direction).
w_{11} and w_{12}	(Hz.)	The undamped, coupled bounce/pitch natural frequencies of the engine/transmission mass on its mounting rubbers.

w_2 (Hz.) — The theoretical decoupled natural frequency of the body mass in pure, undamped bounce (constrained to move only in the z direction).

w_{21} and w_{22} (Hz.) — The undamped, coupled bounce/pitch natural frequencies of the body on the springs k_3 and k_4.

w_3 (Hz.) — The theoretical undamped, decoupled natural frequency of the front "axle" mass m_3 (mass constrained to move only in the z direction).

w_4 (Hz.) — The theoretical undamped, decoupled natural frequency of the rear axle mass m_4 (mass constrained to move only in the z direction).

w_5 (Hz.) — The theoretical undamped, decoupled natural frequency of the combined engine/transmission and body masses on the road springs. The rate of the engine mounting springs assumed infinite. (Masses constrained to move in phase in the z direction only.)

w_{51} and w_{52}	The undamped coupled bounce/pitch frequencies of the body and engine/transmission masses on k_3 and k_4 (masses in phase).
w_{10} (Hz.)	The theoretical decoupled, undamped natural frequency of the body/engine/transmission axles masses, bouncing in phase on the tyre springs.
μ (dimensionless)	The mass ratio m_1/m_7.
ϕ and ψ (radians)	Phase angles.
γ dimensionless	The index that determines the rate of the non-linear viscous damping characteristic.

CO-ORDINATES.

z axis	The axis normal to the road surface.
x axis	The axis parallel with the vehicle longitudinal axis.
y axis	The axis parallel with the transverse axis of the vehicle.
θ	Rotation about the y axis.

See fig. 3.1. for axes convention.

1. A TECHNICAL REVIEW OF PUBLISHED LITERATURE.

1. A TECHNICAL REVIEW OF LITERATURE PUBLISHED CONCERNING: ENGINE/TRANSMISSION MASS SUSPENSION AND ITS FREE VIBRATIONS. THE EFFECT OF VEHICLE VIBRATION ON PASSENGER COMFORT. TECHNIQUES FOR INVESTIGATING VIBRATIONS IN MOTOR VEHICLES.

1.1. The suspension of the automobile engine/transmission unit and its free vibrations.

The vibrations, which produce most passenger discomfort in the automobile, are the vibrations which result from the oscillations of the "secondary" masses which are attached to the vehicle body mass. The vibrations of the "secondary" masses produce accelerations of the vehicle body, or "primary" mass. These vibrations are then transmitted to the passengers.

The effect of the vibration of the "secondary" axle masses, on passenger comfort, have been dealt with in detail over a number of years. Theories are well developed and results are predictable (references 8 & 9). Fig. 1.1. (a) & (b) show the usual vibration models chosen for most of these early investigations. The amount of work done on the effect of the engine/transmission mass vibration, on vehicle riding comfort, is small in comparison. This is because it has been generally assumed that movements of the mass are small, and the vibrations which result are of such small magnitude, as not to affect passenger comfort. A paper by Engles (reference 7), however, shows that this is not correct and gives a good introduction to the problem.

If the only requirement of the engine/transmission mass suspension was to isolate the natural vibrations of the mass, which are excited by road irregularities or front wheel out of balance, then the solution would be to mount the mass rigidly into the body structure. However, this measure would result in intolerable engine and transmission noise being transmitted to the body of the vehicle. Therefore a compromise has to be arrived at, so that noise transmission is a minimum, and excessive engine/transmission movements will not result, if soft noise-attenuating mounting rubbers are used. (These movements will result from engine torque oscillations and force inputs from the front suspension.) Excessive movements cannot be tolerated because of the limited space available, to accommodate travel, and because of the restricted compliance of drive shafts and the exhaust system. Soft mounting rubbers combined with a high damping rate to give the required control will satisfy these two conflicting requirements.

The acceleration of the engine/transmission mass should be a minimum to achieve increased passenger comfort. This implies that the movement of the mass should be a minimum on its mounting system. Low rate engine/transmission mounting rubbers would decrease noise transmission to the passenger compartment, but result in increased movement of the suspended mass. If mounting rubbers of a low rate were used, in conjunction with suitable hydraulic dampers, the acceleration of the mass at its resonances could be reduced without increasing noise transmission, assuming

that soft rubbers are used to locate the dampers. In this study of the effect of hydraulic damping, interposed between the engine/transmission mass and the vehicle body mass, upon vehicle ride, no modifications to the engine/transmission mounting spring rates or geometry are made. Only the hydraulic damping, in parallel with the mounting rubbers, is added to change the 'standard' engine/transmission suspension.

The engine/transmission mass is given only two degrees of freedom, vertically in the z direction, and rotation about the transverse y axis, for the theoretical study in this work. Vibrations, of both the theoretical mathematical model, and the actual vehicle used in the experimental investigations, are excited by generating harmonic and transient force inputs (at the tyre/road interface of the front axle, in the z direction) respectively. The theoretical study takes no account of the influence of the propeller shaft or exhaust system 'coupling'.

Engles (reference 36 paper 15) shows that power unit mounting spring rates should be such that the natural frequency of the power unit, in bounce on its mounts, is less than .7 times the idling speed frequency of the engine in order to isolate the vibrations that are generated by the engine itself. Engles also reports that for a damping factor of .4, which in respect of noise transmission to the vehicle body structure is considered the maximum value, the reduction in resonant amplitudes of the engine/transmission mass is approximately 60%. Engles in this paper

also shows that a soft (low 'Shore' hardness) rubber with high inherent damping is best suited for engine/transmission mounts, e.g. butyl rubber.

Pickford, in his paper (reference 25), shows that a 'soft' engine/transmission suspension system is beneficial at high engine R.P.M. in reducing 'cab deck vibration' of trucks. Pickford shows that the natural mounting frequency of the power unit should be less than 40% of the idle frequency. This represents 80% isolation with no damping.

Reference 20, "Analysis of steady state engine shake" by Mather, stresses the benefit of decoupling the natural pitch vibrations of the power unit. He shows that coupling of the natural vibrations of the power unit, about transverse axes, results from the mass centre not being in the same plane as the spring centre axis. The two natural frequencies for the mass, with two degrees of freedom (bounce and pitch about a transverse axis), will lie further apart the stronger the coupling. Mather concludes that decoupling is desirable, in order to narrow the frequency band, for the purpose of easier control of the reaction, which excitation of the engine/transmission mass produces, on the vehicle structure.

Horovitz (reference 13) and Harrison (reference 11) are excellent papers dealing with the theory of the geometry of vehicle power unit suspension. Harrison postulates that the front mounts should support the weight of the engine/transmission

mass, and also absorb oscillating torques produced by the engine. He shows that the mounting rubbers should be positioned on the principal axis (least moment of inertia). The rear mount he considers must be positioned so that pitching motion is stabilised. This is the 'centre of percussion theory', i.e.

$$a + b = \frac{j_1 + m_1 a^2}{m_1 b^2} \qquad \ldots \quad 1.1.(1)$$

Harrison also gives some rule of thumb design criteria for engine mounting. Over rough terrain he suggests that the power unit will be subjected to 3g. maximum vertical acceleration. The shear stress of the mounting material should be limited to 30lb./in.^{2} and compressive strain to 12%.

1.2. Vehicle 'Shake'.

'Shake' may be defined as the beam-like vibrations of the vehicle body, excited by front road wheel imbalance, road irregularities or engine/transmission mass vibrations.

Stepp (reference 31) in his paper, "A computer technique for designing engine mounts to control shake", illustrates how the mounts can be designed to control 'shake'. He reports that the main function of the engine mounting system must be to support the engine under all conditions, and as a secondary function to control forces transmitted from the engine

to the vehicle structure. The mountings must reduce forces transmitted to the structure from the engine mass, and also reduce noise transmission to the passenger compartment to a satisfactory level. For shake control, he postulates that the engine must act as a dynamic absorber and that the mounts should be designed to feed large forces into the car structure, equal and opposite to the suspension force inputs. Stepp's theory shows that, for ideal engine mounting, the system should be completely decoupled giving a minimum number of resonant frequencies. These frequencies will, in general, be lower than the highest resonant frequency that would exist with coupling present.

To decouple the frequencies the resultant force applied to the engine by the isolators, when the engine is displaced in translation, must pass through the c. of g., or the resultant of the forces in each isolator, resulting from a rotation of the mass, must be zero. These conditions are satisfied when the elastic and principal axes coincide.

Engles (reference 36 paper 15) reports that the accelerations of the car body, for a front mounted engine, are much larger at the front of the body than the accelerations at the rear, in the 5 to 15 Hz frequency range. This indicates that most body 'shaking' results from motion of the power unit. He also shows that the main vehicle suspension dampers excite

the natural vibrations of the engine/transmission mass by transmitting shocks produced by road irregularities.

The work of Engles (reference 7) indicates that separating the engine mass from the main body mass by springs results in higher body accelerations, which will result in decreased 'riding' comfort. However, if it is accepted that the engine must be isolated from the body by springs, in order to reduce noise transmission, then some possible advantages can be gained. It should be possible to use the vibration energy of the engine/transmission mass, produced by its motion, to balance the vibration energy generated by the displacement of the front 'axle' mass, and hence reduce the car body motion. This may be achieved by design of the engine/transmission suspension system. The paper by Engles shows the advantage of looking at phase plots of motion of the engine, body and wheel masses to study the effect of 'balancing'. The conclusion reached is that for a conventional vehicle layout, for optimum balancing, it is necessary that the phase shift of the engine motion relative to the motion of the body should approach 180 degrees below wheel mass resonance. The declining remainder of 'resonance boosting' of the natural oscillations of the engine mass should intersect with the rising resonance curve of the wheel mass, but only to the extent that the 180 degree phase shift in the resonance range between wheel mass and body mass is maintained.

Lloyd-Nedley (reference 19) in his paper, "The effect of wheel non-uniformities on tyre and wheel assembly and the vehicle", describes 'smooth road shake' which is experienced in cars travelling over smooth surfaces. In American cars this 'shake', which can be felt, and is uncomfortable to the car occupants, occurs in the frequency range 11 to 17 Hz. This is in the 'wheel hop' frequency range. This 'shake' input force, which is independent of road surface conditions, is proved by Lloyd-Nedley to be produced by tyre non-uniformities and wheel runout. He concludes that it is the first harmonic of the wheel and road irregularities that produce this 'shake', and that the peak to peak values of the runout curves are not an indication of the amount of 'shake' that the tyre/wheel assembly produces in the vehicle. Practically, to reduce the induced 'shake', Lloyd-Nedley describes how the wheels and tyres may be indexed on assembly so that the first harmonics of the runouts subtract, i.e. the first harmonics are 180 degrees apart.

Kojima, Osaka, Hazemoto and Arita in their paper, "Control of shake in trucks" (reference 17), define 'shake' as the resonance that can occur in a vehicle travelling over any road surface, but which is generally excited by tyre/wheel imbalance. Their work shows that it is possible to use the engine/transmission mass, on its mounts as a 'dynamic absorber', to control this resonant condition of chassis or body bending.

In the paper a mathematical model representing the pitching and bouncing of the engine, body and cab, bouncing of the unsprung axle masses and the bending of the chassis frame is considered. Because the horizontal, roll and yaw vibrations are considered to be decoupled from the vertical vibrations, they are not taken into account. From the equations of motion, vertical acceleration of the passenger cab is calculated, for a range of engine mount stiffness and damping factors.

The optimum mounting spring rate and damping rate (in the vertical direction) to achieve effectiveness as a 'dynamic absorber' is selected from a carpet plot. Minimum cab vertical acceleration, produced by the 'shake' vibration, is shown to be theoretically achieved, with mounting rubbers of high inherent damping. The mounting rate constant can take a wide range of values without significantly affecting the acceleration level in the cab. Measurements of the cab vertical vibrations, made by the authors on a vehicle equipped first with the original engine mounts and then on a vehicle fitted with the butyl rubber mounts (to give better control of the 'shake' vibration) confirmed their theoretical study.

It is essential to include in this survey a study of published literature on the following topics: The effect of vehicle vibration on passenger comfort. The effect of changing vehicle parameters on the vibration behaviour of the vehicle. A complete picture of the vibration characteristics of the motor

vehicle and its effects on passenger comfort can then be built up.

1.3. 'Vehicle ride' and passenger comfort.

1.3.1. A survey of some published comfort criteria.

Published information indicates that 'riding comfort' of the automobile depends upon the peak accelerations and the frequency of the vibrations encountered by the passengers (reference 4).

The frequency content of the vibrations of any spring/mass system is determined by the system resonances, and the acceleration peaks by the severity of the force inputs.

The different methods of assessing human response to vehicle vibration, which have evolved, can be classified as follows:

1. Subjective ride measurements.
2. The results of shake table analysis.
3. Objective ride simulator tests and ride measurement in the vehicle.

Subjective comfort curves.

These curves are based upon the subjective response of the individual to a given vertical acceleration at a given frequency. The most important curves are discussed below.

The Reiher and Meister comfort curves.

These curves are based upon the results of standing

ten individuals, in turn, on a shake table and subjecting them to sinusoidal vibrations in a vertical direction at a given frequency for fifteen minutes and recording their responses. The curves are plotted to show vertical acceleration of the shake table against forcing frequency. Six zones of comfort are defined in accordance with the following table:

Zone of comfort.	Human response.
0	Imperceptible.
1	Barely perceptible.
2	Distinctly perceptible.
3	Slightly disagreeable.
4	Disagreeable.
5	Unbearable.

The curves are shown in fig. 1.2.

The Janeway recommended limit.

This comfort limit is based upon a survey of shake table results published prior to 1950. The results are pertinent to vertical vibrations. The comfort limit is determined by three straight lines*. The equations of the straight lines* being given by the expression:

$$J = Kzw^{x} \qquad \ldots \qquad 1.3.1.(1)$$

'w' is the forcing frequency (c.p.s.) and 'z' is the vibration amplitude (in.). (* straight line with log. scales).

When w equals 1 to 6 Hz, K equals 1/6 and x equals 3.

When w equals 6 to 20 Hz, K equals 1 and x equals 2.

When w equals 20 to 60 Hz, K equals 20 and x equals 1.

These three sets of constants will give the three straight lines, which are easily interpreted. The limit is shown in fig. 1.2.

The Dieckman criterion.

This criterion is based upon a comfort index 'K', which is frequency-dependent. The curves were established from shake table experiments and backed up by ride tests on a vehicle. On this scale the index K = 100 is taken as being intolerable for 'off the road vehicles' and K = 30 as being intolerable for road vehicles.

The comfort limit is based on levels of constant acceleration up to 5 Hz, constant velocity from 5 Hz to 40 Hz, and constant displacement above 40 Hz, viz:

$K = zw^2$. 0 to 5 Hz. ... 1.3.1. (2)

$K = 5zw$. 5 to 40 Hz. ... 1.3.1. (3)

K = 200 z. above 40 Hz. ... 1.3.1. (4)

where 'z' is the amplitude (m.m.) and 'w' = frequency (c.p.s.)

The Dieckman comfort curves are shown in fig. 1.2. Work carried out by Woods (reference 32) indicates that irrespective of a person's height, build or weight, the human body undergoes its most unpleasant resonance in a vertical direction at 4.5 Hz. Work that he carried out to compare the

effects of sinusoidal and random vertical vibrations on human comfort show that, for the same R.M.S. acceleration value, random vibrations are more acceptable to the human by half a comment on a six comment scale, viz: 1 - neutral; 2 - some unpleasant effects; 3 - some unpleasant effects, cannot be ignored; 4 - definitely unpleasant; 5 - most unpleasant; 6 - unacceptable.

Other comfort criteria.

These criteria to be described are not based upon acceleration/frequency relationships.

Professor Eldik-Thieme (reference 6) outlines a basis for assessing riding comfort quality, in railcars, due to Sperling. This criterion could be applied to road vehicles. The product of 'work done' and 'jerk' (the rate of change of acceleration) is considered. If 'z' is the displacement amplitude (m.m.) and 'w' the forcing frequency (Hz.), a comfort index, represented by the following equation, is considered. It is formulated as the result of subjecting 25 subjects to sinusoidal vibrations and recording their responses.

$$W_z(\text{comfort index}) = 2{\cdot}7\ \sqrt[10]{z^3 w^5} \quad \ldots\ldots\ 1{\cdot}3{\cdot}1(5)$$

In 1956, as a result of further work, a correction factor F(w) was introduced into the equation to give:

$$W_z = 2{\cdot}7\ \sqrt[10]{z^3 w^5\ F(w)} \quad \ldots\ldots\ 1{\cdot}3{\cdot}1(6)$$

Values of F(w), for a range of frequencies, are given in graphical form in reference 6. As a guide to index values expected, $W_z = 1$ is considered to result from a quality of riding comfort that is good and $W_z = 3.5$ is considered barely satisfactory. A vehicle will travel over a variety of surfaces; to take this into account Sperling arrives at an average comfort index, W_z (average).

$$W_z(\text{average}) = \sqrt[10]{\frac{l_1 W_{z1}^{10} + l_2 W_{z2}^{10} + l_n W_{zn}^{10}}{l}} \quad .1.3.1(7)$$

where $l = l_1 + l_2 + l_n$ = the sum of distances of a particular journey, and W_{z1}, W_{z2}, W_{zn} are calculated using equation 1.3.1.(6).

The work of Mauzin and Sperling, reported by Eldik-Thieme, shows that for a vertical acceleration of $\sqrt{2}$ x the same lateral acceleration, at a given frequency (w), the same comfort index will result.

Sperling also develops a method of acceleration level analysing, in his work, as a method of assessing an overall comfort index, for a random input, using Miners Law. This method relies upon counting the number of occurrences (n) of a given acceleration amplitude, at a given frequency (w). If n is the total number of occurrences, n_1, n_2 ... n_n are the occurrences at different acceleration amplitudes and w_{z1}, w_{z2} ... w_{zn} are the comfort indices (calculated using equation

1.3.1.(6)) at each acceleration level, then

$$W_z \text{ average} = 10\sqrt{W_{z1}^{10}.\frac{n_1}{n} + W_{z2}^{10}.\frac{n_2}{n} \ldots W_{zn}^{10}.\frac{n_n}{n}} \quad \ldots 1.3.1(8)$$

Vibration response histories may be analysed by obtaining the power spectral density of the signal. The area under the curve can be measured and used to give a comfort index for the particular vehicle under investigation. The area can be used to assess riding comfort because the area under a P.S.D. curve equals the vibration energy of the system being analysed over the chosen frequency range.

Reference 10 ("Human response to low frequency noise and vibration", by J.C. Guignard) contains a table which shows various harmful, frequency-dependent effects of structural vibration and airborne (noise) vibration upon man. This table indicates that all the resonant vibrations, which may be excited in the motor vehicle, have a detrimental effect upon the comfort of the occupant. Vibrations in the (0 - 100) Hz. range reduce the comfort of the vehicle. Vibrations in the (100 - 200) Hz. range will induce fatigue over a period of time and may even produce permanent damage to the body. The paper stresses that a potentially annoying vibration can be perceived visually, irrespective of the presence of mechanical sensations of motion.

1.3.2. The effects of changing some vehicle parameters on ride comfort and vehicle safety.

The results of Mitschke's work (reference 22) show the effects of changing vehicle parameters on vehicle riding comfort and safety (effectiveness of tyre to road adhesion or variation of dynamic wheel load).

His results show that the changing of the sprung mass of the vehicle by a factor of two produces a twofold increase in the vertical body acceleration in the case of the lighter vehicle. The ratio of dynamic wheel load to static wheel load is approximately the same for the unladen and laden cases, which indicates a decrease in riding safety for the lighter vehicle, since the variation in the ratio of dynamic to static wheel load does not decrease proportionally with the static load.

Changes to suspension spring rates, with the other vehicle parameters fixed, to give a range of body frequencies from (.7 - 2.5) Hz., indicate that body acceleration decreases as the body frequency decreases. The maximum values decrease in proportion to the suspension stiffness. Hence a small reduction in the natural frequency of the suspension will result in a large increase in ride comfort. Decreasing the suspension spring stiffness decreases dynamic to static wheel loads at the body natural frequency, but increases the ratio at wheel hop frequencies, so decreasing the vehicle safety. Therefore,

softening a vehicle suspension reduces vehicle safety if wheel hop is excited.

Finally Mitschke shows the effect of changing suspension damping rates, with the other vehicle parameters remaining fixed. The results of Mitschke are in agreement with the findings in part of this thesis (reference Appendix A.3.). Increasing damping at the wheel to body relative velocity, at which body resonance occurs, produces decreases in both body acceleration and dynamic to static wheel load ratios.

In the region of 'wheel hop', he shows that body acceleration at first decreases with increasing damping, but increases again, as the damping is increased further. The magnitude of the dynamic to static wheel load ratio decreases continuously with increasing damping at 'wheel hop' frequency. Mitschke does not quote a numerical value for the optimum damping factor, for a vehicle suspension, to give best riding comfort and vehicle safety. He simply states that for good riding comfort the damping factor should be small and for best road holding the value should be of greater magnitude.

From the theoretical calculations (see Appendix A.3) in this thesis, considering a two degree of freedom system to represent one corner of the vehicle, results show the following: Best wheel control will be achieved with a damping factor of .52 referred to the wheel 'hop' mode. Best ride comfort is calculated

to result from a damping factor of .22, referred to the body 'float' mode. Therefore, as a compromise, to achieve satisfactory wheel 'hop' control and vehicle safety, with a good degree of ride comfort, the damping factor for a passenger car should be of the order .35 referred to the wheel 'hop' mode.

1.4. Experimental techniques for investigating vibrations and 'riding comfort' in motor vehicles.

Techniques that have been used to investigate the vibratory behaviour of the motor vehicle can be put into three categories: viz. Techniques relying upon vibration measurements on a vehicle running in the 'field'; Laboratory vibration tests on the stationary vehicle using a mechanical method of vehicle excitation; Tests using an analogue model or digital model of the vehicle.

1.4.1. Vibration measurements on vehicles in the 'field'.

(a) Subjective assessment of vehicle riding comfort.

This method of assessing vehicle ride is still widely used in the motor industry. The results of these subjective tests are usually reliable, because staff employed to make the assessments are experienced in the art. The 'Motor Industries Research Association' has carried out work to obtain physical measurements of vehicle motion, and compared the results with subjective assessments, in order to obtain an understanding of how people assess riding comfort in passenger cars

(reference 23). The results of Aspinall's and Oliver's tests show that people are capable of detecting small changes in vehicle motion. 15% is quoted as the smallest change detectable, if vehicle suspension changes, or road surface changes, are made, which might produce a range of vertical passenger accelerations of the order 4 : 1 maximum.

(b) Objective measurement of vehicle riding comfort.

The need for objective ride measurements in the 'field' is desirable, in order to produce more operator-independent results. This method should also be less time-consuming than subjective testing. Oliver has reported on the development of a 'ride meter' for evaluating ride comfort in passenger cars (reference 24). This instrument depends upon the measurement of mean or mean square vertical acceleration of the seated passenger, when the car is running over a road surface that produces continuous vibratory inputs to the vehicle. The instrument was calibrated using information from previous work on subjective ride measurements and correlated objective measurements. The instrument integrates the input signal over a period of time ranging from 30 seconds to 6 minutes, depending on the length of time required for a particular test. The instrument incorporates a filter of bandwidth .2 - 50 Hz. Most vibrations of annoyance occur in this range in the motor car.

Engles (reference 36 paper 15) discusses vibration measurement in road vehicles. He describes his technique of acceleration measurement and recording the signals on magnetic tape in the 'field'. Tapes are analysed at a later date in the laboratory. Engles made measurements of the vertical accelerations on the vehicle body, above the axles, and on the seats at various vehicle road speeds. Conclusions reached in his paper are that, irrespective of the road surface excitations, all vehicle resonances will be excited as the vehicle travels forward. He shows that the forward speed of the vehicle affects the response spectrum for the vehicle because of the variation of suspension friction with speed. Engles obtains the acceleration spectrum by subsequent frequency analysis of the recorded acceleration signals for each test. However, he does not attempt to correlate the objective work in this paper with subjective assessments of ride in the same vehicle.

1.4.2. Laboratory investigations of motor vehicle vibrations.

Simulation of vehicle ride. Ride simulators used in the laboratory usually consist of four electro-hydraulic or electro-magnetic vibrators, with the vehicle arranged to rest directly upon them on its tyres.

Mills and Ashley (reference 36 paper 4) report experiments which they carried out to examine the performance properties of vibrators in relation to the problem of measuring motor vehicle

vibrations. The authors point out that by using sinusoidal excitation it is not possible to excite all modes of vibration simultaneously in the vehicle. Their work, however, does give a fundamental understanding of the nature of the vehicle's suspension characteristics, particularly friction and its effects upon vehicle 'ride transfer characteristics'.

Engles, in his paper (reference 36 paper 15), discusses randomly distributed excitation using electro-hydraulic and electro-mechanical vibrators. He comes to the conclusion that, by reason of their design principle alone, expectations of random testing have not yet been fulfilled. Engles describes the use of a vertical excitation rig, driven by a mechanical eccentric, to vibrate each road wheel of the vehicle under test, sinusoidally. A rig that has been built by Mercedes-Benz, which consists of a steel belt running over rollers and a vibrator, thus permitting the inclusion of tyre rotation in tests, is also described by Engles.

Barson, James and Morcombe (reference 36 paper 5) describe the use of electro-hydraulic vibrators, sinusoidal excitations and a rolling drum rig, to investigate vehicle tyre vibration characteristics.

Hodkin (reference 36 paper 7) discusses the basic principles and the use of electro-hydraulic vibrators in automobile vibration testing. This work makes obvious the large

capital outlay required for this type of vibration testing. The comment is made by Hodkin that it is not wise to expect too high a quality of dynamic performance, as this has been found to be a major cause of failure, in the application of hydraulic vibrators. In his low frequency excitation work, to eliminate tyre scrub, Hodkin uses air pads mounted between the tyre platform and the vibrator heads. For the majority of dynamic work the wheel platforms are suspended on three links to minimise tyre scrub. Hodkin shows that the equipment finds prime use below 25 Hz. excitation frequency.

Barrowcliff and Ehlert (reference 1) have conducted road simulated endurance tests utilising magnetic command to electro-hydraulic shakers. They record the random inputs to a vehicle suspension in the field, and duplicate the signals in the laboratory to effect a fatigue test evaluation of the vehicle structure using P.S.D. and peak level counting techniques.

1.4.3. Use of the analogue computer to investigate vehicle vibrations and ride comfort.

The use of analogue computers, in the study of vibratory behaviour of motor vehicles, has generally been confined to linearised and simplified models of the vehicle or more comprehensive models of parts of the vehicle. Generally the excitation inputs have been continuous sinusoidal or single pulses. Chenchanna (reference 3) has simulated one corner of the motor

vehicle on the analogue computer and subjected the tyre spring to a random signal input, which represented the roughness of a 'normal' road, statistically. He uses this model to evaluate ride comfort, by passing the response signal through a filter, which represents human sensitivity to random vibration, and then looks at the acceleration output from the filter. In this simulation the effect of differential damping has been evaluated. Optimum comfort was found to result from a bump rate equal to .4 the rebound rate. Best road holding resulted from a bump rate equal to the rebound rate, i.e. no damping differential.

Non-linear damping rates and spring rates may be generated with modern analogue computers using 'diode function generators'. Modern analogue machines can simulate any mechanical system and account for all non-linearities. However, it would not be feasible to consider representing the vibration model of the complete automobile spring-mass system, because of the size of computer required.

Fig.1.1

(a)

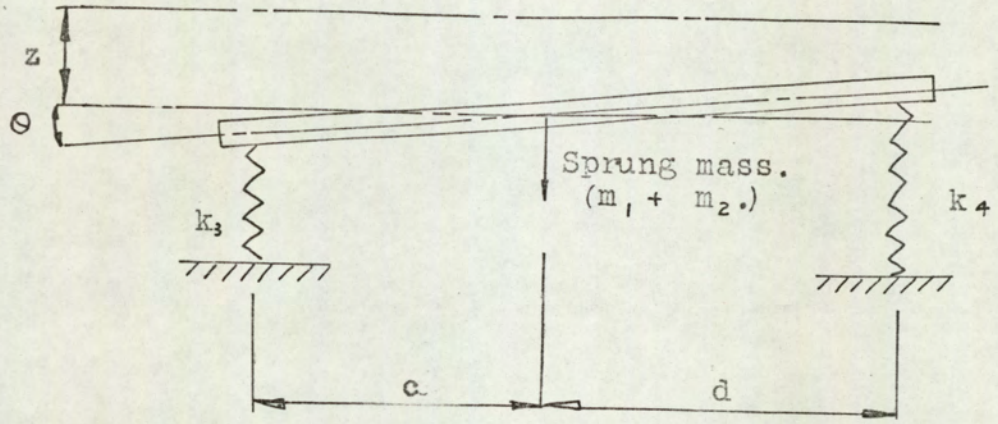

(b)

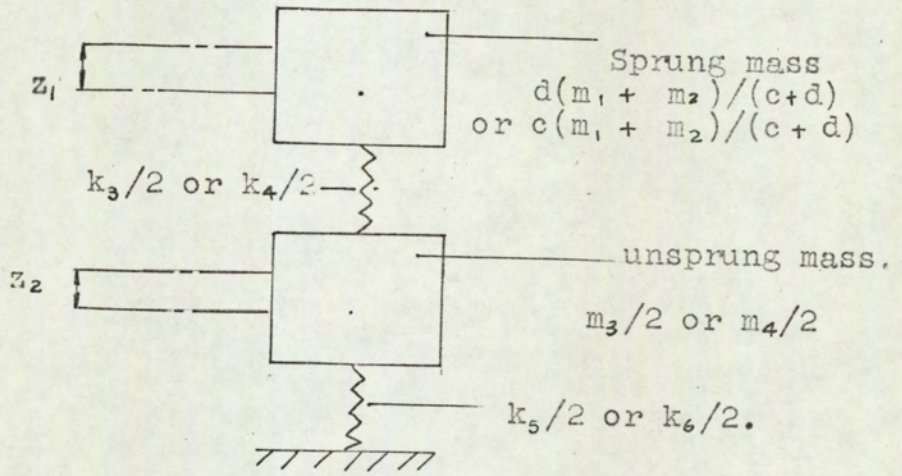

Two degree of freedom vibration diagrams representing:

a) The vehicle sprung mass vibrating with coupled vertical bounce and longitudinal pitch.

b) One corner of the vehicle in coupled bounce.

Fig. 1.2

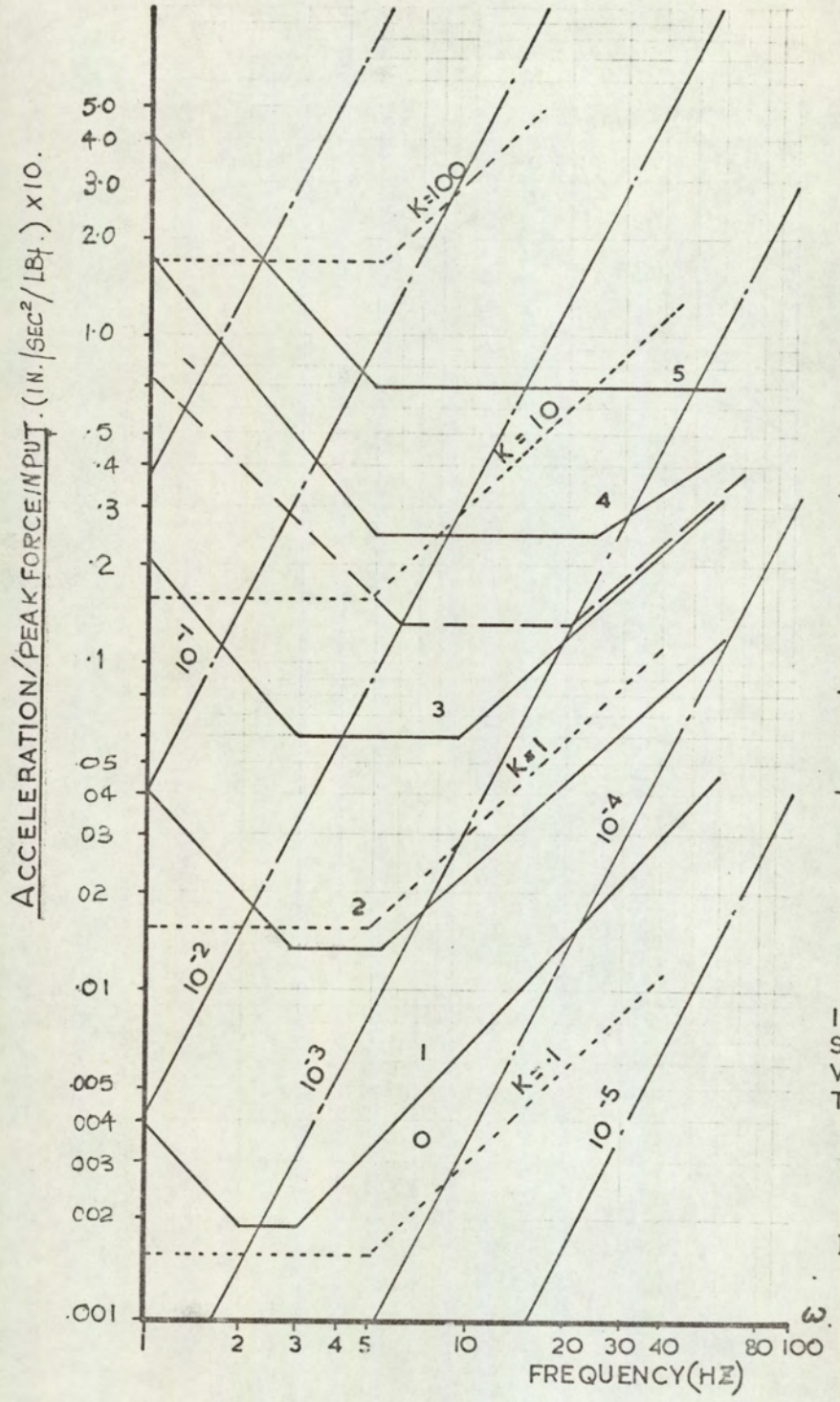

—— REIHER AND MEISTER'S ZONES OF COMFORT. 0-5

— — — JANEWAY'S LIMIT BASED ON SURVEY OF PUBLISHED INFORMATION.

------ DIECKMANN CRITERIA.

—·—·— LINES OF CONSTANT AMPLITUDE.

IN ALL CASES PERSONS SUBJECTED TO SINUSOIDAL VIBRATIONS ON A SHAKE TABLE.

Force input. = 1000 lbf.

SUBJECTIVE COMFORT CURVES.

2. STATEMENT OF THE PROBLEM.

2. THE PROBLEM OF MOTOR VEHICLE 'SECONDARY' MASS VIBRATION, PASSENGER COMFORT, AND THE SELECTION OF METHODS OF ANALYSIS.

2.1. The Vibration Problem.

For any spring-mass-damper system, with 'n' degrees of freedom, there will be associated with it 'n' natural frequencies. The vibrations of such a system are generally coupled, i.e. for any resonant frequency each mass will vibrate at this frequency, to a lesser or greater extent. For preliminary studies of the vibration behaviour of the automobile, the usual approach is to consider the motion of the various masses as being decoupled. This assumption is reasonable for most rigid body systems whose resonant frequencies are not closely coupled and when an answer, of no great accuracy, is required.

As many as eighteen degrees of freedom may be identified in the actual vehicle. In this thesis six degrees of freedom are given to the mathematical model. The method of experimental testing in this work has been chosen such that only the six degrees of freedom, chosen for the mathematical model, are excited together with some structural modes which will be identified.

The effect of the decoupled vibration of the vehicle 'axle' masses on passenger comfort is studied thoroughly from the theoretical standpoint, and the results are familiar (references 8 and 21). However, the amount of theoretical work that has gone

into the study of the free vibrations of the engine/transmission mass, and the effect of engine/transmission mass damping on vehicle vibrations, is small by comparison. Theoretical studies of the spring-mass-damper system, representing the complete motor vehicle, have been impossible until recently, because of the volume of calculations involved. Today digital computers have increased the speed at which calculations can be carried out, with a result that these more comprehensive vibration studies have been made possible. Engles (reference 7) deals with the theory of the free vibrations of the automobile power unit in detail. Papers by Kojima, Osaka, Mizuno, Hazemoto and Arita (reference 17) and Stepp (reference 31) give details of digital computer methods used to design engine mounting rubbers, with the optimum damping and spring rates, to control the 'shake' resonant condition. The 'shake' condition is defined in 1.2. From the conclusions of Kojima, etc., it is evident that increased vehicle comfort will result from a high value of damping in parallel with the power unit mounting springs, the damping effecting dynamic control of the 'shake' vibration. For good noise and engine torque oscillation attenuation the rates of the mounting rubbers should be as low as possible, commensurable with adequate control of excessive power unit movements, which might prove troublesome.

The installation of hydraulic dampers, in parallel with the engine mounting rubbers, will satisfy the increased damping requirement to give better ride comfort by controlling the

structural longitudinal beam vibrations of the vehicle body. It will also prevent excessive dynamic movements of the power unit, which would result if softer mounting rubbers were designed into the engine suspension system.

2.2. Problem Analysis.

In order to assess the effect of increased power unit damping on vehicle ride and passenger comfort it is necessary to obtain the relationship between a known input vibration to the vehicle and the output response on some part of the vehicle body on which the passenger seat is located. (This ratio of output response to input response is known as the 'vehicle ride transfer' characteristic.) It is assumed that the passenger seat will filter the 'shake' and secondary mass resonant vibrations, so that they will not be sensed by the torso of the vehicle occupant. Therefore the seat 'spring' can be omitted, and the number of variables in the analysis will be reduced. The 'shake' and secondary mass vibrations will, however, be felt by the vehicle occupant through his feet which rest on the floor of the vehicle. For these reasons, measurement and calculation of the vehicle acceleration should be made on the vehicle body, and at its c. of g. for reference purposes.

To understand the complete vibration behaviour of the vehicle the 'transfer mobility' for each mass would be beneficial. These characteristics can be arrived at from the calculation of the acceleration response of each mass, by considering the equations

of motion, or by measuring the accelerations,(experimentally) of each mass, and ratioing the acceleration spectrum to the spectrum of the force input to the system.

2.2.1. Theoretical Analysis.

The analysis of a six degree of freedom system, representing the vibrating motor vehicle, will give a good understanding of its coupled vibration behaviour. The model is shown in fig. 3.1. The body mass, engine mass and axle masses are constrained to move vertically in the 'z' direction. The engine and body masses are also free to rotate about the transverse 'y' axis. Bending motion of the vehicle body is not accounted for, because of the complex nature of the body which makes calculations of second moments of area inaccurate. Horizontal, roll and yaw vibrations are considered to be decoupled from the vertical and the longitudinal pitch vibrations, and they are not accounted for in the analysis.

Because we are particularly interested in the effect of power unit vibrations on passenger comfort, it is considered that a force input at the front tyre/road interface will best excite these vibrations. In order to simplify analysis, a sinusoidal forcing function is the logical choice. Equations of motion for each mass can be generated using Newton's Laws, and then solved to yield the peak acceleration response of each mass in the system, in the frequency domain. By dividing the peak acceleration response by the peak force input, at a given frequency, the

acceleration responses will be correctly 'weighted'. This 'weighted' acceleration response is known as the 'transfer mobility', referred to a particular mass. From these 'transfer mobility' characteristics the effect of changing system parameters can be investigated. The 'transfer mobility' of the body mass, or the 'vehicle ride transfer characteristic' is of particular interest from the vehicle ride and comfort point of view.

2.2.2. Experimental Analysis.

The problem of experimentally assessing the effect of hydraulically damping the motor vehicle engine/transmission mass on the 'vehicle ride transfer characteristic' could be tackled using any one of the following techniques:

1. Simulating vehicle ride conditions in the laboratory, by exciting the complete vehicle using electro-dynamic vibrators (reference 36 paper 7). Forcing functions may be sinusoidal, or some other simple continuous function, or a random reproduction of the special density of a road surface, recorded in the 'field' (reference 1).
2. Subjectively assessing vehicle ride comfort in the 'field' on an actual test vehicle, employing experienced 'ride engineers'.
3. Objectively, making ride measurements in the 'field', by taking physical measurements of a parameter which gives a value to the riding quality of the vehicle, e.g. using a 'ride meter', which measures and integrates the mean or

$(R.M.S.)^2$ value of the vehicle passenger vertical acceleration over a given period of time, and gives the riding comfort as a percentage (reference 24). Objective ride measurements can also be made, by analysing tape recordings made in the 'field' at a later date in the laboratory.

4. Simulating simplified models of the motor vehicle, and obtaining the 'vehicle ride transfer characteristic' for various input functions, using an analogue computer (reference 3).

5. Transiently exciting the test vehicle, in the time domain, in the laboratory. Magnetic tape recordings of the input and output transients which have been transferred to punched tape can be processed, using a digital computer programmed to perform the required Fourier Transform Analysis (references 15 and 33), to give the 'vehicle vibration transfer' characteristics, in the frequency domain.

The first four methods listed here have all been used, by various workers, in experimental studies of the vibration behaviour of motor vehicles. Because of the non-availability and high capital cost of the necessary test equipment, techniques one, three and four are ruled out. Method two cannot be considered, because physical measurement of vibration signals is of prime importance in the work.

Technique number five appears to be the most suitable technique for the investigation, because of the availability of data logging equipment, and a digital computer for transient information processing. For the tests a transient input can be generated at the front tyre/road interface, so making the theoretical and experimental forcing conditions compatible. So far as the author is aware this experimental method of obtaining the motor vehicle 'vibration transfer characteristic', in the frequency domain, from measurements made in the time domain, has not been used previously. The effects of tyre/wheel rotation on vehicle vibration are not to be accounted for using this technique.

Changes made to engine/transmission mass damping and the effects on passenger comfort should not be considered in isolation from the other vehicle parameters which affect vehicle ride. These are studied by making changes to the parameters in the mathematical model, and noting the effect on the 'vehicle ride characteristic', or by investigating a simplified two degree of freedom system representing one corner of the vehicle.

3. THEORETICAL INVESTIGATIONS.

3. THEORETICAL INVESTIGATIONS.

3.1. Choice of an equivalent vibration diagram to represent the automobile spring-mass-damper system (see fig. 3.1.).

A complete automobile vibratory model, considering the engine mass and axle masses to be separated from the body structure by springs and dampers, has a minimum of sixteen degrees of freedom. If structural bending modes are considered, extra degrees of freedom will result. To mathematically analyse such a system would be a formidable task, even with the aid of a digital computer. For this study of the effect of engine/transmission mass damping on vehicle ride, six degrees of freedom are considered to be sufficient to work with. The vibration diagram is shown in fig. 3.1. The vehicle is symmetrical about its longitudinal axis. The horizontal, yaw and roll displacements are considered to be decoupled from the vertical and longitudinal pitch displacements and are not taken into account in the analysis. The force inputs (in the frequency domain) at the front tyre/road interface, are assumed to be of equal magnitude and in phase, at both the nearside and offside 'tracks'. Spring and damping laws are assumed to be proportional to the relative displacements and velocities respectively. The damping non-linearities, that occur in practice, are linearised by equating the work done by the damper to the work done by an equivalent linear damper and calculating its new

equivalent linear rate (for theory of equivalent linearisation see Chapter 3.2.).

3.1.1. Theoretical analysis of the mathematical model.

Analysis is carried out considering 'steady state' conditions. The equations of motion are developed using Newton's Laws of motion and by considering each mass in turn as a 'free body'. The forcing function generated P_3 cos.wt. is applied, in the 'z' direction, at the front tyre/road interface.

Equations of motion.

Vertical motion of the engine/transmission mass (m_1); mass constrained to move in the z direction.

$$m_1\ddot{z}_1 + v_1(\dot{z}_1 + a\dot{\theta}_5 - \dot{z}_2 - c\dot{\theta}_6) + v_2(\dot{z}_1 - b\dot{\theta}_5 - \dot{z}_2 - l\dot{\theta}_6) + k_1(z_1 + a\theta_5 - z_2 - c\theta_6) + k_2(z_1 - b\theta_5 - z_2 - l\theta_6) = P_1\cos.(wt + \psi_1) \quad \ldots\ldots\ldots\ldots\ldots 3.1.1(1)$$

Vertical motion of the body mass (m_2); mass constrained to move only in the z direction.

$$m_2\ddot{z}_2 + v_3(\dot{z}_2 + c\dot{\theta}_6 - \dot{z}_3) + v_4(\dot{z}_2 - d\dot{\theta}_6 - \dot{z}_4) - v_2(\dot{z}_1 - b\dot{\theta}_5 - \dot{z}_2 - l\dot{\theta}_6) - v_1(\dot{z}_1 + a\dot{\theta}_5 - \dot{z}_2 - c\dot{\theta}_6) + k_3(z_2 + c\theta_6 - z_3) + k_4(z_2 - d\theta_6 - z_4) - k_2(z_1 - b\theta_5 - z_2 - l\theta_6) - k_1(z_1 + a\theta_5 - z_2 - c\theta_6) = P_2\cos.(wt + \psi_2) \quad \ldots\ldots\ldots 3.1.1(2)$$

Vertical motion of the 'front axle' mass (m_3); mass constrained to move only in the z direction.

$$m_3\ddot{z}_3 + k_5z_3 - k_3(z_2 + c\theta_6 - z_3) + v_5\dot{z}_3 - v_3(\dot{z}_2 + c\dot{\theta}_6 - \dot{z}_3) = P_3\cos.wt. \quad \ldots\ldots\ldots\ldots 3.1.1(3)$$

Vertical motion of the rear axle mass (m_4); mass constrained to move in the z direction.

$$m_4\ddot{z}_4 - v_4(\dot{z}_2 - \dot{z}_4 - d\dot{\theta}_6) - k_4 z_2 + (k_4 + K_6)z_4 + k_4 d\theta_6 + v_6\dot{z}_4 = P_4\cos.(wt + \psi_4) \quad \ldots\ldots\ldots \quad 3.1.1(4)$$

Pitching motion of the engine/transmission mass (m_1); mass constrained to rotate about a transverse axis through its c. of g.

$$-j_1\ddot{\theta}_5 - v_1(\dot{z}_1 + a\dot{\theta}_5 - \dot{z}_2 - c\dot{\theta}_6)a + v_2(\dot{z}_1 - b\dot{\theta}_5 - \dot{z}_2 - l\dot{\theta}_6)b - k_1(z_1 + a\theta_5 - z_2 - c\theta_6)a + k_2(z_1 - b\theta_5 - z_2 - l\theta_6)b = P_5\cos.(wt + \psi_5) \ldots\ldots\ldots\ldots 3.1.1(5)$$

Pitching motion of the body mass (m_2); mass constrained to rotate about a transverse axis through its c. of g.

$$-j_2\ddot{\theta}_6 - v_3(\dot{z}_2 + c\dot{\theta}_6 - \dot{z}_3)c + v_1(\dot{z}_1 + a\dot{\theta}_5 - \dot{z}_2 - c\dot{\theta}_6)c + v_2(\dot{z}_1 - b\dot{\theta}_5 - \dot{z}_2 - l\dot{\theta}_6)l + v_4(\dot{z}_2 - d\dot{\theta}_6 - \dot{z}_4)d - k_3(z_2 + c\theta_6 - z_3)c + k_1(z_1 + a\theta_5 - z_2 - c\theta_6)c + k_2(z_1 - b\theta_5 - z_2 - l\theta_6)l + k_4(z_2 - d\theta_6 - z_4)d = P_6\cos.(wt + \psi_6) \ldots\ldots\ldots\ldots 3.1.1(6)$$

The manipulation and the digital computational matrix method, which is used to solve the equations 3.1.1.(1) to 3.1.1.(6) is given in the appendix (A.1.1. and A.1.2.). The solution yields the values for $\ddot{z}_1$, $\ddot{z}_2$, $\ddot{z}_3$, $\ddot{z}_4$, $\ddot{\theta}_5$, & $\ddot{\theta}_6$, in the 'steady state' for a range of forcing frequencies. The various system 'transfer mobilities' are generated by ratioing the values of $\ddot{z}_1$ to $\ddot{\theta}_6$ by the amplitude of the forcing function (P_3).

3.2. Linearisation of damping rates.

Figs. 4.13. and 4.14. are the characteristics for the hydraulic dampers taken from the test vehicle. Figs. 4.17. and 4.18. are graphs of static hysteresis measured in the vehicle suspension. It is clear that these characteristics are not linear with velocity. The equations of motion, which have been derived to describe the mathematical model of the vehicle, are linear second order equations of the form:

$$m_n\ddot{z}_n + v_n\dot{z}_n + k_n z_n = P_n \cos. wt. \quad \ldots \quad 3.2.1.(1)$$

The damping term in the practical system will however be of the form $(v^1_{hn}\dot{z}^{\gamma}_n + F_n)$ where $v^1_{hn}\dot{z}^{\gamma}_n$ is the hydraulic component of the damping and F_n is the Coulomb damping component.

3.2.1. Linearisation of a non-linear velocity-conscious damping rate.

Jacobs and Ayres (reference 16) describe a method of linearising non-linear velocity-conscious damping rates. They show that the work done by a non-linear viscous damper can be equated to the work done by an equivalent linear viscous damper, i.e.

$$v^1_{hn}\dot{z}^{\gamma}_n = v_{hn}\dot{z}_n \quad \ldots \quad 3.2.1.(2)$$

The work done by the non-linear damper taken from the vehicle can be calculated from the area under the experimentally obtained force/velocity characteristic. This area can be calculated using Simpson's Rule.

If 'W_E' is the work done on the extension stroke and 'A_E' is the area under the experimental characteristic on the extension stroke then:

$$A_E = W_E \quad \ldots \quad 3.2.1.(3)$$

Similarly for the compression stroke:

$$A_C = W_C \qquad \ldots \qquad 3.2.1.(4)$$

If 'K_n' is the velocity limit for the practical characteristics and 'R/K_n' is the rate of the equivalent linear damper, then:

$$R = (W_C + W_E) / K_n \qquad \ldots \qquad 3.2.1.(5)$$

Therefore 'V_{hn}' , the equivalent linear rate (also equal to 'R/K_n'), is given by the expression:

$$V_{hn} = (A_E + A_C)/K^2 \qquad \ldots \qquad 3.2.1.(6)$$

The units of 'V_{hn}' are lbf./in./sec. or N./m./sec.

3.2.2. Transformation of a Coulomb damping characteristic to a characteristic which is linearly velocity conscious.

The Coulomb damping characteristics of the front and rear suspensions for the test vehicle are shown in figs. 4.17. and 4.18. Van Brommel (reference 2) proves that the equivalent linear viscous damping rate V_{in} of a Coulomb damping constant is given by

$$V_{in} = 4/\pi \quad (F_n / K_n) \text{ lb./in./sec. or N./m./sec.} \quad .. \quad 3.2.2.(1$$

where 'F_n' is the Coulomb or hysteretic damping constant and 'K_n' is the maximum relative velocity of the equivalent viscous damper.

3.2.3. The total equivalent linear velocity damping rate.

The viscous damping and the Coulomb damping for both the engine/transmission suspension and the main vehicle suspension will be in parallel.

Therefore $V_n = V_{hn} + V_{in}$ lbf./in./sec. or N./m./sec. .. 3.2.2.(2)

where 'n' is a subscript, which locates the particular damper in the mathematical model.

3.3. Equations for the calculation of the decoupled and undamped natural frequencies of the mathematical model of the vehicle.

For a linearly vibrating single degree of freedom spring-mass system as shown in fig. 3.2. the natural frequency is given by the equation:

$$W_{nx} = \frac{1}{2\pi}\sqrt{k_x/m_x} \text{ Hz.} \quad \ldots\ldots\ldots 3.3(1)$$

If each mass of the mathematical model is taken in turn, their natural frequencies will be given by the following equations:

Front axle mass. (m_3)

$$W_3 = \frac{1}{2\pi}\sqrt{(k_3 + k_5)/m_3} \text{ Hz.} \ldots\ldots 3.3(2)$$

Rear axle mass. (m_4)

$$W_4 = \frac{1}{2\pi}\sqrt{(k_4 + k_6)/m_4} \text{ Hz.} \ldots\ldots 3.3(3)$$

Engine/transmission mass (m_1) in pure bounce.

$$W_1 = \frac{1}{2\pi}\sqrt{(k_1 + k_2)/m_1} \text{ Hz.} \ldots\ldots 3.3(4)$$

Body mass (m_2) in bounce on the suspension springs.

$$W_2 = \frac{1}{2\pi}\sqrt{(k_3 + k_4)/m_2} \text{ Hz.} \ldots\ldots 3.3(5)$$

Body/engine/transmission masses ($m_1 + m_2$) in bounce on the suspension springs.

$$W_5 = \frac{1}{2\pi}\sqrt{(k_3 + k_4)/(m_1 + m_2)} \text{ Hz.} \ldots\ldots 3.3(6)$$

Body/engine/transmission/axle masses in bounce on the tyre springs.

$$W_{10} = \frac{1}{2\pi}\sqrt{(k_5 + k_6)/(m_1 + m_2 + m_3 + m_4)} \text{ Hz.} \ldots 3.3(7)$$

3.4. The equations for theoretical determination of the damping factors associated with the decoupled vibration of the masses for the mathematical model (fig.3.1.).

For a linear single degree of freedom system as shown in fig. 3.2., the damping factor is defined by η_x

Where $\eta_x = V_x / V_{x\ crit.} = v_x / 2k_x / w_{\eta x}$ .... 3.4(1)

and $V_x = 2\sqrt{k_x m_x}$ ..... 3.4(2)

w_{nx} is the natural frequency associated with the spring-mass system in fig. 3.2.

If the two degree of freedom system shown in fig. A.3.1. is considered to represent one corner of the model of the vehicle vibration model and it is also completely decoupled in its modes of natural vibration, then the damping factors will be given by the following expressions:

Damping factor in 'the wheel hop mode' for the front axle mass.

$$\eta_3 = w_3 (V_3 + V_5)/2 (k_3 + k_5) \quad \ldots \quad 3.4.(3)$$

Damping factor in 'the wheel hop mode' for the rear axle mass.

$$\eta_4 = w_4 (V_4 + V_6)/2 (k_4 + k_6) \quad \ldots \quad 3.4.(4)$$

Damping factor of the body mass in the 'pure bounce mode'.

$$\eta_2 = w_2 (V_3 + V_4)/2 (k_3 + k_4) \quad \ldots \quad 3.4.(5)$$

Damping factor of the engine/transmission mass in its 'pure bounce mode'.

$$\eta_1 = w_1 (V_1 + V_2)/2 (k_1 + k_2) \quad \ldots \quad 3.4.(6)$$

Damping factor of the body/engine/transmission masses bouncing in phase on the suspension springs.

$$\eta_5 = w_5 (V_3 + V_4)/2 (k_3 + k_4) \quad \ldots \quad 3.4.(7)$$

The values of w_1, w_2 etc., are calculated using equations 3.3.(2) to 3.3.(7).

3.5. The damping properties of elastomeric materials (ref. 28 & 29).

The damping ratio ($\overline{\delta}$) of an elastomeric material is defined as the viscosity coefficient of the material/the viscosity coefficient necessary to damp the system critically.

The damping ratio is given by the equation:

$$\overline{\delta} = w_\eta \xi / 2E \quad \ldots 3.5.(1) \text{ (ref.29)}$$

where w_n is the natural frequency of the mounting system, in which the elastomer is employed, ξ is the viscosity coefficient of the material and E is the elastic modulus of the material.

The damping factor of the elastomer (δ) is defined by the equation:

$$\delta = w \xi / E \quad \ldots 3.5.(2)$$

$$\text{i.e. } \delta = 2(w/w_\eta)(\delta) \quad \ldots 3.5.(3)$$

Therefore $\overline{\delta} = \delta/2$ at resonance $\quad \ldots 3.5.(4)$

For natural rubber, the damping factor and the elastic modulus of the material can be considered independent of frequency, over the frequency range 0 - 200 Hz.

The material used in the engine/transmission mounting rubbers of the test vehicle is natural rubber, of 'Shore' hardness

55 degrees. In reference 28, a study is made of the dynamic mechanical properties of rubber-like materials. The author indicates that the damping ratio for natural rubber is .05 over the range of excitation 1 - 100 Hz. For the engine/transmission suspension system of the vehicle used in this research, this figure is taken as being the inherent damping ratio for each mounting rubber. In his study of different rubber mounting materials, Snowdon (reference 29) reports that they should possess high damping, in order to reduce vibration amplitudes at resonance. He also reports that rubber materials should be free from increase in dynamic modulus, with increasing forcing frequencies, for best vibration isolation.

Synthetic rubber is a poor vibration isolator, because of its poor damping properties and modulus change, with frequency. Filled Butyl rubber is the exception, affording good isolation at high frequencies as a result of its high inherent damping.

Snowdon (reference 29) reports that high damping is desirable in a mounting system if the springs supporting the mass are fixed to a non-rigid foundation. The high damping suppresses the natural modes of vibration of the non-rigid foundation. Since the motor vehicle engine/transmission mounting rubbers are attached to a non-rigid body structure, it is expected that increased damping in the mounting system will improve the riding comfort in the vehicle by reducing structural vibrations or 'shake'.

* Note in references 28 and 29, the term 'damping ratio' refers to the % of critical damping in a complete suspension system, and the term 'damping factor' refers to the internal properties of the rubber in isolation from the mounting system. In mechanical engineering textbooks generally the term 'damping factor' refers to the % of critical damping in a complete suspension system. This latter interpretation of terminology is used in this thesis.

3.6. Fourier transformation theory - transformation of a function from the time domain to the frequency domain.

The frequency response characteristic of a vibrating system is of fundamental importance. However, to obtain the experimental frequency response for the complete automobile directly, using electro-dynamic vibrators, is costly (ref. 1.4.2.).

For this reason, in this research the experimental response has been arrived at from a knowledge of the transient response time histories of the transiently excited automobile and the transient forcing function.

3.6.1. Transfer of data from the time domain to the frequency domain (reference 15).

Both the 'input' and 'response' transients are transferred from the time domain to the frequency domain using the same theory. This theory is true for any shaped time history.

The Fourier transform of a time function is defined by the expression:

$$f_n(w) = \int_0^{\infty} f(t)e^{-jwt}\,dt. \quad \ldots\ldots\ldots 3.6.1(1)$$

Consider the transient time history shown in fig. 3.3. The time history is divided into n rectangles. For the n^{th} rectangle

$$f_n(w) = \int_{tn-1}^{tn} A_n e^{-jwt}\,dt. \quad \ldots\ldots\ldots 3.6.1(2)$$

This expression can be integrated and expressed in real and imaginary parts.

Real part: $\mathrm{Re}.f_n(w) = A_n \delta t\,(\sin\phi \cos(2n-1)\phi/\phi)$ ..3.6.1(3)

Imaginary part: $\mathrm{Im}.f_n(w) = -A_n \delta t(\sin\phi \sin(2n-1)\phi/\phi)$.3.6.1(4)

where $\phi = w\delta t/2$ and is known as the normalising parameter.

Therefore, to obtain the frequency spectrum from the time history, the transient is divided into 'n' rectangles of base δt.

Then a value of frequency, from the frequency range of interest, is taken and the sum of $\mathrm{Re}.f_n(w)$ and $\mathrm{Im}.f_n(w)$, for the 'n' rectangles, is computed. The absolute value of f (w) is given by:

$$f(w) = (\mathrm{Re}.(f(w))^2 + \mathrm{Im}.(f(w))^2)^{\frac{1}{2}} \quad \ldots \quad 3.6.1.(5)$$

and the phase angle ψ by:

$$\psi = \tan^{-1} \mathrm{Im}f(w) \,/\, \mathrm{Re}f(w) \qquad 3.6.1(6)$$

These expressions are computed for the range of values of 'w' of interest, to give a complete frequency spectrum. f(w) is computed digitally, the values of 'A_n' being measured by hand from the time history, or more easily, as described in this thesis (see Chapter 4.3.2.), using data logging equipment.

If it is assumed that one complete oscillation, in the time domain, can be defined by no less than 4 points, then the maximum frequency for which accurate results can be expected is:

$$w_{max} = 2\pi\delta t/3 \text{ rads/sec. or}$$

$$\delta t = 2.0950/w_{max} \text{ seconds.} \quad \ldots\ldots\ldots\ldots 3.6.1(7)$$

3.6.2. The Fourier Transform of a step function.(reference 14).

The Fourier transform of a unit step function f(t) which is defined by:

$$f(t) = \begin{cases} A \text{ for } t > 0 \\ 0 \text{ for } t < 0 \end{cases}$$

is given by the expression:

$$f(w) = \pi.\delta(w) + \frac{1}{jw} \quad \ldots\ldots\ldots 3.6.2(1)$$

where f(w) is the amplitude of the Fourier Transform, in the frequency domain, at frequency (w), and $\delta(w)$ is defined as the Delta function, i.e. at $w = 0$ $f(w) = \infty$ Fig. 3.4. shows the theoretical Fourier Transform of a step function of constant amplitude (A), equal to 510 lbf. This theoretical curve will be true for a step function of infinite duration. Fig. 3.4. also shows the experimental Fourier Transform of the modified step input of a same steady state amplitude as recorded in the experimental investigations, (see fig. 4.22a) but of finite duration (3.125 seconds). The transform is obtained using the theory from Chapter 3.6.1. and the computer programme, Fig. 4.10.

3.7. Theoretical Results.

The theoretical results are presented in tabular and graphical form.

3.7.1. System Constants.

Referring to fig. 3.1. and the notation (pages xiii-xxii). Numerical values for the system constants. For determination of the values see Chapter 4.1.2.

Vehicle - Hillman Minx Saloon 1968.

Table 3.1.

Constant.	Numerical Value.	Units.	Constant.	Numerical Value.	Units.
a	4.17	in.	m_6	1.93	lbf./in./sec.^{2}
b	22.9	"	m_7	1.00	"
c	52.15	"	m_8	.855	"
d	46.3	"	m_9	.155	"
f_3	$\pm$50	lbf.	m_{10}	5.127	"
f_4	$\pm$25	"	P_3	1,000	lbf.
j_1	140	lbf.in.sec.^{2}	v_1	44.8	lbf./in./sec.
j_2	6660	"	v_2	4.74	"
k_1	2720	lbf./in.	v_3	19.64	"
k_2	534	"	v_4	13.19	"
k_3	180	"	v_5	10	"
k_4	190	"	v_6	10	"
k_5	1800	"	v_{i1}	4.8	"
k_6	1800	"	v_{h1}	40	"
l	29.41	in.	v_{i2}	.91	"
m_1	1.01	lbf./in./sec.^{2}	v_{h2}	3.83	"
m_2	3.22	"	v_{i3}	3.74	"
m_3	.347	"	v_{h3}	15.9	"
m_4	.55	"	v_{i4}	1.87	"
m_5	2.3	"	v_{h4}	11.32	"

3.7.2. The decoupled, undamped natural frequencies for the mathematical model of the vehicle (fig. 3.1.).

The theory for the calculation of these frequencies is given in Chapter 3.3. and the calculations are presented in Appendix A.2.2.

Table 3.2.

Decoupled mass and mode of vibration.	Undamped, decoupled natural frequency. (Hz.)
Front axle assembly (m_3) in pure bounce on the tyre and suspension spring.	w_3 = 12.03 Hz.
Rear axle assembly (m_4) in pure bounce on the tyre and suspension.	w_4 = 9.6 Hz.
Engine mass (m_1) in pure bounce on its mounts.	w_1 = 9.0 Hz.
Body mass (m_2) in pure bounce on the suspension springs.	w_2 = 1.7 Hz.
Body/engine/transmission masses (m_5) in pure, in phase, bounce on the suspension springs.	w_5 = 1.49 Hz.
Body/engine/transmission/axle masses (m_{10}) in pure, in phase, bounce on the tyre springs.	w_{10} = 4.33 Hz.

3.7.3. The coupled bounce/pitch natural frequencies of the engine/transmission mass on its mounting springs.

The theory and calculation of these frequencies is given in Appendix A.2.3. The natural frequencies of the coupled bounce/pitch modes of vibration of the engine/transmission mass are:

$w_{1,1}$ = 9 Hz. and $w_{1,2}$ = 5.4 Hz. and the position of the transverse pitch axles are 240" behind the engine/transmission mass c. of g. and .6 inches in front of the c. of g. respectively.

3.7.4. The coupled bounce/pitch natural frequencies of the body/engine/transmission masses, vibrating in phase on the suspension springs.

The theory and calculation of these frequencies is given in Appendix A.2.4. Referring to Appendix A.2.4.:

$w_{5,1}$ = 1.56 Hz. $w_{5,2}$ = 1.43 Hz.

The transverse pitch axes are located 18" behind the vehicle c. of g. and 13.2" in front of the c. of g. respectively.

3.7.5. The coupled, undamped natural frequencies of the mathematical model in fig. 3.1.

The natural frequencies are obtained using an iterative matrix method which is described in Appendix A.1.4. Computer programme 'Damper 01' was compiled to compute the frequencies (reference Appendix A.1.5.).

The natural frequencies associated with the test vehicle were computed using the numerical values for the relevant masses, inertias and spring rates from table 3.1. The natural frequencies obtained from the iteration are, in descending order:

12.1 H_3 ; 11.7 H_3 ; 9.6 H_3 ; 7.75 H_3 ; 1.66 H_3 and 1.32 H_3

These can be identified with the natural frequencies obtained for the decoupled vibration modes, above. (The natural pitch/bounce frequencies of the engine/transmission mass on its mounts are 11.7 H_3 and 7.75 H_3).

3.7.6. The damping factors associated with the decoupled vibration of the mathematical model (model completely inherently and hydraulically damped).

Table 3.3.

Decoupled mass and mode of vibration.	Associated damping factor.
Front axle mass (m_3) in pure bounce on the tyre and suspension springs.	n_3 = .566 in the 'wheel hop' mode.
Rear axle mass (m_4) in pure bounce on the tyre spring and suspension spring.	n_4 = .35 in the 'wheel hop' mode.
Body/engine/transmission masses (m_5) in pure, in phase bounce on the suspension springs.	n_5 = .416 in the 'body float' mode.
Engine/transmission mass (m_1) in pure bounce on its mounting rubbers.	n_1 = .43.

3.7.7. 'Transfer mobility' characteristics of the vehicle model.

The 'transfer mobility' is defined in the introduction (part iii). Derivation of the 'transfer mobilities' for the various parts of the mathematical model of the motor vehicle is given in Chapter 3.1.1. Computer programme 'Damper 14' (see Appendix A.1.3.) is compiled to solve the equations of motion for the mathematical model.

The theoretical 'transfer mobilities' $\ddot{z}_1/P_3$ to $\ddot{\theta}_6/P_3$ are presented in graphical form (figs. 3.5. to 3.10.) For these theoretical investigations a sinusoidal forcing input, in the frequency domain, of amplitude P_3 = 1000 lbf. at the front tyre/road interface is considered.

The graphs show the effect that changes to the system damping have on the 'transfer mobilities' of the system masses.

3.8. Discussion of the theoretical results.

The object of studying simplified mathematical models of complex mechanical vibrating systems is to indicate the possible behaviour of the system, and to use the results as a design aid to improve the system. In this project the effect of damping the natural resonances of the engine/transmission mass on its mounting springs upon the 'riding comfort' of the vehicle occupants is of particular interest. A measure of vehicle 'riding comfort' for different damping conditions is obtained by looking at the acceleration response, in the frequency domain, of the vehicle

body mass, for a known force input at the front tyre/road interface, with reference to the mathematical model of the vibrating motor vehicle in fig. 3.1.

3.8.1. The natural frequencies of vibration for the mathematical models.

In order to get a measure of the natural frequencies that can be expected for the model, it is useful to look, first, at the undamped decoupled vibration behaviour of the mathematical model. Each mass is considered in turn as a single degree of freedom spring-mass system. The decoupled, undamped natural frequencies for the mathematical model are shown in table 3.2.

These frequencies will not be exact compared with those for the actual vehicle, because damping is not included and spring non-linearities are not accounted for. Also, the masses are assumed to be vibrating as single degree of freedom systems on rigid foundations, the flexibilities of the body structure not being accounted for. Foundation non-rigidities will tend to raise these theoretical natural frequencies (reference 12). This technique of single degree of freedom system analysis is widely used to estimate the natural frequencies of vibration for the motor vehicle. The results shown in table 3.2. indicate that the front wheel 'hop' frequency of 12.03 Hz. is close to the natural frequency of the engine/transmission mass, in pure bounce, on its mounting rubbers (9 Hz.). The work of Engles (reference 7) shows that for a vehicle of conventional layout (front engined, rear wheel drive), if the dominant frequency of resonance of the engine/

transmission mass on its mounts lies close to, or at the front 'unsprung' mass resonant frequency, optimum 'balancing' of the forces produced by these masses will result and the body motions will be a minimum.

The values calculated for the coupled bounce/pitch natural frequencies for the engine/transmission mass on its mounts, considered to be fixed to a rigid structure, are 9 Hz. and 5.4 Hz. (see Appendix A.2.3.). The values of the coupled bounce/pitch natural frequencies for the body, engine and transmission masses vibrating in phase on the suspension springs are 1.56 Hz. and 1.43 Hz. (see Appendix A.2.4.). The undamped, decoupled natural frequency of the rear axle mass vibrating as a single degree of freedom mass on the suspension and tyre springs, in the 'z' direction, is calculated to be 9.6 Hz.

The values of the coupled, undamped natural frequencies for the six degree of freedom mathematical model in fig. 3.1. are calculated using a matrix iteration technique (see Appendix A.4.1.). The results obtained, in descending order, are: 12.1, 11.7, 9.6, 7.75, 1.66 and 1.32 Hz. These frequencies can be identified with reference to the frequencies calculated in the decoupled, undamped calculations (see table 3.2.). The frequency at 12.1 Hz. can be identified as the coupled natural frequency of the front wheel mass, restrained to move in the 'z' direction only. The resonance at 9.6 Hz. is the coupled natural frequency of the rear axle mass, restrained to move in the 'z' direction. The

resonances at 1.56 and 1.43 Hz. are the coupled natural frequencies of the body mass bounce/pitch mode. These latter two frequencies are known as the 'primary ride' natural frequencies for the vehicle. The frequencies at 11.7 and 7.75 Hz. can be identified as the bounce/pitch frequencies of the engine/transmission mass on its mounts. These two frequencies are higher than the undamped, decoupled bounce/pitch natural frequencies predicted for the engine/transmission mass. All the resonances above 5 Hz. can be described as being associated with the 'secondary' ride comfort of the vehicle. It is assumed that that natural frequencies calculated for the coupled mathematical model will be nearer the natural frequencies for the actual vehicle than the ones calculated using the decoupled theory, because the coupled model is a more accurate representation of the vehicle. Damping will produce some resonance frequency shifting. This effect can be assessed by referring to the theoretical 'transfer mobility' characteristics for the mathematical model (figs.3.5 to 3.10).

3.8.2. The 'transfer mobility' characteristics for the mathematical model.

'Transfer mobility' is defined in the introduction (part iii). The 'transfer mobility' characteristics (figs. 3.5. to 3.10) are computed in the frequency domain. They show the effects of three different conditions of damping upon the vibration response of the masses which constitute the mathematical model. The three

conditions of damping considered are:

(i) Inherent damping only in the system.

(ii) The engine/transmission suspension and the main vehicle suspension inherently and hydraulically damped. Inherent tyre damping.

(iii) The main vehicle suspension inherently and hydraulically damped. Inherent damping, only, in the engine/transmission suspension. Tyres inherently damped.

The damping rates shown in table 3.1.(account of the differential rates, extension and compression, is taken in the equivalent linear viscous damping rate calculations - see Appendix A.2.1.), are substituted into the mathematical model above 3 Hz. excitation frequency. This frequency represents a suspension damper piston velocity of 10"/sec. for a .5" vibration amplitude. Below this frequency of excitation the suspension damping rates substituted into the mathematical model are v_3 = 15 lbf./in./sec. and v_4 = 5 lbf./in./sec. This is done to take account of the discontinuity of the hydraulic suspension damping rates in the region of 10"/sec. piston velocity. For the computation of the 'transfer mobilities' (using computer programme Damper 14 - see Appendix A.1.3.), all the other system parameters are fixed and taken from table 3.1.

The system resonances can be identified from the 'system damping only' transfer mobilities. It is evident that

the hydraulic suspension damping modifies the 'coupling' in the mathematical model. The dominant body mass resonance predicted at 1.32 Hz., in the coupled frequency computation, is completely modulated.

Engine/transmission mass damping does not modify the 'transfer mobility' in the mode associated with the resonant body motion at 1.7 Hz. The resonance that can be identified at 2.5 to 3 Hz. is associated with the in phase, bounce/pitch resonance of the complete vehicle on its tyre springs. Because of the closeness of the natural frequencies, associated with the dominant modes of vibration of the front unsprung mass and the engine/transmission mass, these resonances cannot be separated in the 'transfer mobility' characteristics.

The engine/transmission mass 'transfer mobility' characteristics (fig. 3.5.) show that hydraulic damping of the engine/transmission mass produces a 70% reduction in the resonant amplitude at the dominant engine/transmission natural frequency compared with the vehicle model with no hydraulic engine/transmission damping. The reduction at the 3 Hz. resonance for the same considerations is some 30%.

Most important from the vehicle riding comfort standpoint is a study of the 'transfer mobility' for the body mass (m_2). It is assumed that the passenger seat will filter out the frequencies of vibration above 5 Hz. As a result, it is more correct to look at the vibration characteristics for the body mass of the vehicle

rather than the response of the passenger. This enables a complete spectrum of the vibrations encountered by the passenger to be investigated (includes vibrations which would be sensed by the car occupants' feet). The 'vehicle ride transfer characteristics' for the vehicle model are shown in fig. 3.6.

From this figure it is evident that the hydraulic damping of the engine/transmission mass produces a 60% reduction in the resonant amplitude at 12 Hz. and a 30% reduction at 3 Hz. (compared with the vehicle with no hydraulic engine/transmission damping).

A study of the 'transfer mobility' characteristics for the front 'unsprung' mass, for the different conditions of damping (in fig. 3.7.), shows that engine/transmission damping has no effect upon the acceleration response, for this mass, over the frequency range considered.

Fig. 3.8. shows the 'transfer mobility' characteristics for the rear 'unsprung' mass (m_4), for the three different conditions of system damping. The trends are the same as for the characteristics already looked at. Hydraulic engine/transmission damping completely modulates the resonant amplitudes above 5 Hz. (The undamped amplitudes are small to begin with, because the excitation input is applied in the plane of the front axle.)

A study of the theoretical 'transfer mobility' characteristics for the engine/transmission mass (m_1), considered in pitch about a transverse axis through its c. of g. (fig. 3.9.), shows that the additional hydraulic engine/transmission damping

does not modify the engine/transmission mass amplitudes below 5 Hz. However, above this frequency the resonances are modulated. The effect of hydraulic engine/transmission damping upon the 'transfer mobility', associated with the pitching of the vehicle body mass (fig. 3.10.), shows the same trends as the characteristic for the pitching of the engine/transmission mass (m_1). The addition of hydraulic engine/transmission damping to the already inherently damped model with only hydraulic suspension damping added, produces a 35% modulation of the resonant amplitude at 3 Hz. and a 65% modulation at the 12 Hz. resonance.

3.8.3. The damping factors for the mathematical model.

Table 3.3. shows the damping factors associated with the decoupled pure bounce vibration of the test vehicle. This table gives the damping as substituted into the mathematical model, in terms of the non-dimensional damping factor η.

For the inherently damped model the associated factors are: .05 critical for the engine/transmission suspension; .11 critical for the front 'unsprung' mass and .015 critical for the rear 'unsprung' mass. The factors associated, with the vehicle under investigation, with hydraulic and inherent engine/transmission suspension and main vehicle suspension damping are: .566 critical for the front 'unsprung' mass, .35 for the rear unsprung mass and .43 for the engine/transmission mass (for calculations see Appendix A.2.1. and A.2.5.).

The latter damping factor was chosen for the test vehicle

after reference to the theoretical study in Appendix A.4. and with reference to the work of Kojima, etc. (reference 17) and the work of Engles (reference 7).

The values of the suspension damping factors, associated with the combined inherent and hydraulic damping of the suspension, compare with the findings of the theoretical study to find the optimum damping requirements for a vehicle suspension (in Appendix A.3.). This study shows that, as a compromise, for best riding comfort and road holding the factor should be .35 critical.

It is obvious that the values of damping which might be substituted into the mathematical model are infinite.

The particular advantage of developing a comprehensive mathematical model and the analysis technique as described, to study the vibration characteristics of the motor vehicle, is that the effect of changing any damping condition can be understood quickly.

3.9. Conclusions to theoretical investigations.

The conclusions arrived at from this theoretical study may be applied to any passenger car, with a front mounted engine/transmission and similar dimensions and mass distribution.

The natural frequencies predicted for the undamped, decoupled mathematical models are near to those calculated for the undamped, coupled model of the vehicle. However, it must be assumed that the resonances computed for the coupled mathematical model are nearer to those which can be expected to be measured on the actual test vehicle.

The 'transfer mobilities' computed for the mathematical model, in the frequency domain, show the theoretical advantage of increasing the damping factor for the engine/transmission mass suspension, from the low value of .05 critical, associated with the inherent damping of the rubber mounts, to .43 critical, produced by introducing hydraulic damping in parallel with the mounts. This increased damping gives approximately 60% reduction in the amplitude of the vehicle body mass 'transfer mobility' or vehicle 'ride transfer' characteristic at the 12 Hz. resonance (dominant natural frequency of the engine/transmission mass), and 30% reduction at the 3 Hz. resonance (the dominant natural frequency of the vehicle mass in bounce on the tyre springs).

The value of the engine/transmission suspension damping has no effect upon the amplitude of the 'primary' vehicle body mass resonant mode at 1.7 Hz.

The theoretical investigations carried out show how a mathematical model, with six degrees of freedom, can be analysed to predict the vibration behaviour of the motor vehicle.

The analysis technique developed provides a useful tool to study the effect of any vehicle parameter listed in table 3.1. upon the 'transfer mobilities' of a motor vehicle.

Fig. 3.1

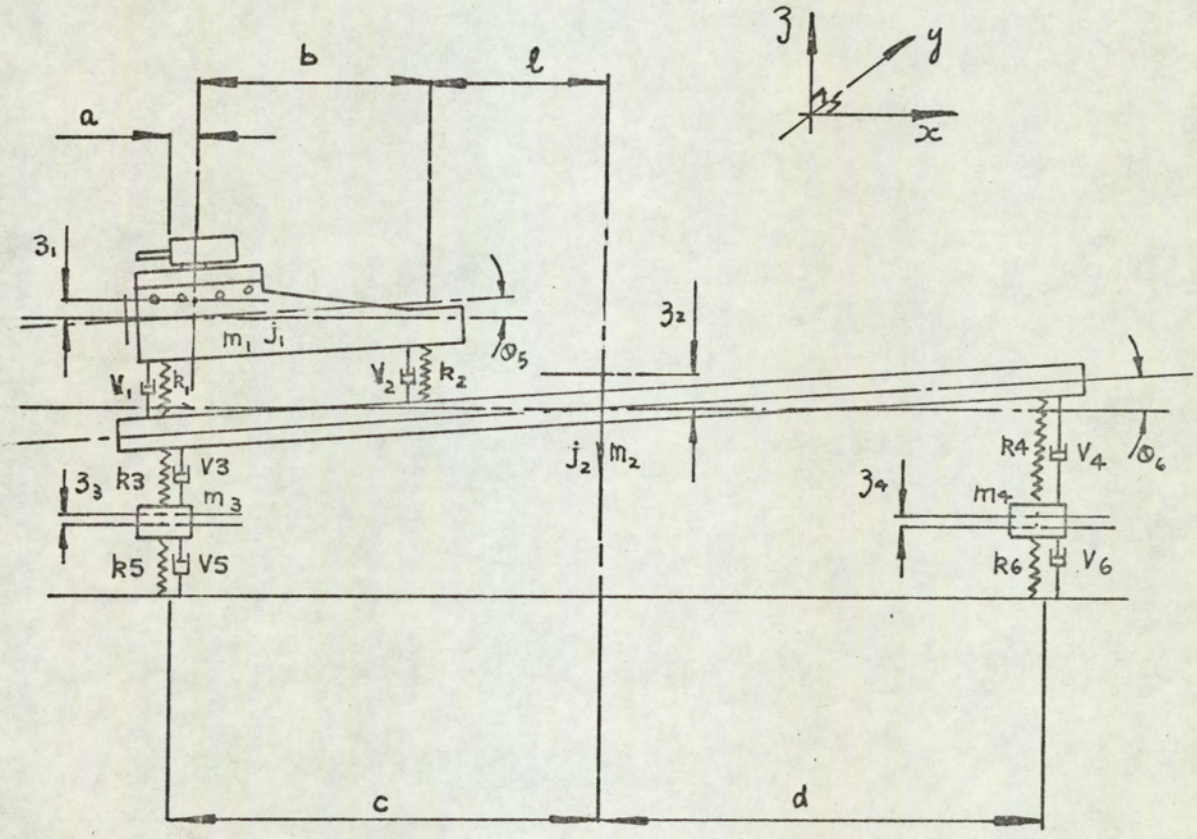

EQUIVALENT VIBRATION DIAGRAM OF VEHICLE.

Fig. 3.2

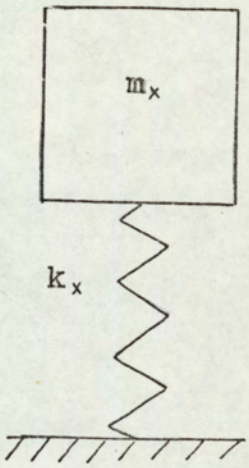

A Single Degree of Freedom Spring-Mass System.

Fig. 3.3

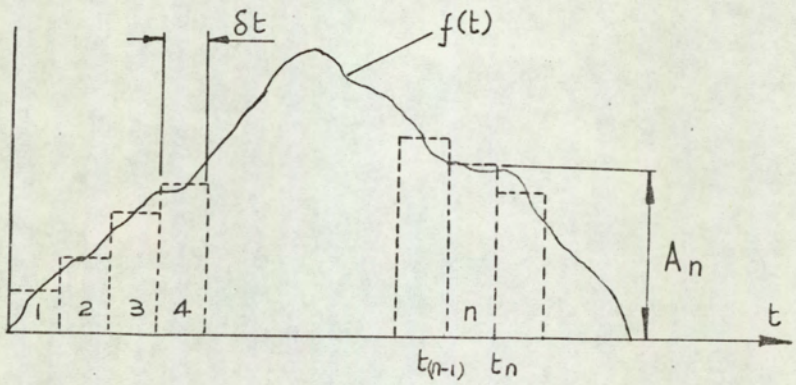

A Staircase Function approximation of a transient for Fourier transformation evaluation.

Fig. 3.4 Graphs showing Fourier Spectrums of:

a) A 'step' function (theoretical spectrum.)

b) A modified 'step' function as shown in fig. 4.22 a.

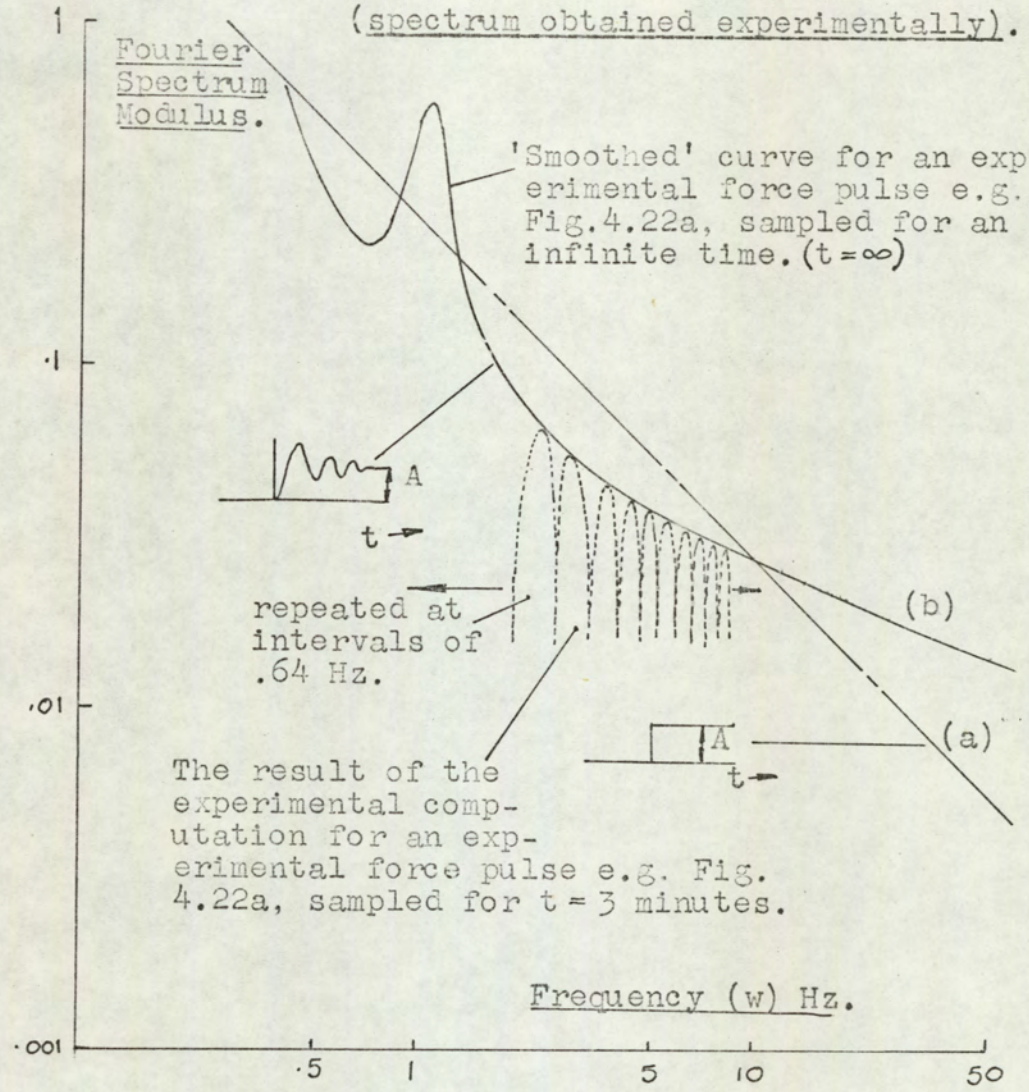

Fig. 3.5 The theoretical 'transfer mobility' $\ddot{z}_1/P_3$ frequency spectrum for various conditions of model damping.

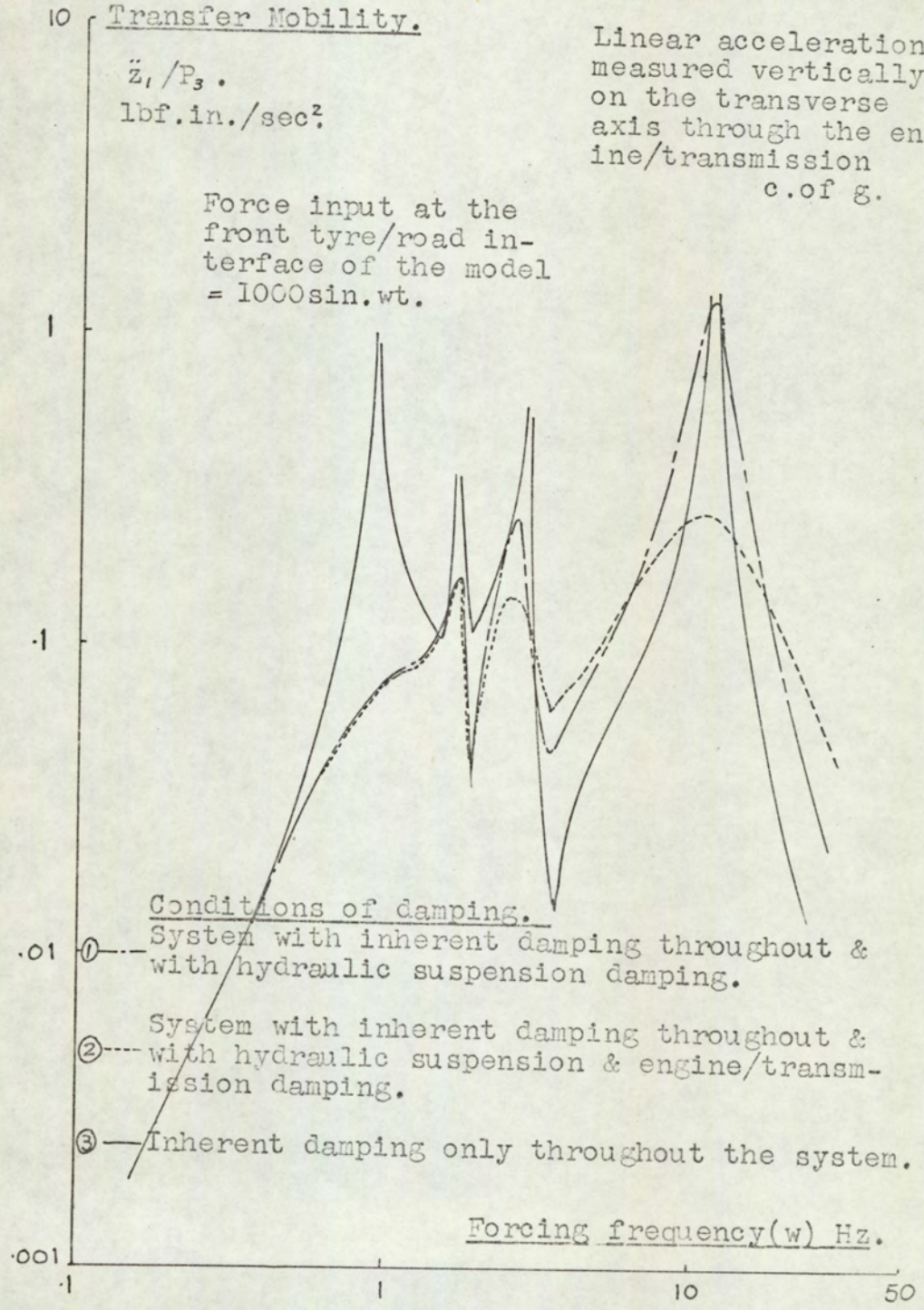

Fig. 3.6 The theoretical 'transfer mobility' $\ddot{z}_2/P_3$ frequency spectrum, or vehicle 'ride transfer' characteristic, for various conditions of model damping.

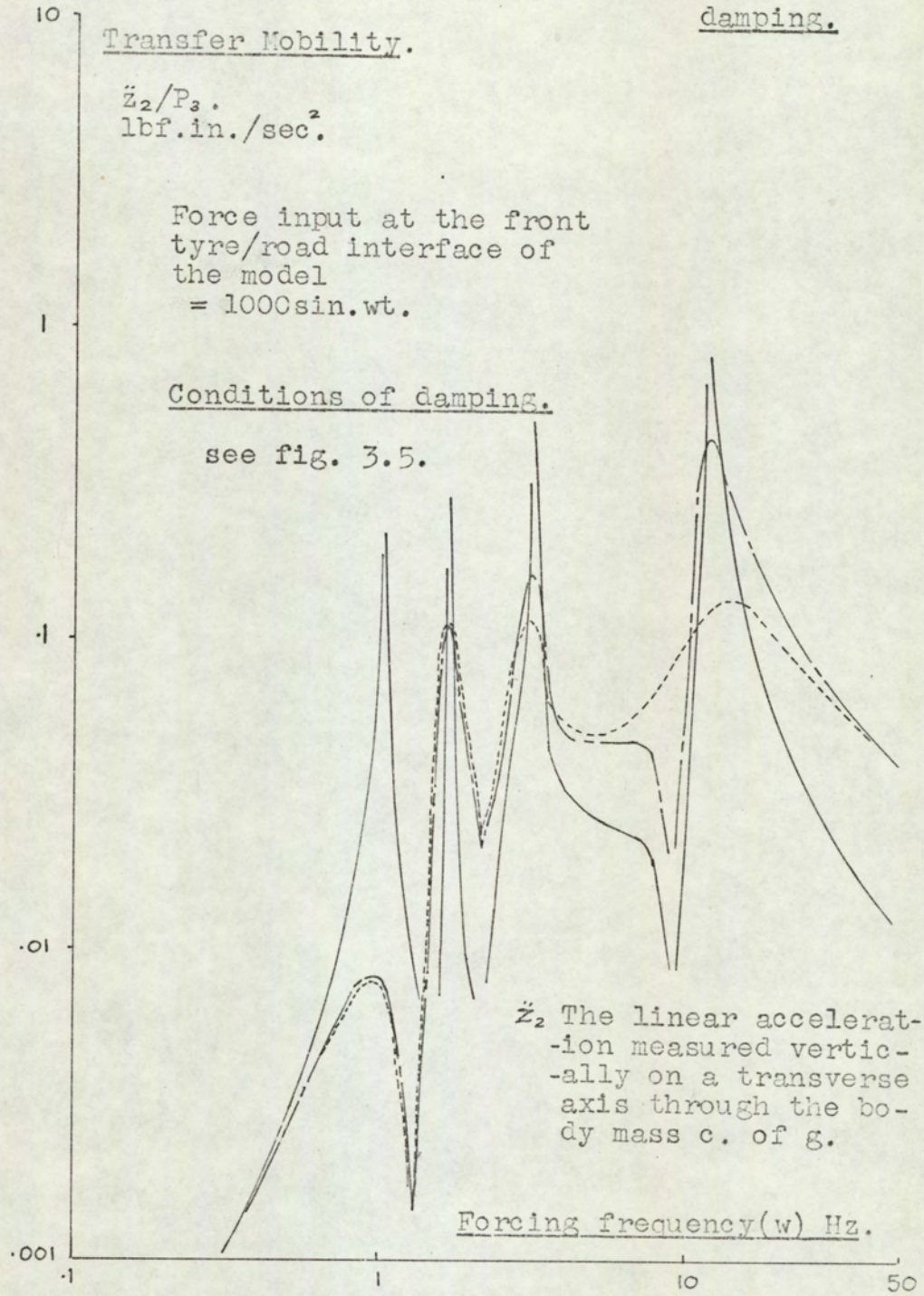

Fig. 3.7. The theoretical 'transfer mobility' $\ddot{z}_3/P_3$ frequency spectrum, for various conditions of model damping.

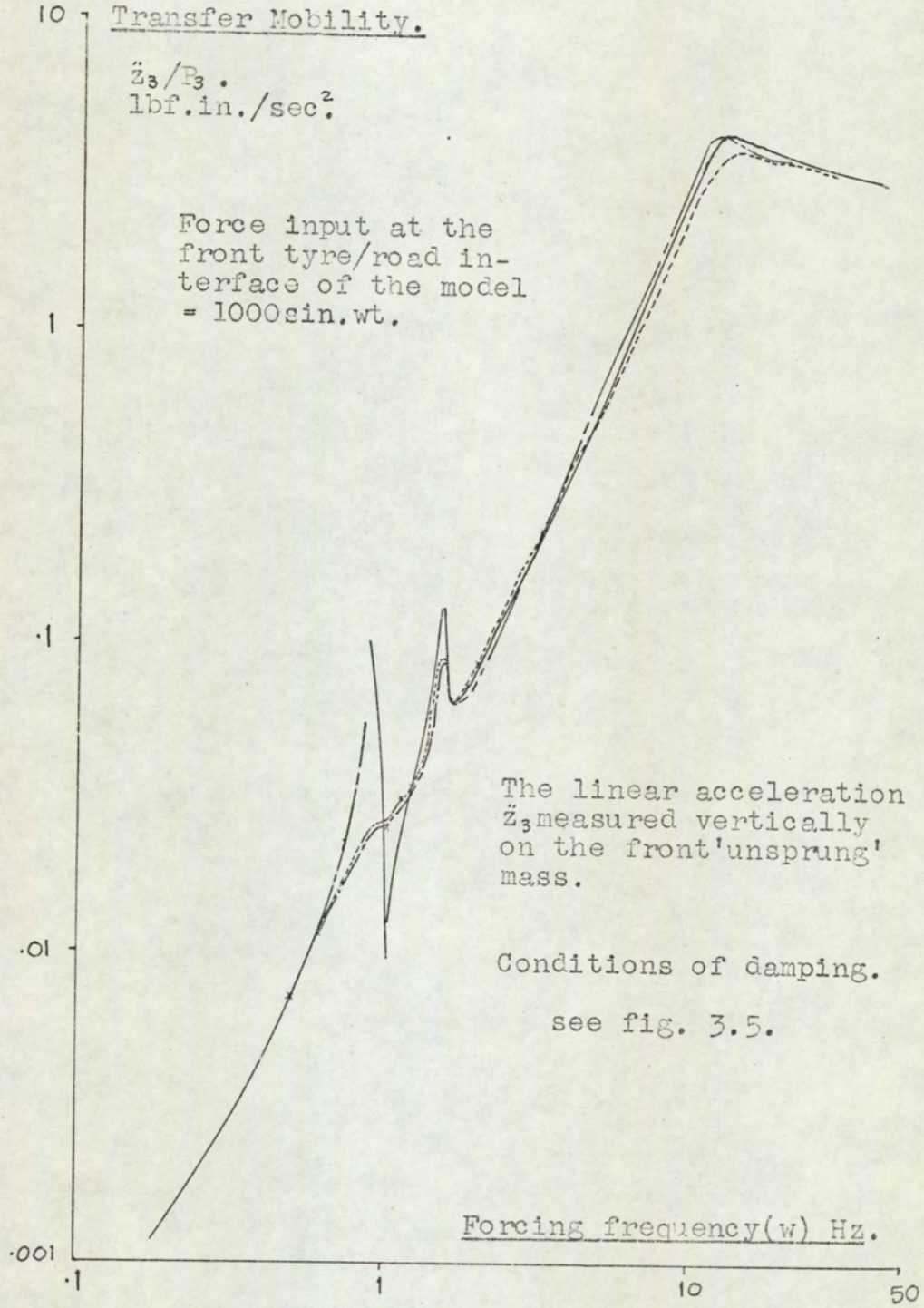

Fig. 3.8 The theoretical 'transfer mobility' $\ddot{z}_4/P_3$ frequency spectrum, for various conditions of model damping.

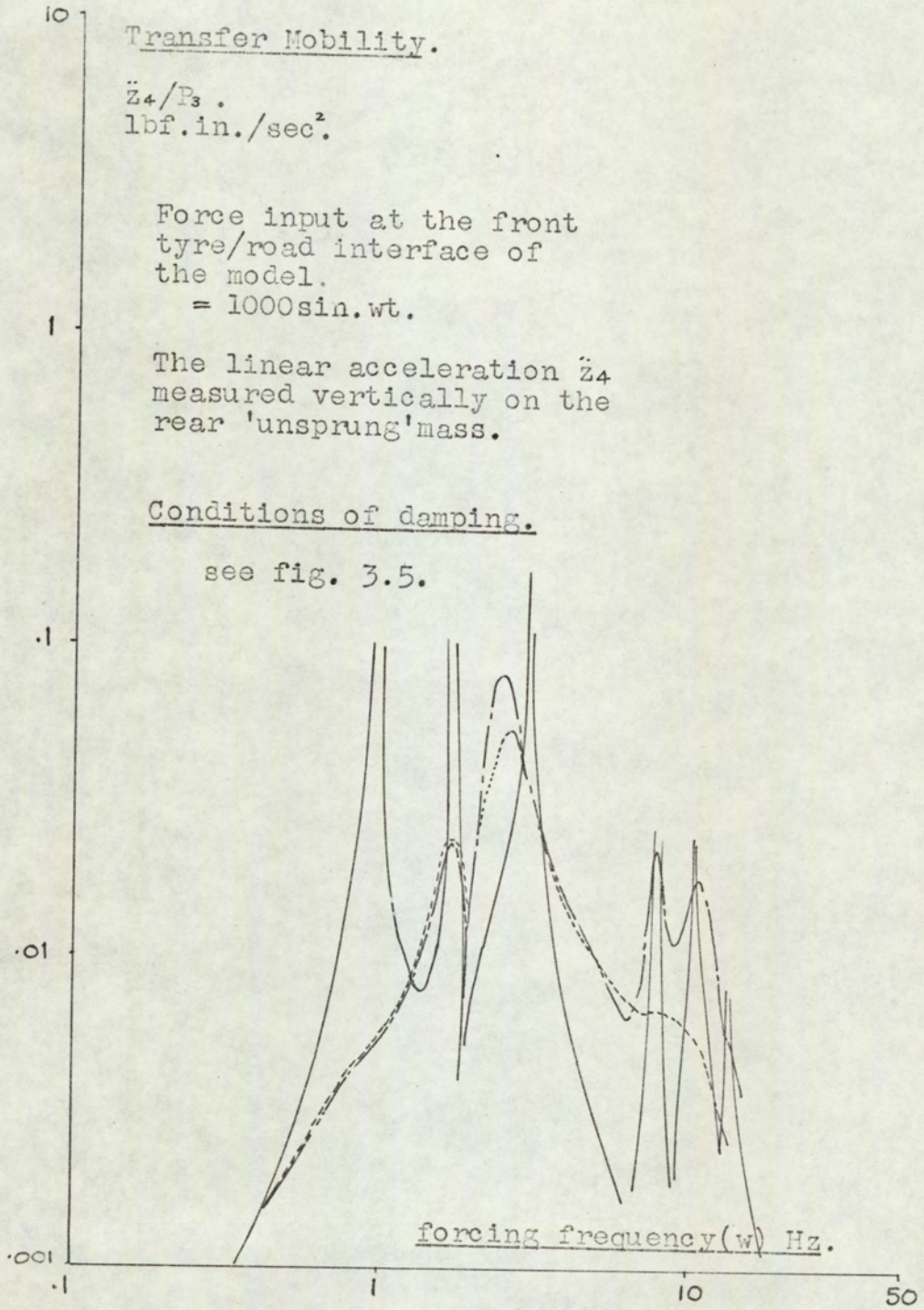

Fig. 3.9 The theoretical 'transfer mobility' $\ddot{\Theta}_5/P_3$ frequency spectrum, for various conditions of model damping.

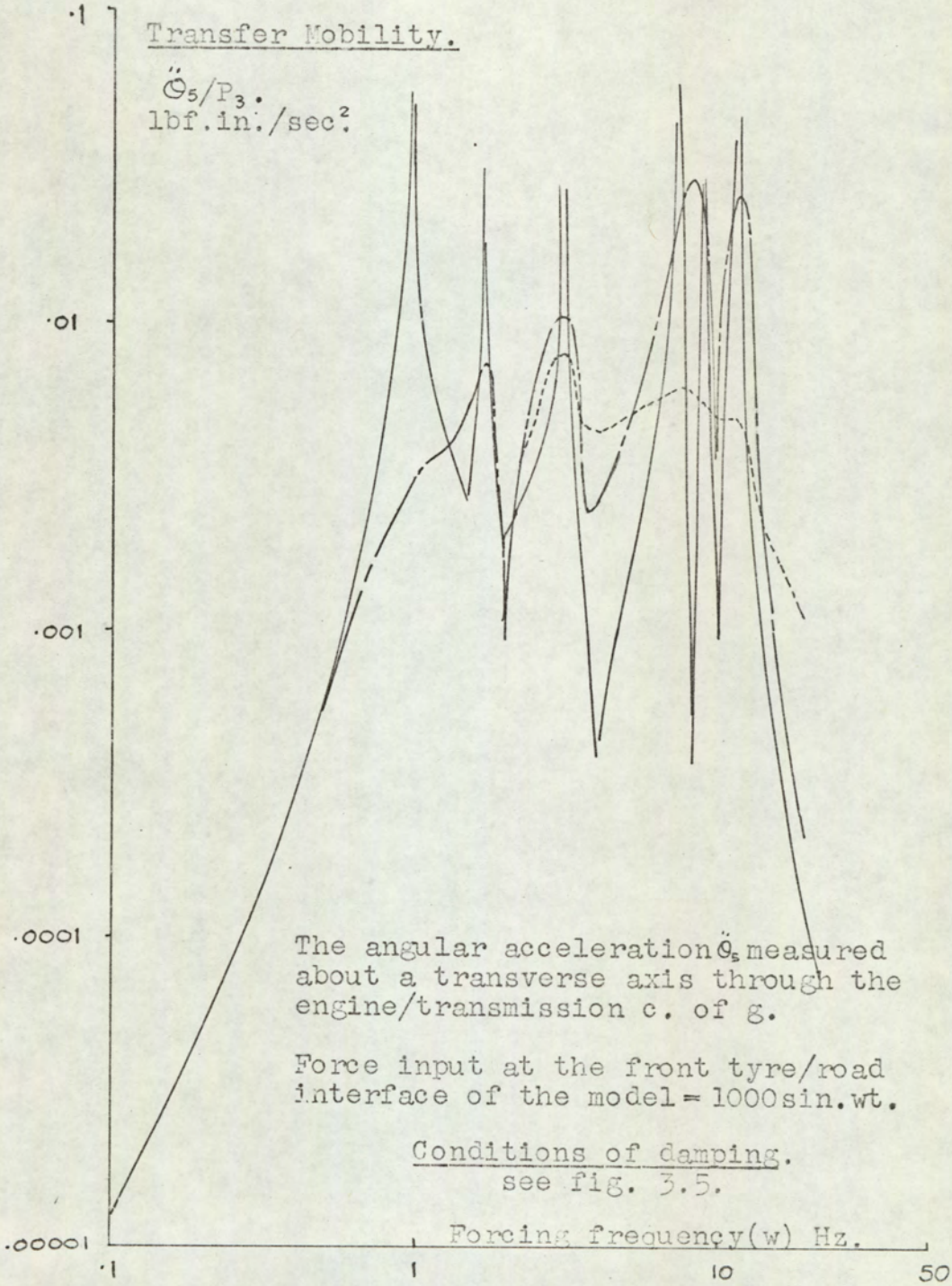

Fig. 3.10. The theoretical 'transfer mobility' $\ddot{\Theta}_6/P_3$ frequency spectrum, for various conditions of model damping.

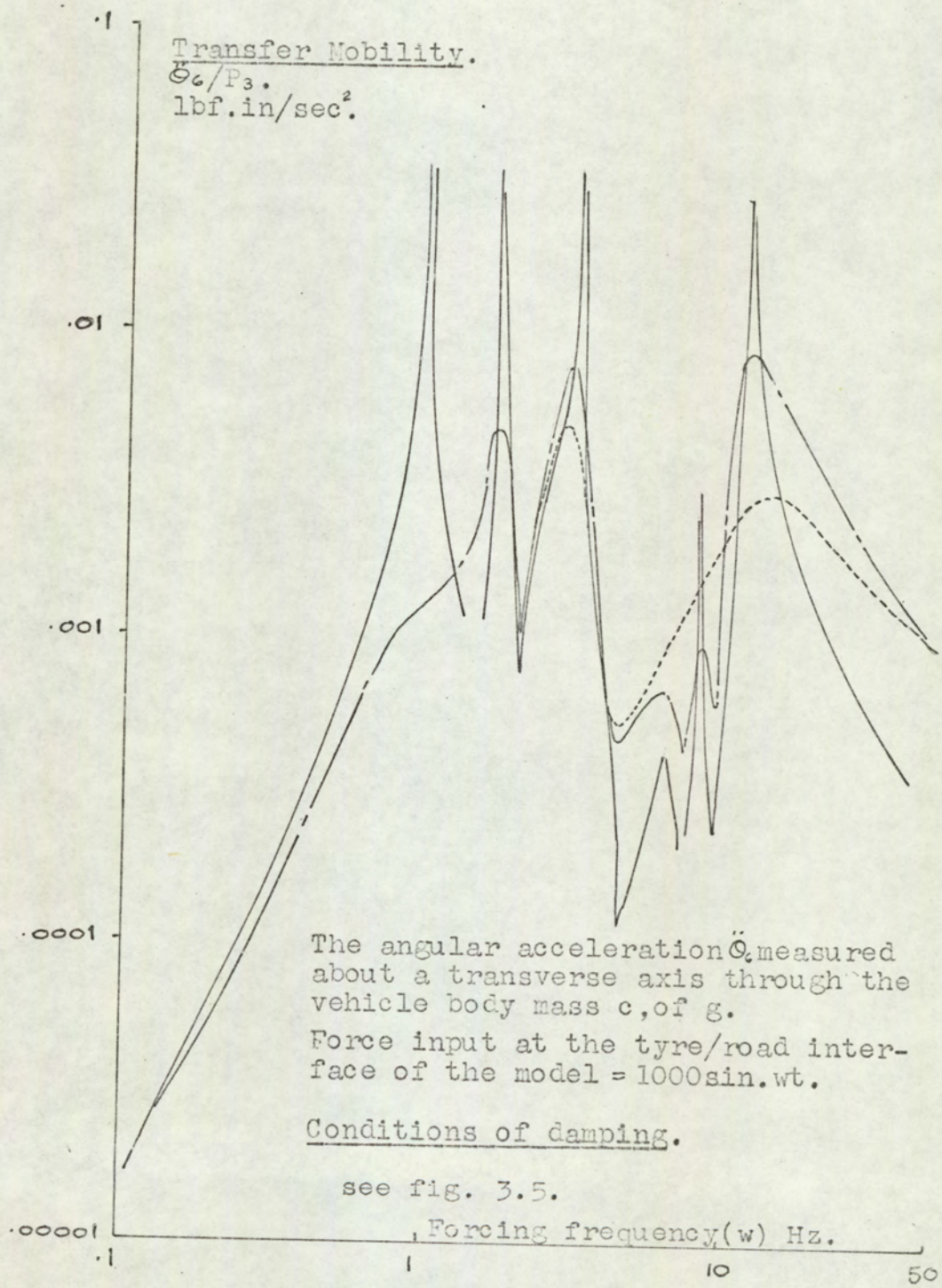

4. EXPERIMENTAL INVESTIGATIONS.

4. EXPERIMENTAL INVESTIGATIONS.

4.1. Experimental Equipment and Procedures.

4.1.1. Experimental Equipment.

In the theory (Chapter 3.6.1.) it is shown that it is possible to obtain the 'transfer mobility' (acceleration response/ force input, at a given forcing frequency), in the frequency domain, for a mechanical structure, from a knowledge of the time histories of the input and the output transients. Acquisition and analysis of the transient data needs a minimum of specialised equipment. These factors make the transient testing technique attractive for obtaining the 'transfer mobility' of the various masses which constitute the motor vehicle, and in particular the 'transfer mobility' of the body mass or the 'vehicle ride transfer characteristic'.

Reference 7 indicates that, irrespective of the excitation at the road wheels of a vehicle as it passes over a random road surface, all the resonant frequencies will be excited to different degrees. Because we are particularly interested in the free vibrations of the engine and their effects on 'riding comfort', excitation at the front road wheels is selected (ref. Chapter 2.2.1.).

The forcing transient chosen for the experimental investigations is a modified step input. This is generated by lifting the front of the stationary vehicle in such a way that the

front suspension is extended. The tyres are just clear of the 'road' surface. The vehicle is then released from an overcentre supporting strut, and the modified step input generated (see fig. 4.2 2.a). The natural frequencies of the resulting response will lie in the frequency range 0 - 15 Hz., if the structural resonances are ignored (see calculations, Chapter A.2.2.,and theoretical results, Chapter 3.7.2. - 3.7.5.).

4.1.1.1. Choice of instrumentation suitable for transient low frequency vibration measurement and recording.

W. Donaghue (reference 5) surveys instrumentation available for vibration measurement and recording. He specifies instrumentation most suitable for vehicle vibration investigations. Stathopoulos (reference 30) and Riedel (reference 27) describe the application of accelerometers, amplifiers, filters and magnetic tape recorders for shock measurement. Ellis and Perry (reference 36, paper 10) review instrumentation for various aspects of vehicle testing, including accelerometers, filters and recorders.

(i) Measurement of Linear Acceleration.

There is a variety of accelerometers, which have been used by various workers, for measuring the vertical acceleration on the motor vehicle.

The accelerometer selected for this research must have a flat frequency response over the frequency range 0 - 50 Hz. and it must be sufficiently sensitive to give a voltage output

at .05g. acceleration. If the transient forcing function is generated at the front tyre/road interface the maximum acceleration will be recorded on the front axle. It will be of the order 6g. maximum.

Piezoelectric accelerometers have been used to measure vehicle vibrations and initially they were tried in this experimental work. They exhibit a flat response from D.C. to 1,000 Hz., providing they are matched with a suitable charge amplifier, which should have a flat response down to D.C. However, it was evident that this type of accelerometer suffers from a high temperature sensitivity and unless adequately shielded large D.C. 'drift' results. It also exhibits a high cross axis sensitivity. For these reasons it was not considered suited for low frequency vibration measurements on the vehicle.

The inductive or differential transformer type accelerometer was not considered for use in this work, because of its inferior low frequency response and because of the A.C. power supply requirement. (Connected to a D.C. supply the instrument will measure 'jerk' or the rate of change of acceleration.)

Strain gauge accelerometers were found to be the most suitable type to measure vehicle body accelerations. They have a flat frequency response over the frequency range 0 to 50 Hz. The transducer is easy to calibrate and has low cross axis sensitivity. The strain gauge accelerometer consists, basically, of a mass which is suspended on a resistance wire. As the

vibrating mass is subjected to changes in acceleration, the suspension wire will undergo resistance changes, and the current output from the instrument will be modulated in accordance with the acceleration level. This accelerometer has a higher sensitivity and output for a given acceleration than the Piezoelectric transducer. The J.L.T. accelerometer chosen for this project has an accuracy of $\pm$ .086% over the frequency range 0 to 50 Hz.

(ii) Measurement of the transient input force function.

The recordings of the acceleration response on a vehicle are of little value unless the level of the input forcing function is known also. For this study of motor vehicle comfort the acceleration response of the body mass is ratioed to the force input, at a given forcing frequency. This ratio is the 'transfer mobility' or the 'vehicle ride transfer characteristic'. R. Woods (reference 33) gives a full account of transient methods of measuring 'mechanical impedance'. In his work the transient forcing function is measured using a Piezoelectric force accelerometer. However, for this research, in which a step input transient is generated, this transducer was not suitable, because its charge is not held for the 'finite' period, during which the step input is applied. A strain gauge type load cell will, however, produce a signal for any period of time when a steady D.C. load is applied to it. The Elliott (Type D- 00) transducer has a flat response from D.C. to 100 Hz. and an accuracy of $\pm$ 1%. For these reasons it was chosen to measure the transient forcing function, at the tyre/road interface, in this project.

(iii) The amplification and recording of the transient signals.

In order to produce a transient signal that can be usefully recorded on a magnetic tape recorder, it is necessary to amplify the transducer outputs. It is usual to couple strain gauge type transducers to carrier amplifiers. For this project Boulton-Paul Aircraft amplifiers have been selected. The carrier amplifier system consists of an oscillator which supplies an A.C. voltage to the transducer. The transducer modulates the carrier signal in accordance with the level of the physical quantity being measured. The signal is then fed into the amplifier for demodulation and amplification. The output signal is converted to D.C. by means of a phase sensitive detector. Accuracy of these amplifiers is quoted as $\pm$ 1%, against a known reference, over the frequency range 0 to 100 Hz.

Because of the decision to use data logging equipment to carry out the necessary analogue to digital conversion of the transient signals, it is necessary to record the signals on magnetic tape. In this project a two channel Elliot-Tandberg F.M. Tape recorder is used. The signal to noise ratio, for this recorder, is quoted as 48 db. with $\pm$ 1% overall accuracy.

Figure 4.1. is a block diagram of the instrumentation used to generate and record the transient vibrating signals.

(iv) Analogue to digital conversion of the recorded signals.

In order that the recorded data can be processed using a digital computer, it is necessary to convert the electrical

analogue of the acceleration response and force input signals, which are recorded on magnetic tape, into digital form. This digital information can then be punched up on tape and accepted by a digital computer.

The data logging equipment available is shown as in figure 4.2. It is capable of sampling at ten times per second maximum. The punch tape machine accepts the signals from the digital voltmeter and gives the digital read-out in punched tape form. The tape can now be accepted by the Elliott 903 Computer for analysis.

4.1.2. Experimental Procedures.

4.1.2.1. Excitation of the vehicle structure and signal recording.

For these vibration tests transient excitation of the vehicle is selected (reference Chapter 2.2.2.). A block diagram of the equipment used for the tests is shown in fig. 4.1.

Figures 4.7. and 4.6. show the instrumentation and vehicle set up to commence a test. For all tests the front of the vehicle is lifted, using a hydraulic jack, onto the over-centre collapsing strut, which supports the vehicle at the front cross member. The length and position of the strut is adjusted so that the vehicle near-side front tyre is just clear of the load cell face plate (see fig. 4.6.). The vehicle is checked for zero inclination in the transverse plane with a spirit level placed on the bonnet. The vehicle is then released from the over-centre supporting strut, by collapsing the strut. A step input is generated

in the plane of the front axle. Before the tests the vehicle static weights at each wheel are measured with the load cell and recorded. Tyre pressures are also checked before the tests (pressure 24 p.s.i. front and rear). Tests are carried out with the vehicle in second gear and with the hand brake on. This is done to maintain a torque resistance in the transmission drive line, as would occur in the 'field'. Because of the height of the load cell above the road surface it is necessary to raise the rear wheels and the off side front wheel, on wooden blocks, to bring the vehicle level in the static condition. To minimise tyre scrub at the front tyres during the drop tests, mineral grease, smeared at the load cell base/concrete floor and the wooden block/ concrete floor interfaces, is effective.

The tape speed selected for all the tests is $3\frac{3}{4}$"/sec. The calibrated output, from the accelerometer channel of the tape recorder, is .5 volts/g. and from the load cell channel of the recorder, 1.4 volts/1000 lbf. The recording time after commencement of the drop is a minimum of 5 seconds, to ensure no signal truncation (see Chapter 3.6.1. and reference 33).

The accelerometer output voltage, from the tape recorder, is calibrated by vibrating the transducer sinusoidally, on a mechanical eccentric rig, over the range of acceleration values of interest.

The load cell output voltage from the tape recorder is calibrated using a pneumatic 'statimeter'.

Vertical acceleration measurements are made at the following stations on the vehicle: the near side front wheel (see fig. 4.6.), the body mass c. of g. (see fig. 4.8.), the engine c. of g. (see fig. 4.9.) and in the near-side front footwell. These measurements are carried out on the test vehicle fitted with hydraulic engine/transmission dampers, with 65 degrees 'Shore' hardness rubber end bushes, the same, with 'Microvon 35' end bushes and for the vehicle without hydraulic engine/transmission dampers. For installation of the dampers see figs. 4.3., 4.4. and 4.5. The excitation and recording procedure for each test is the same.

4.1.2.2. <u>The processing of the records from the practical tests, to obtain the'experimental transfer mobility' characteristics for the test vehicle</u>.

The equipment used to transfer the recorded data from its analogue to digital form is shown in fig. 4.2. From the Fourier Transformation theory (references 15 and 33), in order to reduce 'aliasing' errors, it is assumed that one oscillation in the time plane can be defined by no less than four points. To satisfy this condition it is necessary to slow down the tape recorded signal, because the maximum sampling rate of the data logging equipment is five times per second per channel for a two channel set-up. Using the record and play-back facilities of both the Elliott-Tandberg and an Ampex Tape recorder it is possible to slow the original records down, in the time domain, by a factor of sixty-four. This gives a sampling rate of five times sixty-four = three hundred and

twenty times per second. The maximum frequency, for which accurate analysed results can be expected = $(2.095/2.\pi)$ x 320 = 106 Hz. (reference 15). All the transient records are handled in this way. The tape punch machine produces five-hole tape in Elliott 803 telecode.

Analysis of the tapes, to obtain the 'transfer mobilities' in the frequency domain from the records in the time domain, is carried out using an Elliott 903 computer. This machine is programmed to handle 803 data tapes which are punched up on the data logger. Because of the time taken to produce the Fourier Transform of the input and response data for each test (approximately $1\frac{1}{2}$ hours), the acceleration response channel results, only, are computed for each test (programme shown in fig. 4.11.). The force response is computed for one test result tape only, since the force input is the same for each test (programme shown in fig. 4.10.). The 'transfer mobility' is calculated for each test by ratioing the relevant computed acceleration response spectrum to the computed force input spectrum, over the frequency range 0 to 30 Hz.

4.1.2.3. Determination of the practical hydraulic and Coulomb damping characteristic of the vehicle.

(i) Hydraulic damping characteristic.

The hydraulic damping characteristics of the engine dampers, front suspension and rear suspension dampers are obtained by taking the dampers from the vehicle and then setting them up on

an S.H.M. 'Carding Machine'. This machine is designed to record the variation of the damper resistance over a complete S.H.M. cycle. A complete resistance build-up characteristic is obtained by 'carding' over a range of cycle speeds and then measuring the card to obtain the maximum resistance (bump and rebound) for each test speed. The peak velocity is calculated from a knowledge of the test speed and stroking amplitude. The characteristics are shown in figures 4.12 to 4.14.

(ii) Coulomb damping characteristics.

The Coulomb damping characteristics of the vehicle suspensions are obtained by setting each wheel of the vehicle, in turn, on the load cell used for the transient tests and then recording the normal wheel load and vertical tyre deflection for increments of vertical body displacement. The body of the vehicle is given increments of vertical deflection by raising axles of the vehicle, in turn, on a hydraulic jack. Figures 4.17 and 4.18. show the test vehicle suspension hysteresis curves or Coulomb damping characteristics.

(iii) Determination of other vehicle parameters.

The static vertical spring rates of the test vehicle tyres were supplied by courtesy of the Dunlop Company. Curves are shown in fig. 4.15.

A graph showing the variation of the vehicle tyre damping co-efficient against vehicle forward speed is shown in fig. 4.16. This curve was also supplied by courtesy of the Dunlop Company.

The vertical spring rate characteristics of the engine mounting rubbers (see figs. 4.19. to 4.21.) are obtained by setting the mounts up in fixtures in the same attitude as they are installed on the test vehicle and measuring the load/deflection characteristic for compression and relaxation of the mounts.

The values of the moments of inertia of the engine/transmission mass and body mass (less the engine/transmission mass) about transverse axes through their respective centres of gravity were supplied by courtesy of the Rootes Motor Company.

The remainder of the parameters were taken from reference 34.

4.2. Experimental Results.

The experimental results are presented in graphical form. Figs. 4.12. to 4.32. are the experimental characteristics, obtained for the hydraulic engine and suspension dampers, as fitted to the test vehicle.

Figs. 4.17. and 4.18. are graphs showing the 'static' hysteresis present in the test vehicle suspensions.

Fig. 4.16. is a graph showing the variation of the damping co-efficient, with vehicle forward speed, of the Dunlop C41 (cross ply) tyre as fitted to the test vehicle.

Fig. 4.15. is graphs showing the variations of the vertical rate, with inflation pressure, for the C41 tyre.

Figs. 4.19. to 4.21. are the static rate characteristics of the test vehicle engine and transmission mounting rubber springs.

Figs. 4.22. to 4.28. are sample traces, taken with an ultra-violet recorder from the tape recorded results. The figures show transient force input signals and transient response signals for a range of experimental tests on the vehicle.

Figs. 4.29. to 4.32. are the experimental 'transfer mobilities' which have been computed for different parts of the test vehicle. The results shown have been obtained for a 'standard' vehicle with no hydraulic engine/transmission damping, and for the vehicle fitted with hydraulic engine dampers with characteristics as shown in Fig. 4.12. Tests on the vehicle, fitted with hydraulic engine dampers, were carried out using dampers fitted with:

(a) 65 degrees 'Shore' hardness rubber end fitting bushes.

(b) Polyurethane foam end fitting bushes.

Dampers 64054600 AA X 016 and 64054600 AA X 017 were fitted across the front mounts and damper 64054600 across the rear mount (see figs. 4.3. to 4.5.).

4.3. Discussion of the experimental results.

4.3.1. The test vehicle parameters.

The rate characteristics for the hydraulic engine/transmission dampers used for the experimental tests are approximately linear, compression and extension rates being equal (see fig. 4.12.).

The rate of the hydraulic dampers installed across the front mounts is 20 lbf./in./sec. per damper (installed on the vehicle). The rate of the hydraulic damper across the rear mount is 3.83 lbf./in./sec. (installed on the vehicle).

The rate characteristics of the hydraulic suspension dampers are non-linear (see figs. 4.13. and 4.14.). The characteristics show a differential resistance ratio extension to compression. This differential ratio varies from 1:1 to 3.5:1 over the velocity range zero to 35"/Sec. for the front hydraulic suspension strut, and from 1:1 to 2:1, over the same velocity range, for the rear hydraulic damper. Chenchanna, (reference 3), reports that the best vehicle riding comfort is achieved with a compression rate equal to .4 times the extension rate, and best road holding or riding safety with the extension rate equal to the compression rate. The equivalent linear rates of the non-linear suspension dampers are calculated using Simpson's Rule (see Appendix A.2.1.). The equivalent rate of each front suspension strut is 7.9 lbf./in./sec. (installed on the vehicle). The equivalent rate of each rear suspension damper is 5.6 lbf./in./sec. (installed on the vehicle).

Reference to fig. 4.16. shows that the tyre damping co-efficient is 5 lbf./in./sec. for zero forward vehicle speed. The co-efficient approaches a value of 1 lbf./in./sec. at 25 m.p.h. forward speed. Since the tests are carried out on the stationary vehicle the former value is taken for substitution into the

mathematical model.

The rate characteristics of all the hydraulic dampers used on the test vehicle are obtained by stroking the dampers on a fixed stroke with S.H.M. for a range of crank speeds, using a Girling Damper 'carding' machine (see Chapter 4.1.2.3.).

The friction present in the vehicle suspensions obviously contributes to the system damping. Figs. 4.17 and 4.18 are graphs of the front and rear suspensions static hysteresis as measured on the test vehicle (see procedure used to obtain the characteristics in Chapter 4.1.2.3.). As was to be expected, because of the suspension geometry, the 'stiction' in the McPherson strut front suspension has a higher value than the 'stiction' measured in the leaf spring rear suspension. The values of 'stiction' being $\pm$ 50 lbf. mean and $\pm$ 25 lbf. mean 'per wheel' respectively. These values represent viscous damping rates of 3.74 lbf./in./sec./axle and 1.87 lbf./in./sec./axle respectively (see Appendix A.2.1.).

The rate characteristics of the engine and transmission rubber mounts are shown in figs. 4.19. to 4.21. The procedure for obtaining the characteristics is given in Chapter 4.1.2.3.(iii). The total 'static' hysteresis of the front engine mounts is $\pm$ 50 lbf. mean. The total 'static' rate, in the z direction, as installed on the vehicle, is 2300 lbf./in. The 'static' hysteresis of the rear transmission mount is $\pm$ 20 lbf. mean and its 'static' rate is equal to 450 lbf./in. These results indicate that quite

high heat build-ups may be expected in these mounts, under dynamic conditions, because of the high hysteresis.

4.3.2. Transient excitation data analysis.

Sample results, in the time domain, obtained from a range of transient excitation tests on the vehicle are shown in figs. 4.22. to 4.28. These traces are obtained using an ultra-violet strip paper recorder, connected to the output of the Elliott-Tandberg Tape Recorder.

From these sample recordings, it is evident that the forcing transient records show reasonable repeatability, for all tests, to within the limits of experimental accuracy.

In order to obtain the 'transfer mobilities', in the frequency domain, for various parts of the vehicle, it is necessary to ratio the Fourier spectrum of the transient response records to the Fourier spectrum of the force input transient. (The acceleration spectrum must be referred to the spectrum of the force input, to have any meaning, when comparing the acceleration response of the vehicle for different conditions of damping.)

Fig. 3.4. shows the Fourier spectrum of a typical force input transient as recorded in tests on the vehicle. This spectrum is obtained using the procedure described in Chapter 4.1.2.2. The result is used to ratio all acceleration spectra obtained in this thesis. The typical force spectrum of final amplitude (A), as recorded in the work, is compared with the theoretical force spectrum for a step input of steady state amplitude A (reference 14)

in fig. 3.4. The results are similar, except for the increase in amplitude at the superimposed natural frequency of the experimental force transient.

* Note: To obtain a reasonable number of points on the experimental force spectrum shown in fig. 3.4., it is necessary to

(a) sample the force response for a period of 3 minutes real time using the procedure in Chapter 4.1.2.2. (the Nyquist frequency of the response spectrum = 4π /(real time sampled));

(b) to perform the transform at 0.1 Hz. increments in the region of the natural frequency of the force input transient.

4.3.3. The experimental 'transfer mobility' characteristics.

Definition - see Introduction (iii).

All the 'transfer mobility' characteristics are computed, from the recordings in the time domain, for three conditions of system damping (see Chapter 4.2.).

1. The experimental 'transfer mobility' referred to the vehicle body mass or 'vehicle ride transfer' characteristics.

This characteristic is shown in fig. 4.30. The acceleration response is measured in the z direction at the point of intersection of the vehicle longitudinal axis and a transverse axis through the sprung mass c. of g. (see fig. 4.8.).

Resonances can be detected at 1.5, 3.0, 12, 16 and between 18 and 20 Hz.

The resonance at 1.5 Hz. can be identified as the natural frequency, associated with the dominant mode of vibration, of the 'sprung mass' on the suspension springs. This is a vibration mode with a dominant pitch content (see Appendix A.2.4.).

The resonance at 3.0 Hz. is the resonant mode of vibration associated with the vehicle 'spring mass' vibrating on the tyre springs.

The resonance at 12 Hz. is the resonant mode of vibration associated with the front unsprung mass vibrating, in the z direction, on the tyre and suspension spring.

The resonance at 16 Hz. is the natural frequency of the engine/transmission mass. This is a bounce mode in the z direction with very little pitch content (see Appendix A.2.3.).

The natural frequency that occurs between 18 and 20 Hz. is the frequency of body front end 'shake' mode which is produced when bending of the vehicle body is excited about a transverse axis through the vehicle.

The effect of hydraulically damping the engine/transmission mass upon the vehicle 'ride transfer' characteristics is obvious. At the 12 Hz. resonance the vehicle, tested with hydraulic dampers fitted with (a) hard natural rubber (65 degrees 'Shore' hardness) and (b) polyurethane foam end fitting bushes, shows a 50% reduction in the body mass 'transfer mobility', over the standard vehicle with no hydraulic engine/transmission damping.

At the 16 Hz. resonance a 70% reduction in amplitude is noted for the vehicle tested with the engine/transmission dampers fitted with the 65 degrees 'Shore' hardness rubber fixing bushes. The reduction in amplitude at this frequency for the vehicle fitted with the same dampers with polyurethane foam end bushes is 62%.

At the 'shake' frequency, the vehicle equipped with the engine dampers with 65 degrees 'Shore' hardness rubber fixing bushes shows a 30% increase in riding comfort over the standard vehicle. At this resonant frequency the effect on ride, produced by the engine dampers with polyurethane fixing bushes, is negligible. A certain amount of off resonance amplitude boosting is evident with hydraulic engine/transmission damping. The extra damping does not modulate the amplitude of the resonant modes at 1.5 Hz. and 3 Hz.

The 'vehicle ride transfer' characteristics shown in fig. 4.31. are computed for acceleration responses measured in the z direction in the near side front footwell. The results show the same trends as those computed from measurements of the vertical acceleration made at the vehicle centre of gravity. The apparent reduction in the amplitude with hydraulic dampers with polyurethane end bushes, at the 1.5 Hz. resonance, for these tests is produced as a result of truncation of the particular acceleration data record which occurred during play-back.

2. The experimental 'transfer mobility' referred to the vehicle engine/transmission mass.

This characteristic is shown in fig. 4.29. for the same three conditions of system damping as described in Chapter 4.3.2. The resonances occur at the same frequencies. The 'shake' mode is not evident between 18 and 20 Hz. The amplitude at the 1.5 Hz. resonance is unmodulated with the hydraulic engine/transmission damping. Some off-resonance amplitude boosting is produced with the increased damping. The amplitudes at 12 Hz. and 16 Hz. are modulated by 62% and 30%, respectively, for the vehicle tested with hydraulic engine/transmission dampers with 65 degrees 'Shore' hardness fixing bushes, as compared with the standard vehicle with only inherent engine/transmission damping. The reductions in amplitude for the vehicle tested with the same hydraulic engine/transmission dampers, but with polyurethane foam end bushes are 45% and 17%, respectively.

3. The experimental 'transfer mobility' referred to the front 'unsprung' mass.

A study of these characteristics (fig. 4.3 2.),shown for the same conditions of damping as above, indicates resonances at 1.5, 3, 10, 12, 15 and 19 Hz. Hydraulic engine/transmission damping does not modulate the 'transfer mobility' over the frequency range studied.

Subjectively it was noticed, when driving the motor

car fitted with hydraulic engine/transmission dampers with the different types of damper end fitting rubbers, that noise transmission to the passenger compartment is increased with the natural rubber, 65 degrees 'Shore' hardness end bushes, compared with the car fitted with hydraulic engine/transmission dampers with polyurethane foam end bushes.

The 'transfer mobility' characteristics could equally well have been computed by referring the responses to the Fourier spectrum of a step displacement input.

From the experimental work described in Appendix A.5. it is shown that if a damper is excited at its own natural frequency on its mounting rubbers, at low amplitudes, the damper will become ineffective, because all displacement is taken up by the end fitting rubbers. For the engine dampers used in this project this is not a problem because their natural frequency on the mounting rubbers will be in the frequency range 80 to 100 Hz.

4.4. Conclusions from the experimental results.

The experimental 'transfer mobility' curves, which are computed for three different conditions of engine/transmission damping, from records made in the time domain, show that the vibration behaviour of the motor vehicle is improved when the damping across the mounting rubbers is increased above the inherent value. For this work the value is increased from .05 'critical'

to .43 'critical', referring to the pure bounce mode of the engine/transmission mass on its mounts (body structure is considered rigid).

Engine dampers, fitted with 65 degrees 'Shore' hardness end fixing rubbers, are more effective in reducing the 'secondary ride' resonant amplitudes in the motor vehicle than those fitted with polyurethane foam fixing bushes. This is because, at the natural frequency of the engine/transmission mass on its mounts, displacements will be relatively small and polyurethane will accommodate the amplitudes of displacement rather than transmit them to the damper movement, i.e. the dampers become ineffective. On the other hand, engine dampers, with rubber end fixing bushes, produce more noise transmission from the engine to the body than the polyurethane bushes.

The riding comfort of the vehicle fitted with hydraulic engine/transmission dampers, with 65 degrees 'Shore' hardness natural rubber end fixing bushes to give a damping factor of .43 'critical', in the s direction, will produce an increased riding comfort of the order of some 30% to 60%, over the frequency range 10 Hs. to 20 Hs. There will be some increase in noise transmission to the passenger compartment, compared with a vehicle with inherent engine damping only. The rates of engine and transmission mounting rubbers should be designed in accordance with the theory, in Appendix A.4., to arrive at these results. Better 'shake' control

would result from an engine/transmission damping factor of .22 (see Appendix A.4.), but this small increase would not produce adequate control of the engine under severe vibration input conditions. (The fact that the original vertical rate of the engine/transmission mounting rubbers, as fitted to the test vehicle, was the same as the theoretically calculated optimum value to control body 'shake' was purely coincidental.)

The transient excitation, in the time domain, and subsequent Fourier Transformation techniques, used in this project, to obtain the vehicle 'transfer mobility' characteristics, in the frequency domain, is an addition to the known vehicle vibration testing techniques used today. This method requires less capital outlay for instrumentation compared with the requirements for excitation of the motor vehicle in the frequency domain.

Although the results reported do not enable a direct comparison with published comfort criteria, to give an absolute value of riding comfort, they do enable comparisons of relative 'riding comfort' to be made about a vehicle for different damping conditions.

A study of the acceleration response traces made in the time domain (figs. 4.22. to 4.28.) indicates that the effect of making changes to the system damping, upon the body mass acceleration response, can be measured from these recordings.

Therefore, if only the trends produced by a change in

system damping are of interest, it would be sufficient to study the acceleration response recordings, made in the time domain.

Fig. 4.1

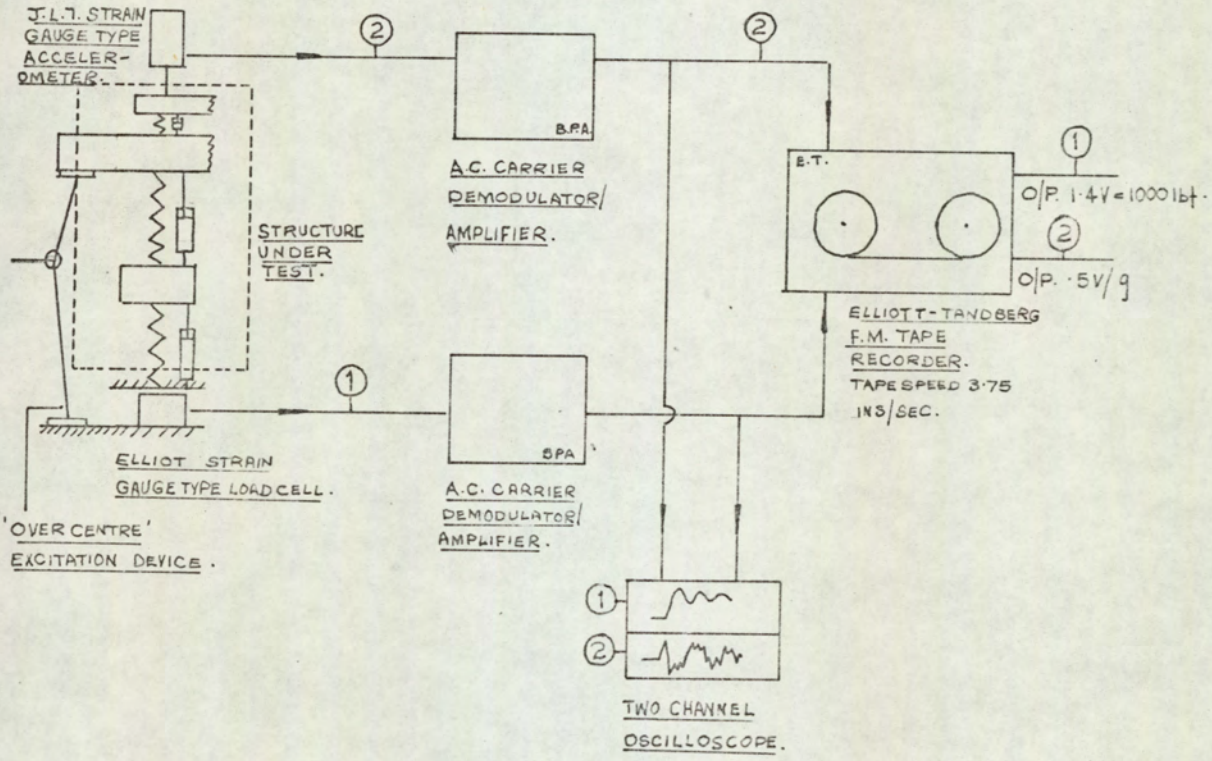

A block diagram of the instrumentation used to generate and record transient vibration signals in the laboratory.

Fig. 4.2

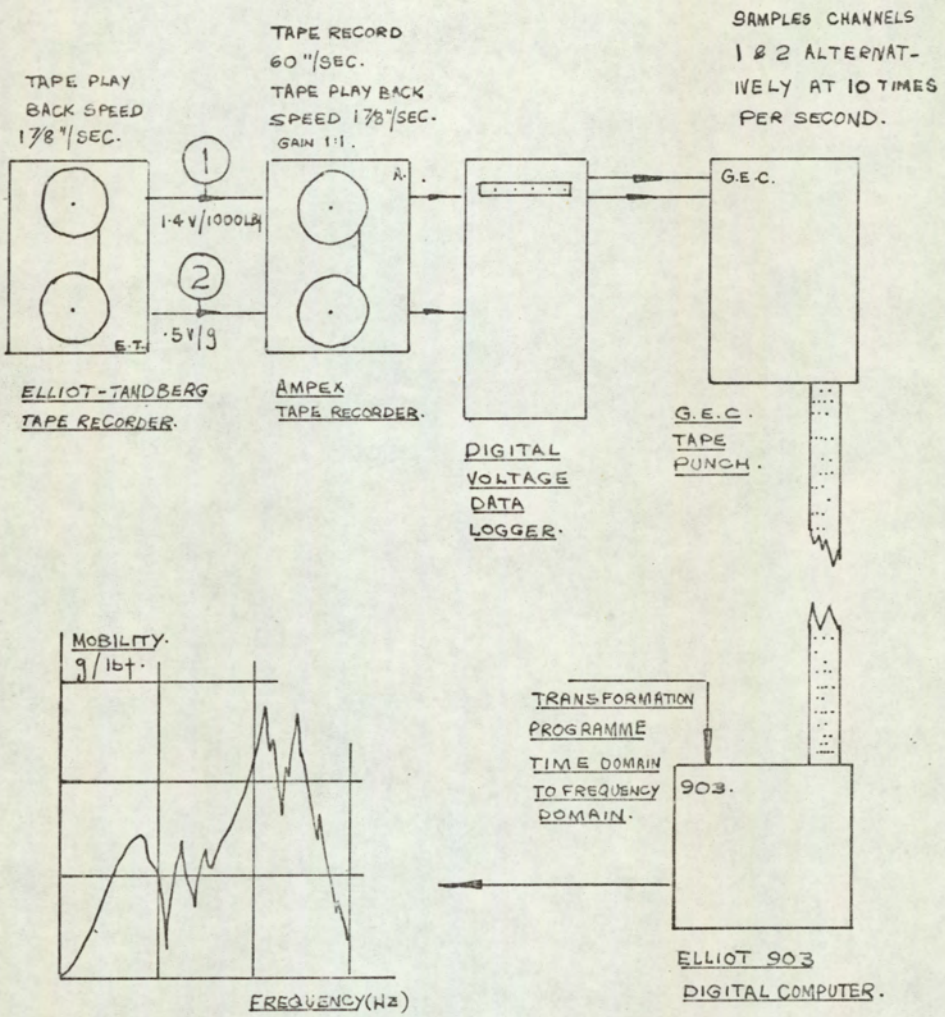

A block diagram of the instrumentation used to perform the analogue to digital conversion of the experimental transient recordings.

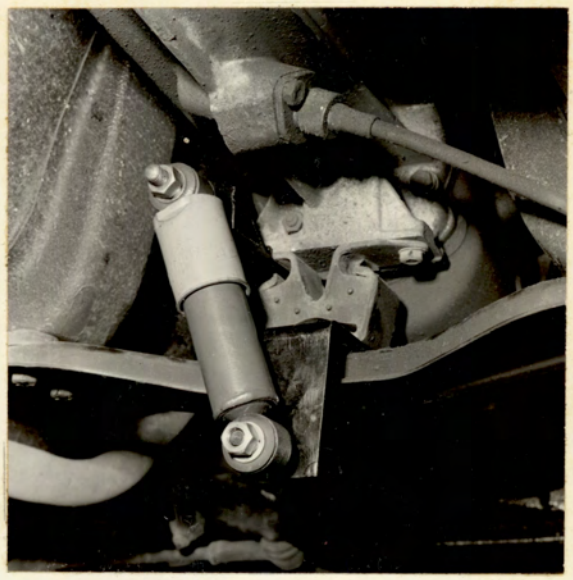

FIG. 4.3 INSTALLATION OF HYDRAULIC DAMPER, IN PARALLEL WITH THE REAR ENGINE/TRANSMISSION MOUNT.

FIG. 4.4 INSTALLATION OF FRONT NEAR SIDE HYDRAULIC ENGINE/ TRANSMISSION DAMPER.

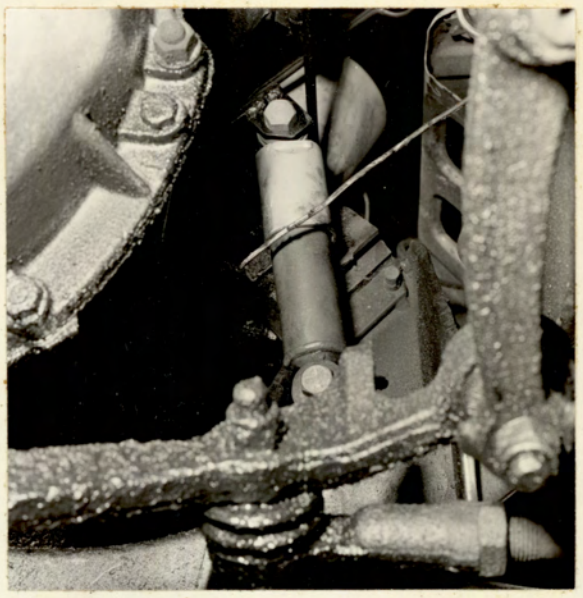

FIG. 4.5 INSTALLATION OF FRONT OFF SIDE HYDRAULIC ENGINE/TRANSMISSION DAMPER.

FIG. 4.6 VEHICLE SET UP TO COMMENCE TEST.

FIG. 4.7. INSTRUMENTATION FOR DATA ACQUISITION.

FIG. 4.8 ACCELEROMETER TO MEASURE THE VERTICAL ACCELERATION ON THE VEHICLE BODY.

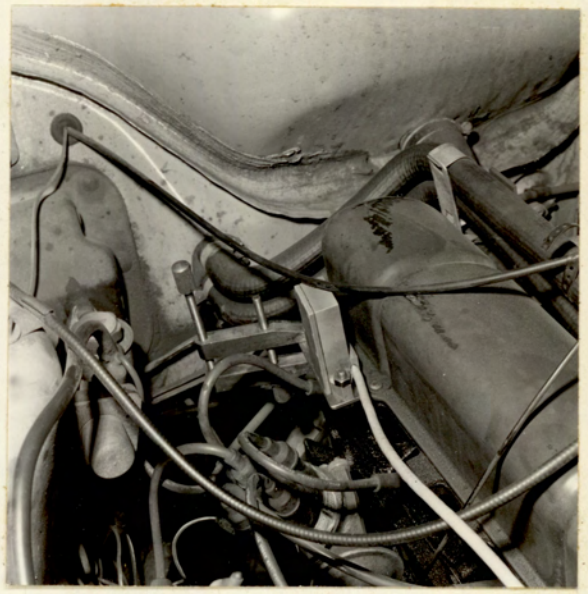

FIG. 4.9 ACCELERATION TO
MEASURE THE VERTICAL ACCELERATION
ON THE VEHICLE ENGINE/TRANSMISSION

FIG.4.10. THE COMPUTER PROGRAMME USED TO TRANSFORM THE DATA LOGGED INFORMATION, OF THE RECORDED FORCE INPUT TRANSIENT, FROM THE TIME DOMAIN TO THE FREQUENCY DOMAIN.

```
DAMP17 MOD3C  RESPONSE TRANSFORMATION  TIME DOMAIN
"BEGIN"                                          TO FREQUENCY
"REAL" X,S1,S2,SUM1,SUM2,B,T,RAV,FF,C1,C3,C4;      DOMAIN;
"INTEGER" P,N;
"ARRAY" A2[1:1200];
"SWITCH" SS:=DATA,LOOP;
"READ" T;
RAV:=0;    N:=0;
DATA: "READ" C3,C4;
RAV:=RAV+C4;
N:=N+1;    "IF" N<15 "THEN" "GOTO" DATA;
RAV:=RAV/15;
N:=0;
LOOP:
"READ" X;
"IF" X < 25000 "THEN"
"BEGIN"
  N:=N+1;   "READ" A2[N];
  A2[N]:=(A2[N]-RAV)/10000;
  "GOTO" LOOP;
"END";
P:=N;
"FOR" B:=.00491 "STEP" .00491 "UNTIL" .0105,
          .0108 "STEP" .00098 "UNTIL"  .015,
          .0196 "STEP" .00491 "UNTIL" .198,
          .245 "STEP" .0491 "UNTIL" .444 "DO"
"BEGIN"
SUM1:=SUM2:=0;
"FOR" N:=1 "STEP" 1 "UNTIL" P "DO"
"BEGIN"
   S1:=A2[N]*T*SIN(B)*COS((2*N-1)*B)/B;
   S2:=-A2[N]*T*SIN(B)*SIN((2*N-1)*B)/B;
   SUM1:=SUM1 + S1;    SUM2:=SUM2 + S2;
   "END";
FF:=SQRT(SUM1*SUM1 + SUM2*SUM2);
C1:=ARCTAN(SUM2/SUM1);
"PRINT" FREEPOINT(5),B,PREFIX('   '),FF,C1;
"END"
"END";
Z
```

FIG. 4.11 THE COMPUTER PROGRAMME USED TO TRANSFORM THE DATA LOGGED INFORMATION OF THE RECORDED ACCELERATION RESPONSE TRANSIENTS, FROM THE TIME DOMAIN TO THE FREQUENCY DOMAIN

```
DAMP17 MOD2C  RESPONCE TRANSFORMATION   TIME DOMAIN TO
      READ A1 ONLY PERFORM ANALYSIS ON A1 ONLY; FREQUENCY
"BEGIN"                                              DOMAIN,
"REAL" X,S3,S4,SUM3,SUM4,B,T,VAV,SUMVAV,FA,C2,C3,C4;
"INTEGER" P,N;
"ARRAY" A1[1:1200];
"SWITCH" SS:=DATA,LOOP;
"READ" T;
VAV:=0;   N:=0;
DATA: "READ" C3,C4;
VAV:=VAV+C3;
N:=N+1;    "IF" N<15 "THEN" "GOTO" DATA;
VAV:=VAV/15;    N:=0;
LOOP:  "READ" X;
"IF" X<50000 "THEN"
"BEGIN"
   N:=N+1;    A1[N]:=X;
  "READ" X;  A1[N]:=(A1[N]-VAV)/10000;
   "GOTO" LOOP;
"END";
P:=N;
"FOR" B:=.00491 "STEP" .00491 "UNTIL" .0105,
         .0108 "STEP" .00098 "UNTIL" .015,
         .0196 "STEP" .00491 "UNTIL" .198,
         .245 "STEP" .0491 "UNTIL" .444 "DO"
"BEGIN"
SUM3:=SUM4:=0;
"FOR" N:=1 "STEP" 1 "UNTIL" P "DO"
"BEGIN"
   S3:=A1[N]*T*SIN(B)*COS((2*N-1)*B)/B;
   S4:=-A1[N]*T*SIN(B)*SIN((2*N-1)*B)/B;
   SUM3:=SUM3 + S3;    SUM4:=SUM4 + S4;
"END";
FA:=SQRT(SUM3*SUM3 + SUM4*SUM4);
C2:=ARCTAN(SUM4/SUM3);
"PRINT" FREEPOINT(5),B,PREFIX('   '),FA,C2;
"END"
"END"
"END";
%
```

Fig. 4.12

CHARACTERISTICS OF VARIOUS HYDRAULIC ENGINE DAMPERS

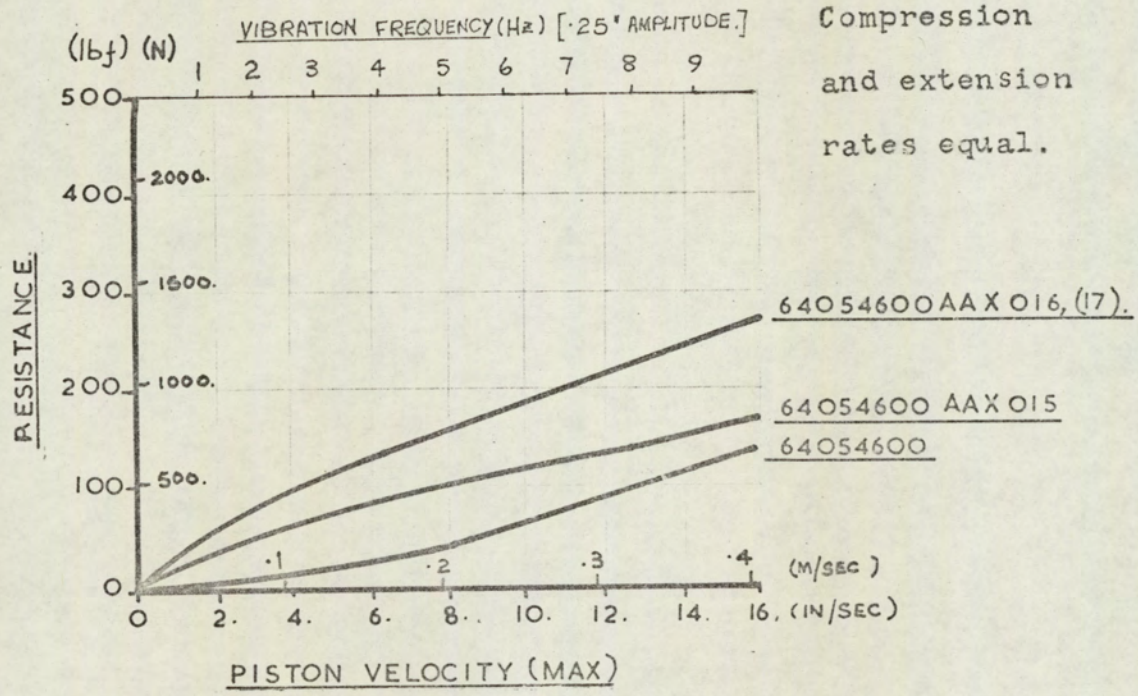

Fig. 4.13.

CHARACTERISTIC OF HYDRAULIC DAMPER BETWEEN FRONT AXLE & BODY.

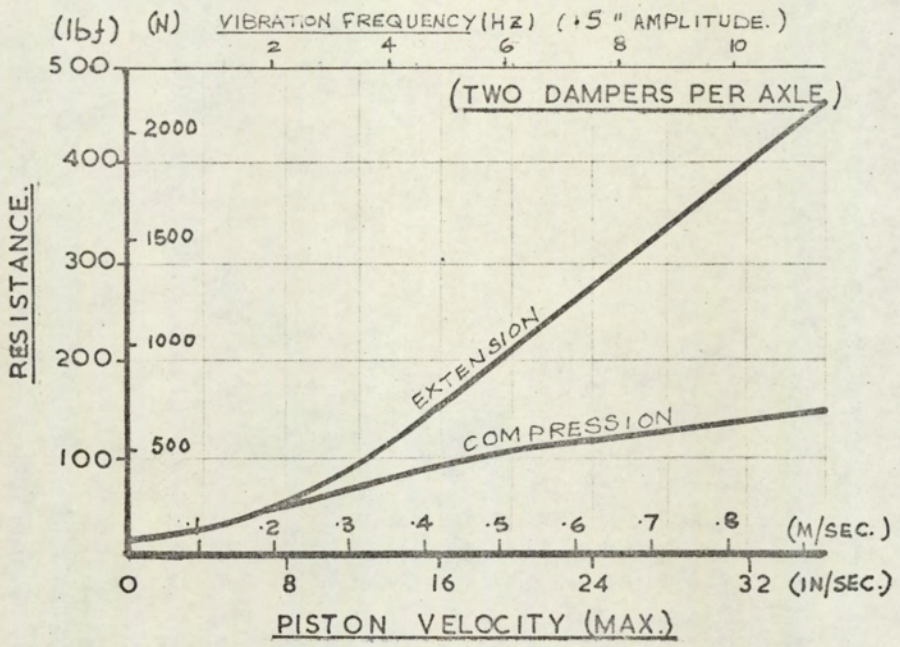

Fig. 4.14.

CHARACTERISTIC OF HYDRAULIC DAMPER BETWEEN REAR AXLE & BODY.

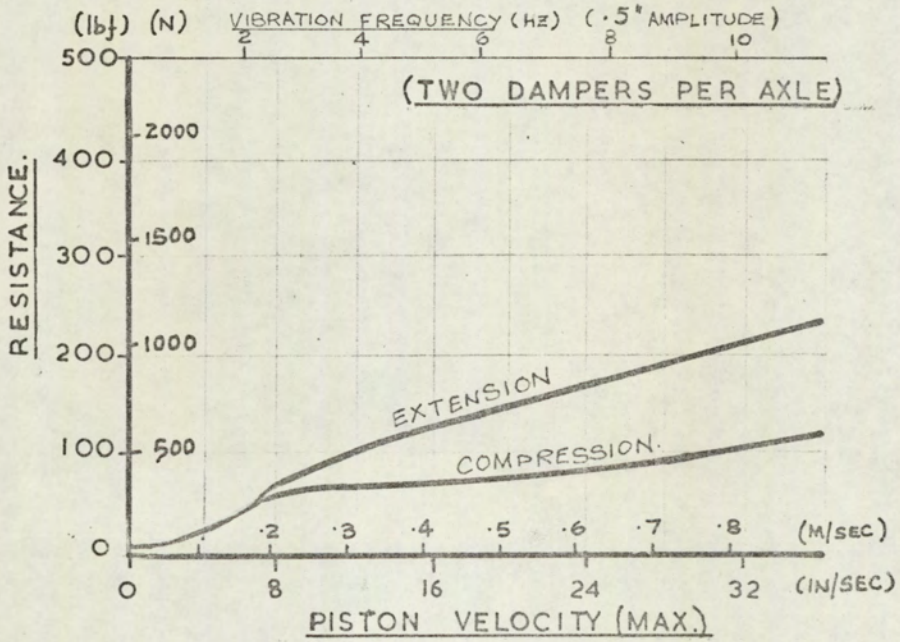

Fig. 4.15.

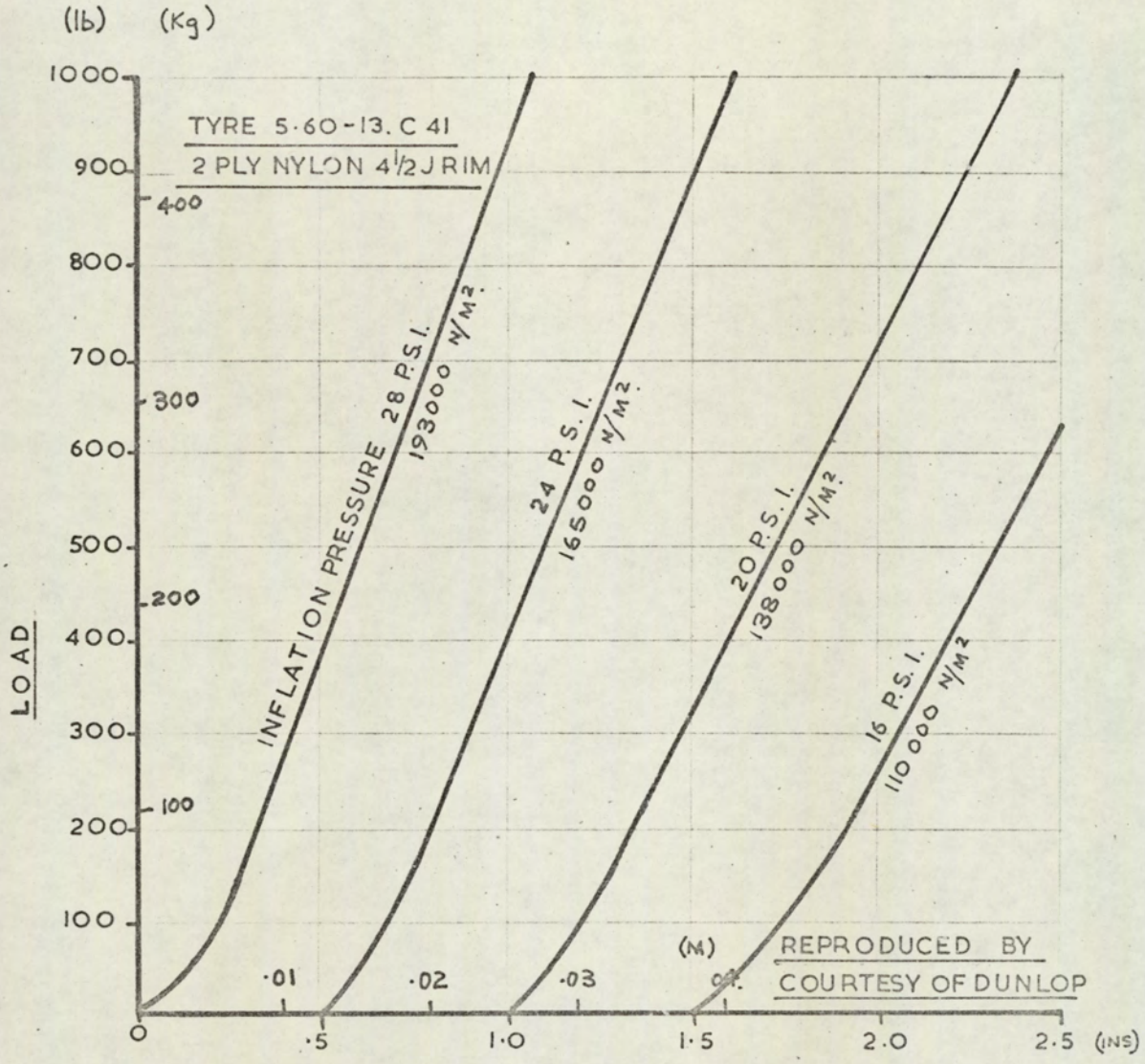

DEFLECTION IN 'Z' DIRECTION NORMAL TO THE AXLE.

VARIATION OF VERTICAL TYRE RATE WITH INFLATION PRESSURE (WHEEL STATIC.)

Fig. 4.16.

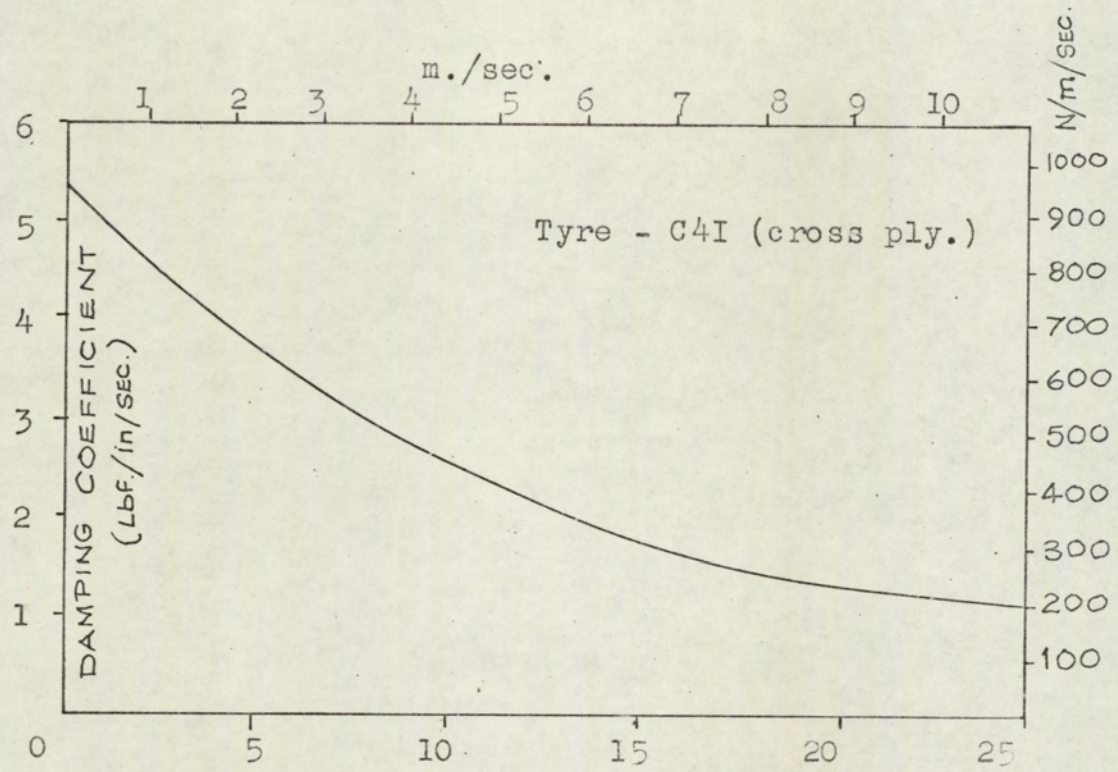

A graph showing the variation of the tyre damping coefficient with the forward speed of the vehicle.

Reproduced by courtesy of Dunlop Ltd.

Fig. 4.17.

Graphs showing the 'static hysteresis' measured in the front suspension of the test vehicle.

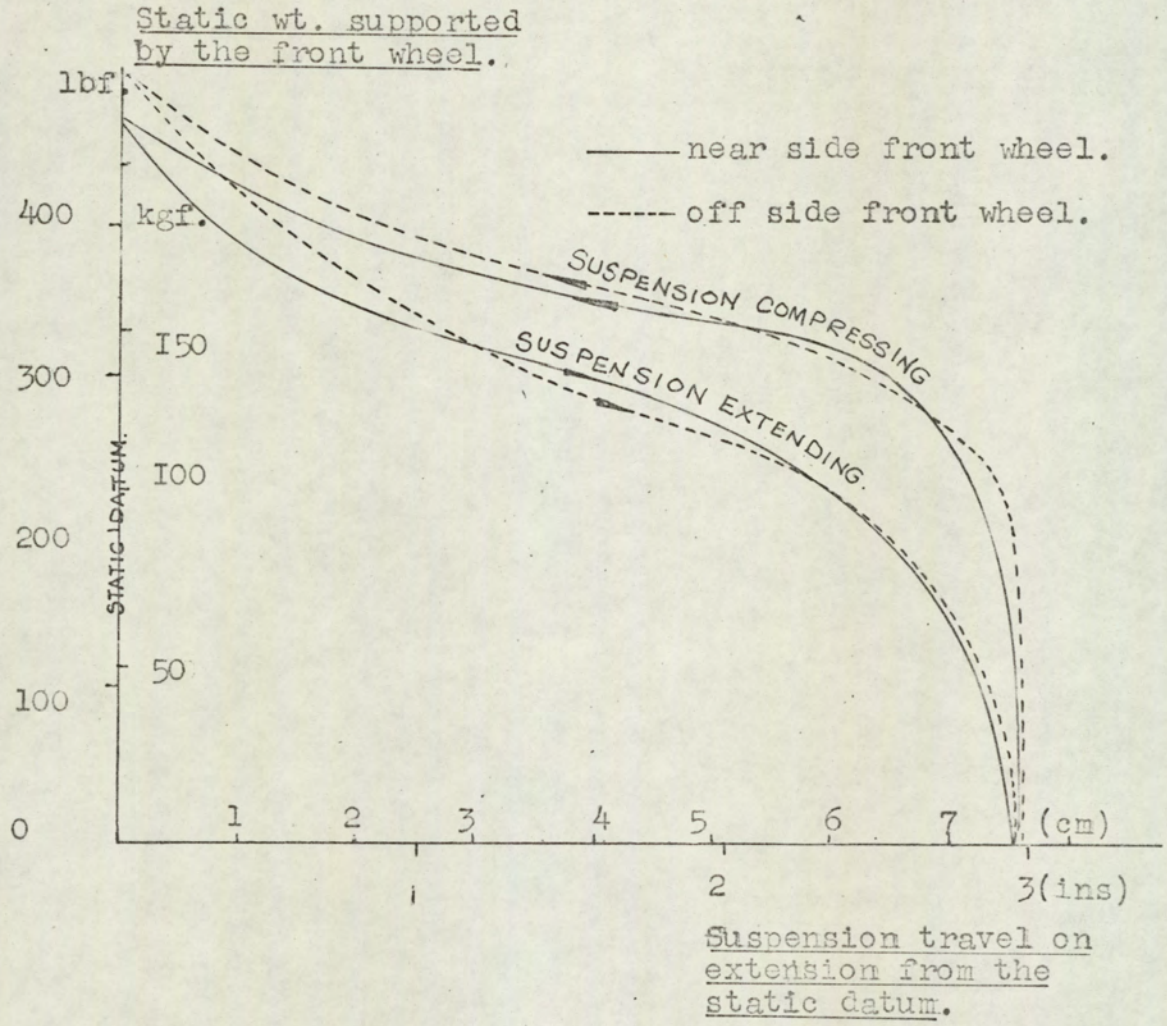

Fig. 4.18.

Graphs showing the 'static hysteresis' measured in the rear suspension of the test vehicle.

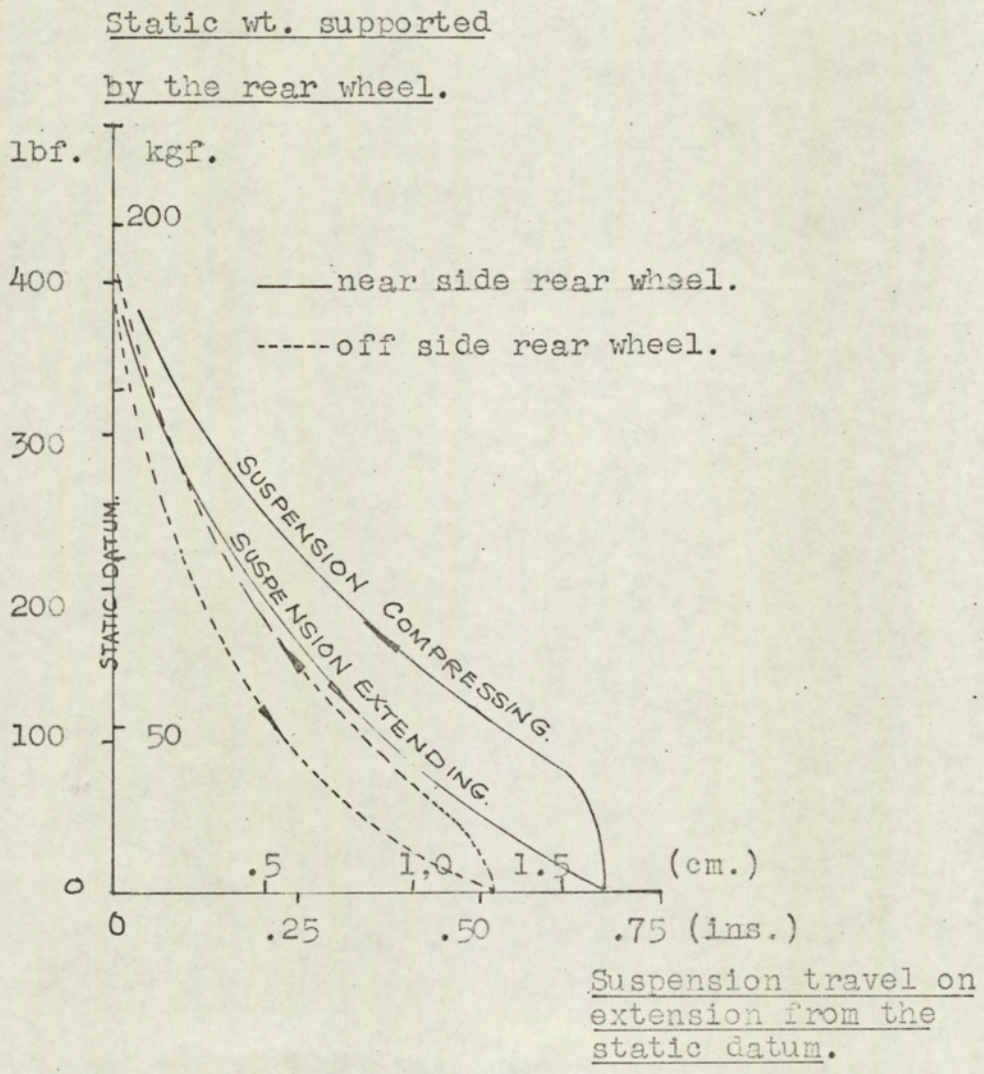

Fig.4.19.

The static vertical rate of the off side engine/transmission mounting rubber as installed on the test vehicle.

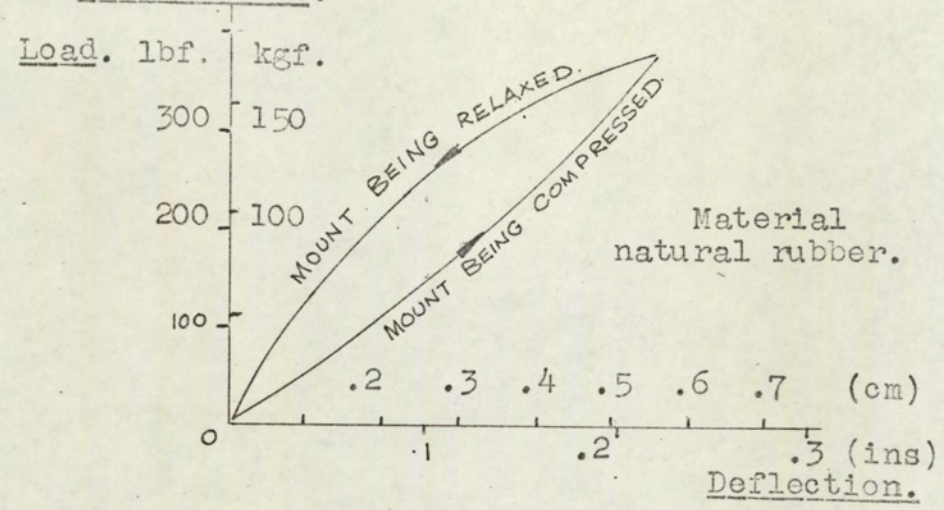

Fig. 4.20

The static vertical rate of the near side front engine/transmission rubber as installed on the test vehicle.

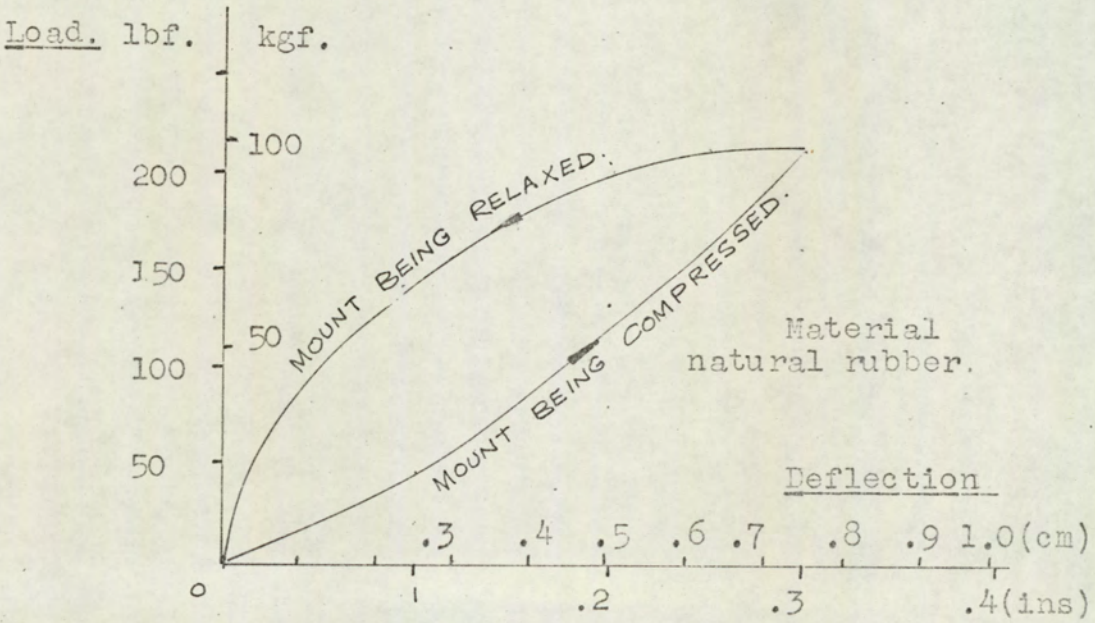

Fig. 4.21.

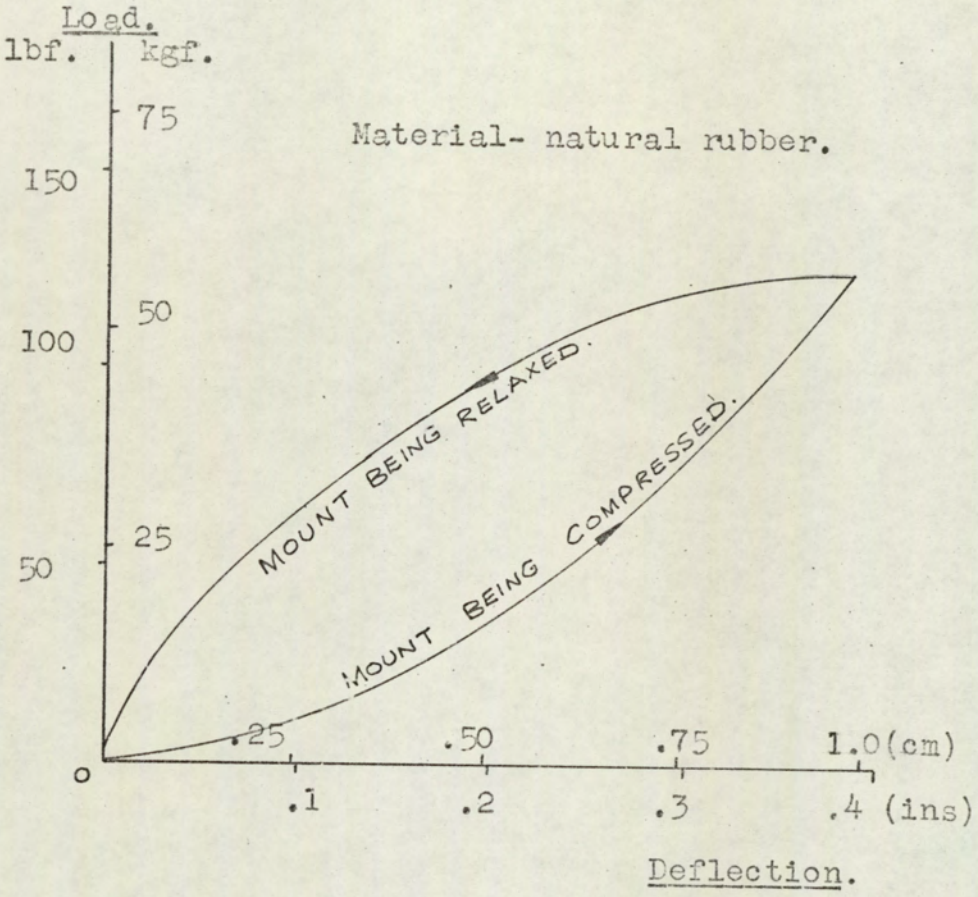

The static vertical rate of the rear engine/transmission mounting rubber, as installed in the test vehicle.

Figs. 4.22. - 4.28.

A sample of the force and response transient recordings made on the test vehicle

Figs. 4.22 a & b. Recordings of a) the force input & b) the acceleration response transients. Acceleration measured vertically at the body mass c. of g. No hydraulic engine/transmission damping.

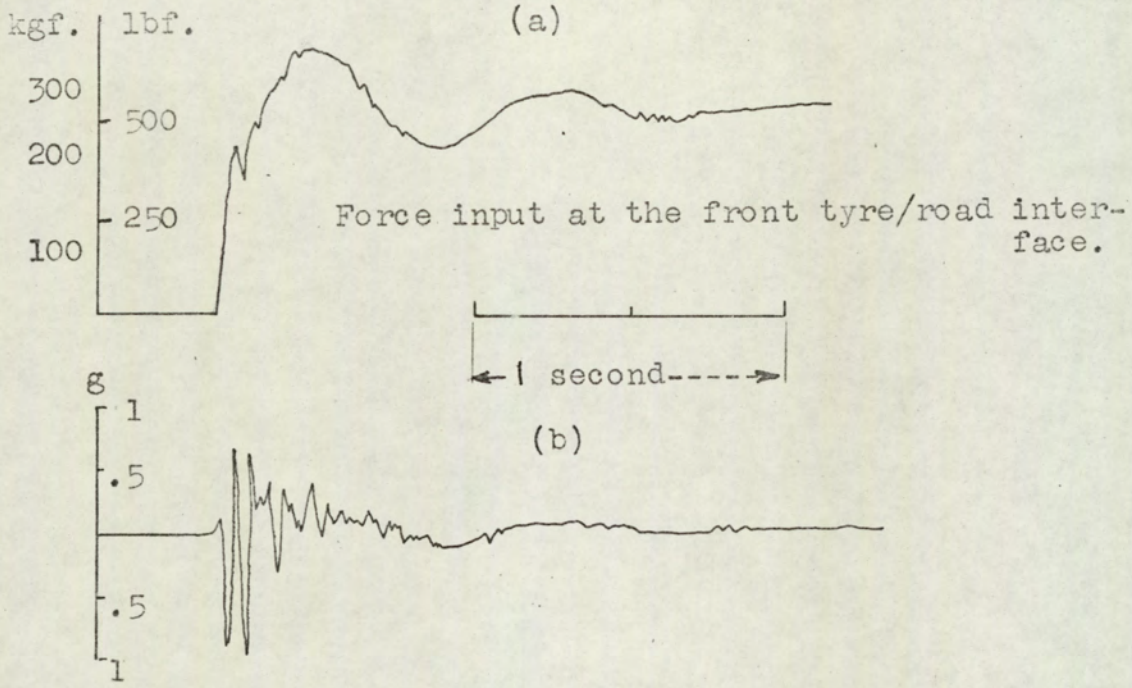

Figs. 4.23 a & b. Transient records as above, but the test vehicle fitted with hydraulic engine/transmission dampers with 65° 'Shore' rubber end bushes.

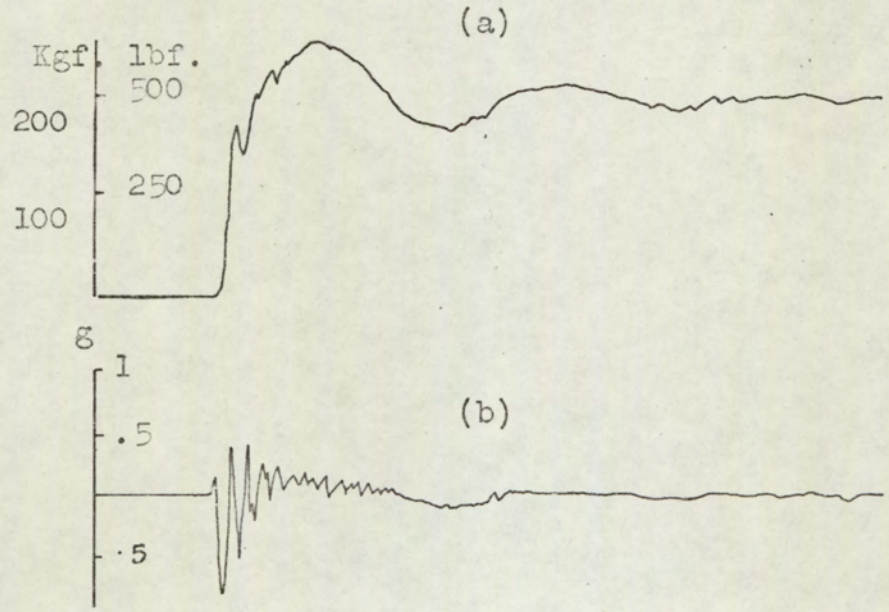

Figs. 4.24 a &b. Recordings of a) the force input & b) the acceleration response transients. Acceleration measured vertically at the engine/transmission mass. Vehicle fitted with hydraulic engine/transmission dampers with polyurethane foam fixing bushes.

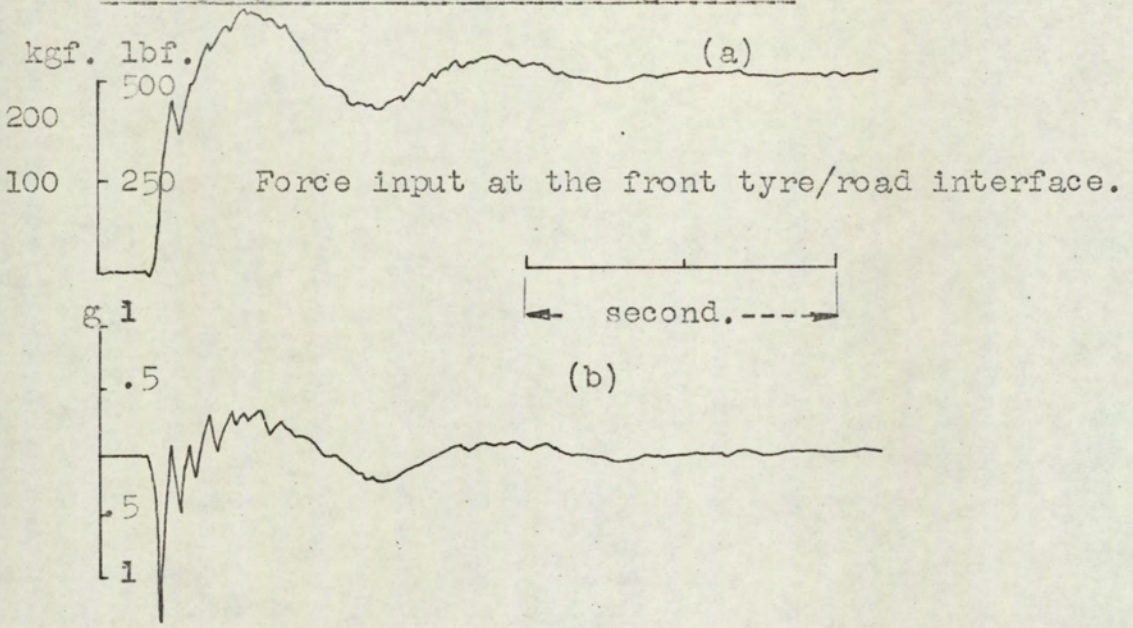

Figs. 4.25. a & b Test conditions as above, but with the acceleration measured vertically at the body mass c. of g.

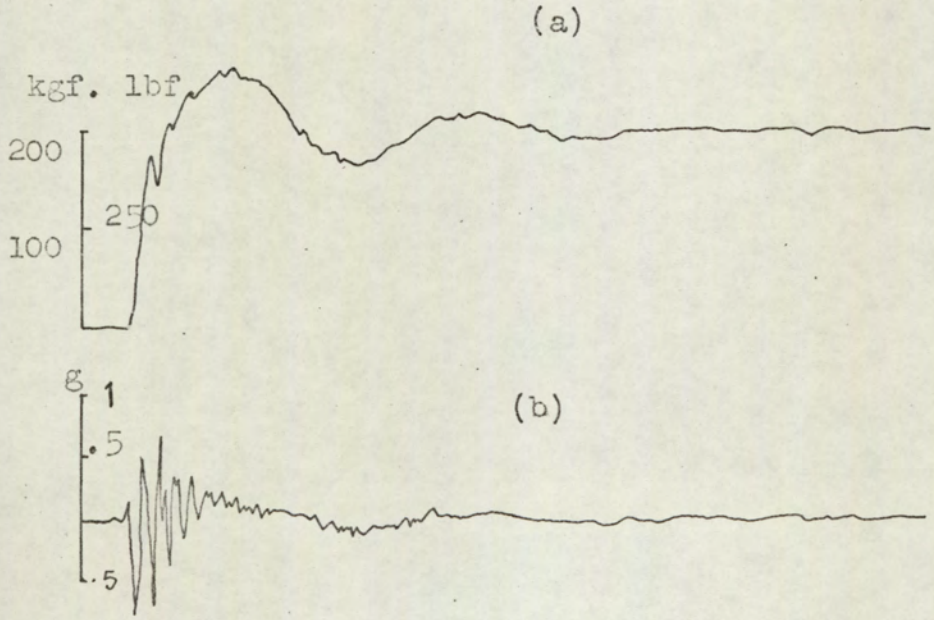

Figs. 4.26 a & b. Test conditions as in Fig. 4.24 No hydraulic engine/transmission damping.

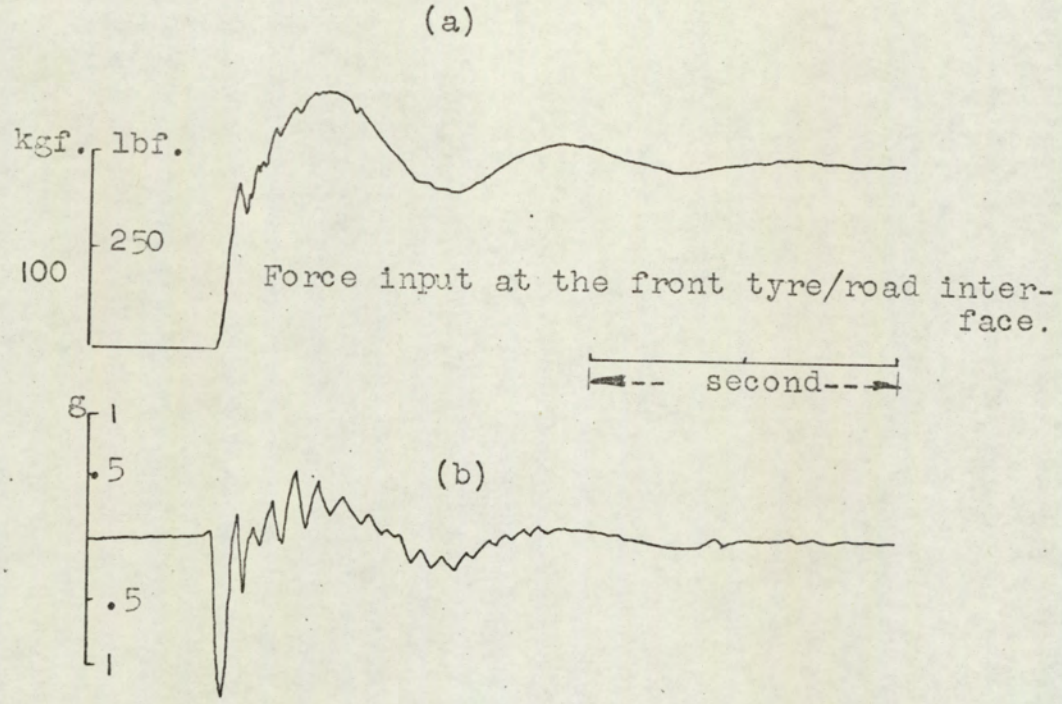

Figs. 4.27 a & b. Recordings as above, but with the test vehicle fitted with hydraulic engine/transmission dampers with 65° 'Shore' rubber end bushes.

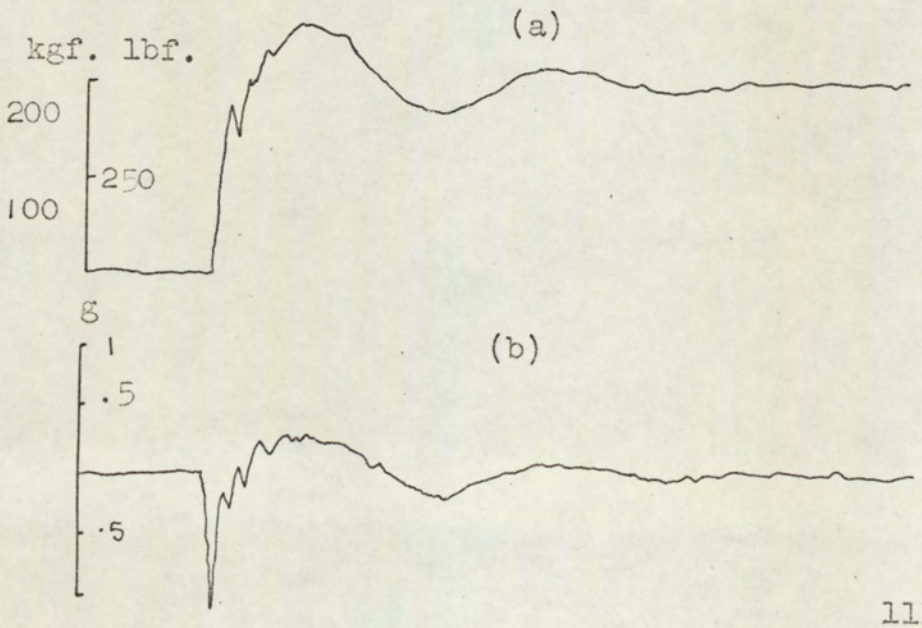

Figs. 4.28 a,b & c. Recordings of the vertical acceleration on the front 'unsprung' mass.

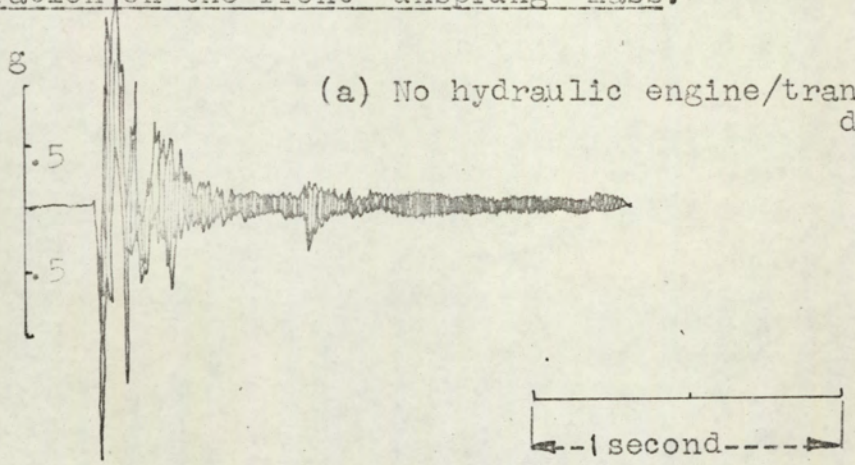

(a) No hydraulic engine/transmission damping.

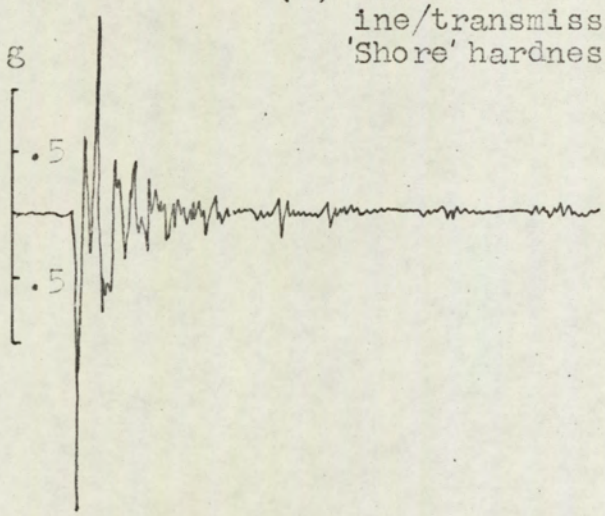

(b) Vehicle fitted with hydraulic engine/transmission dampers with 65° 'Shore' hardness rubber end bushes.

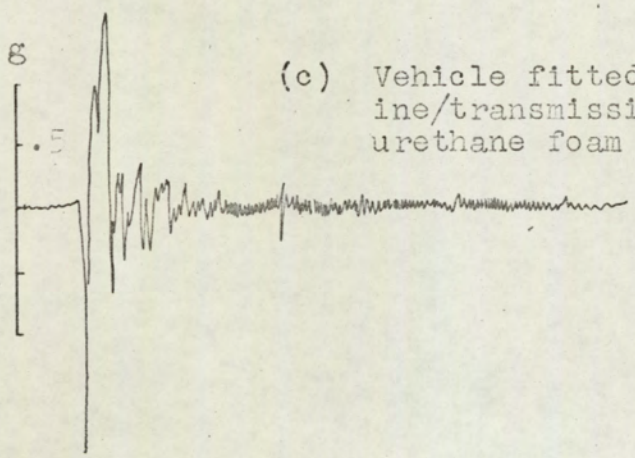

(c) Vehicle fitted with hydraulic engine/transmission dampers with polyurethane foam end bushes.

Fig. 4.29 The experimental 'transfer mobility' $\ddot{z}_1(w)/P_3(w)$ frequency spectrum for various conditions of test vehicle damping.

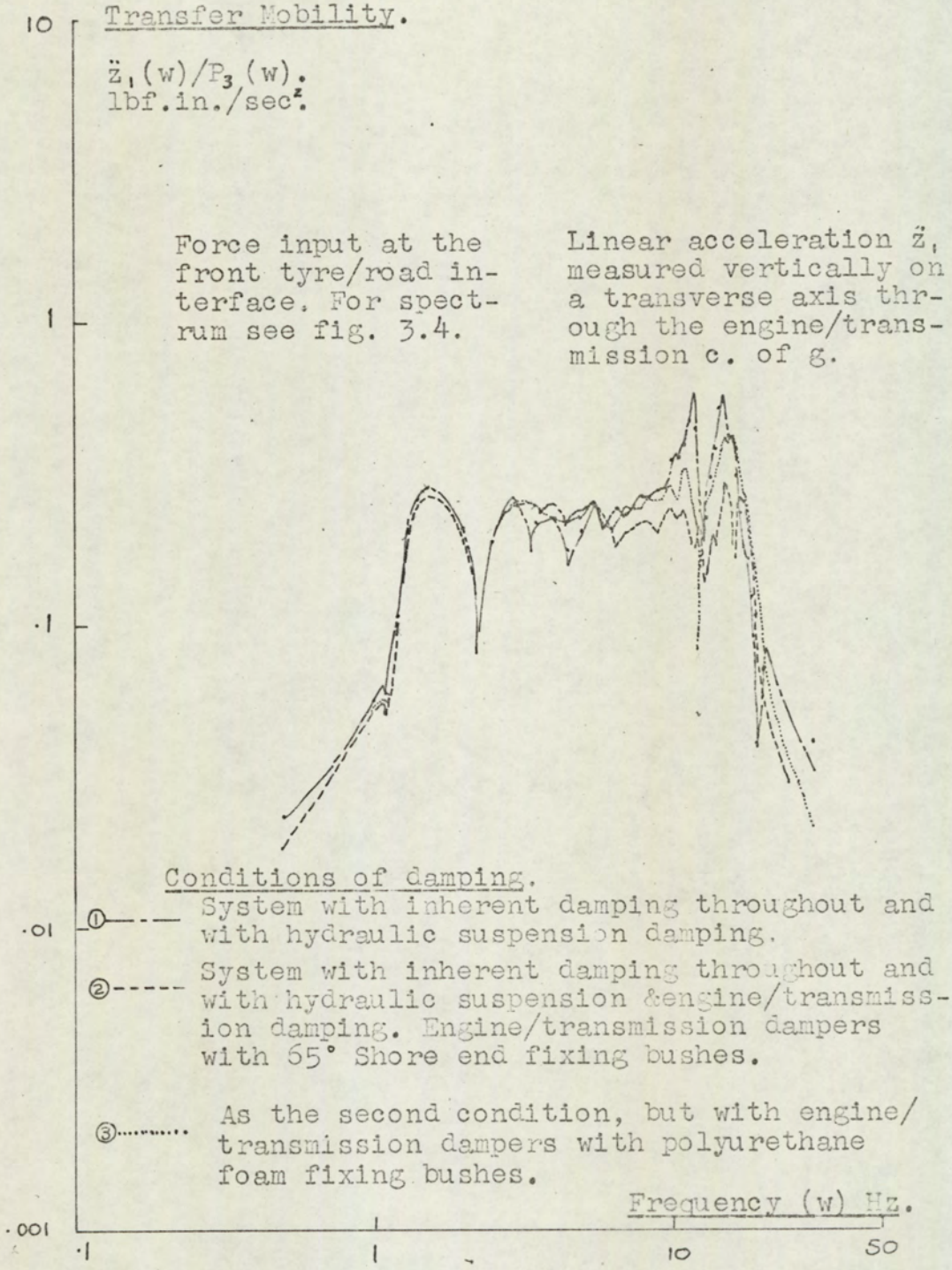

Fig. 4.30 The experimental 'transfer mobility' $\ddot{Z}_2(w)/P_3(w)$. frequency spectrum for various conditions of test vehicle damping.

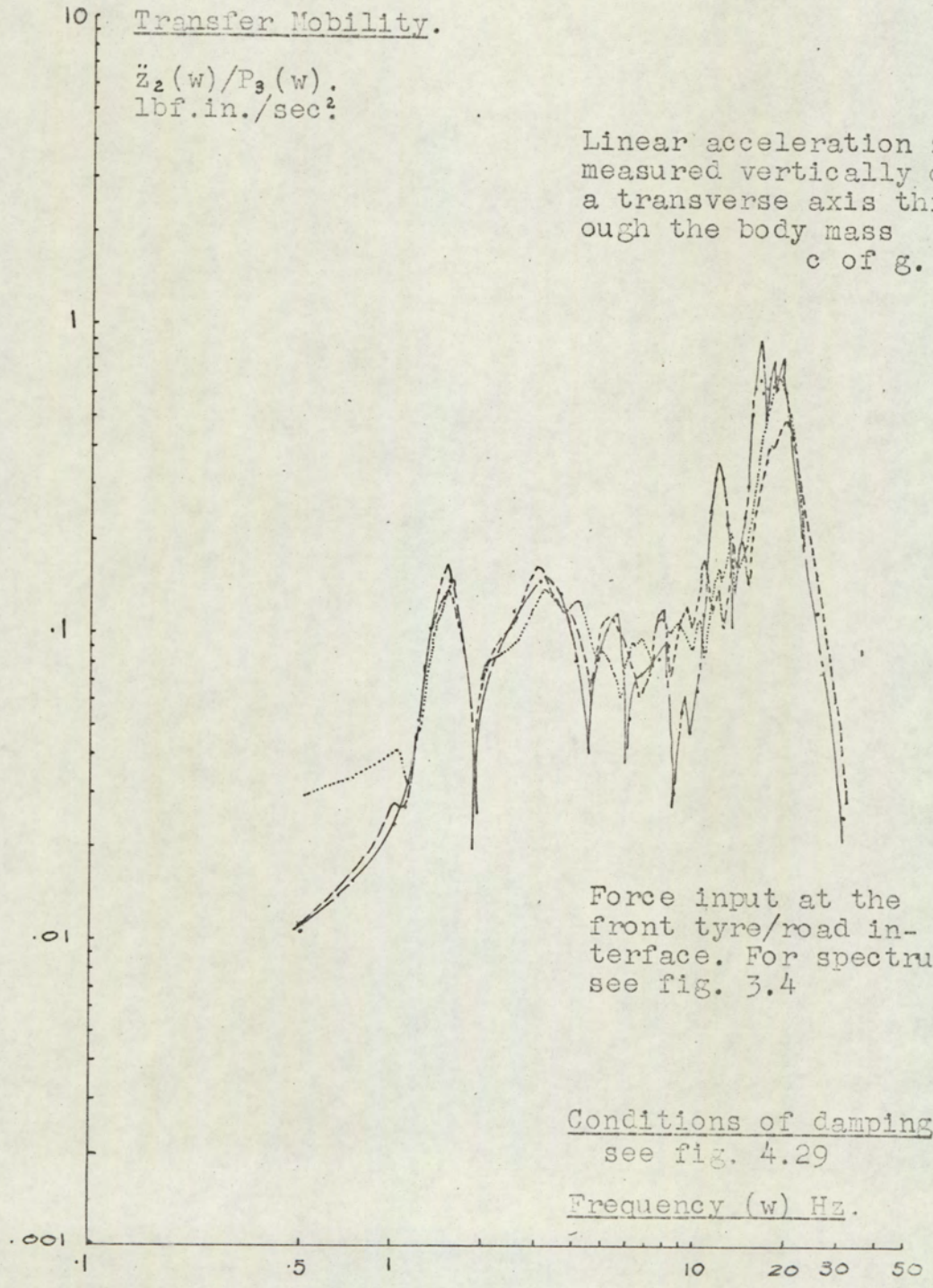

Fig. 4.31. The experimental 'transfer mobility' $\ddot{z}_{FW}(w)/P_3(w)$ frequency spectrum for various conditions of test vehicle damping.

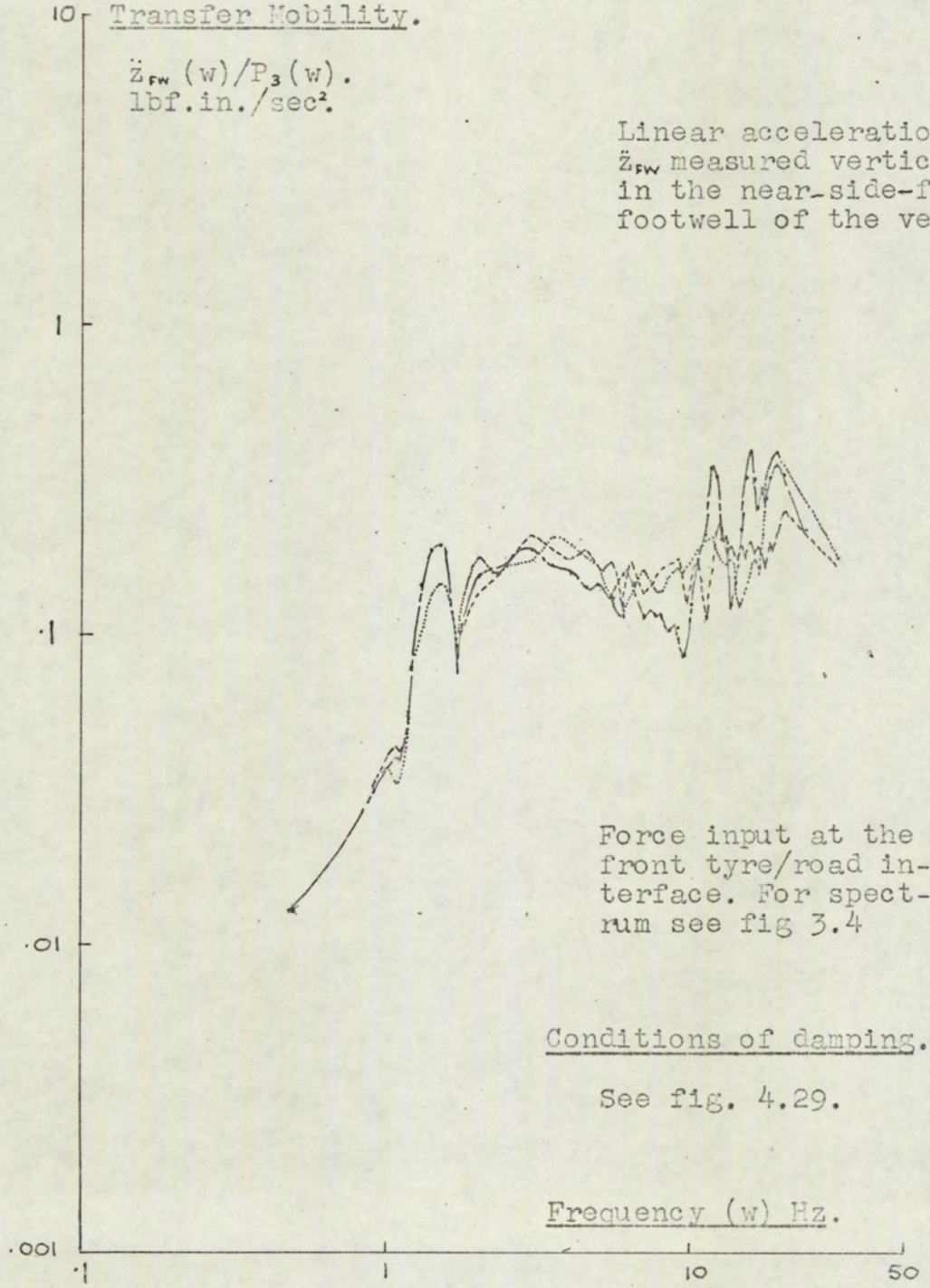

Fig. 4.32 The experimental 'transfer mobility' $\ddot{z}_3(w)/P_3(w)$ frequency spectrum for various conditions of test vehicle damping.

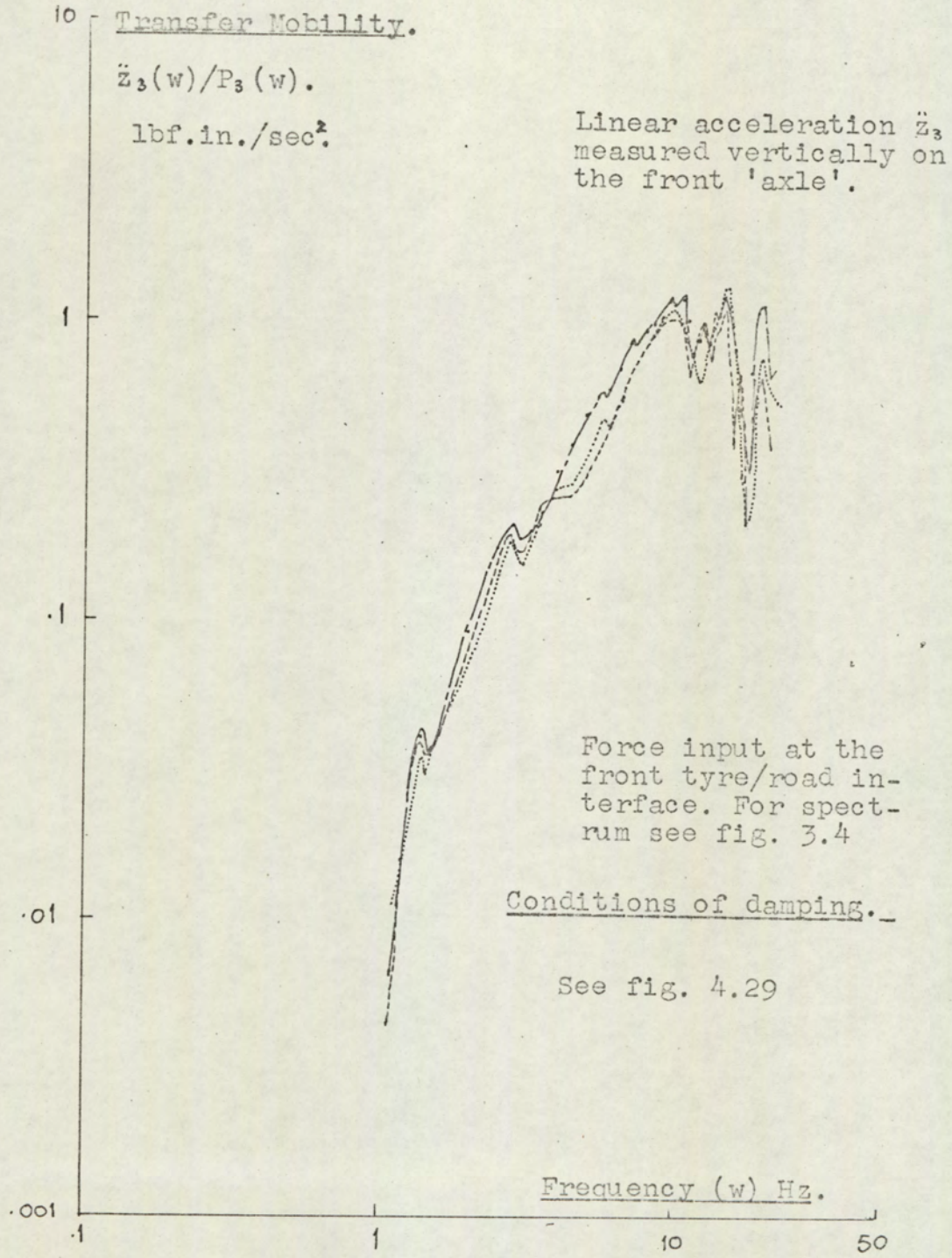

5. A COMPARISON OF THE THEORETICAL AND EXPERIMENTAL INVESTIGATIONS.

5. A COMPARISON OF THE THEORETICAL AND EXPERIMENTAL INVESTIGATIONS.

5.1. The investigation techniques.

The experimental investigations were carried out to assess the effect of engine/transmission mass damping on the vibration properties of the automobile and also to check the validity of the mathematical model which was generated to represent the vehicle.

The choice of the experimental and theoretical investigation techniques to study the vibration characteristics of a mathematical model, and the vehicle that it represents, were influenced by the availability of the following test equipment: a digital computer, to carry out any lengthy digital analysis which might occur (both in the theoretical and experimental investigations); an analogue-to-digital converter and punch tape read-out; and an instrumentation tape recorder and vibration recording transducers and amplifiers. This equipment makes the transient excitation and subsequent Fourier Transformation analysis techniques attractive for the experimental determination of the 'transfer mobilities' for the test vehicle, in the frequency domain, from recordings made in the time domain.

It should be possible to generate a mathematical model of any mechanical system. For this thesis a six degree of freedom

spring-mass-damper system has been developed (see fig. 3.1.), to represent the vibrating automobile. In order to study the effect of the engine/transmission mass damping upon the 'riding comfort' of the vehicle it is necessary to obtain the 'transfer mobility' for the body mass of the vehicle on which the passengers ride (reference Chapter 2.2.).

The transient analysis technique used for the experimental work has not been used before, as far as the author is aware, to obtain the vibration characteristics for the motor vehicle in the form of 'transfer mobilities'. The technique is established as a method of obtaining 'mechanical impedance' (the reciprocal of 'mobility') in other fields (see reference 33).

The overall accuracy of the experimental investigations depends upon the accumulative errors, which can be expected in the recording and analysis instrumentation, and the repeatability of the excitation force input. For this work the overall accuracy of the instrumentation is 14%. However, since the tests were carried out in succession, it has been assumed that the direction and magnitude of errors remain the same throughout the tests. Thus, it is reasonable to compare the experimentally computed 'transfer mobilities', to assess the effect of engine/transmission damping upon 'vehicle ride'.

The accuracy of the theoretical investigations, in the frequency domain, is a function of the analytical techniques used

to solve the equations of motion for the mathematical model, and the accuracy of the various vehicle parameters which are substituted into the equations. The effects of non-linearities will also have an effect upon the results.

5.2. The natural frequencies of vibration.

There is good agreement between the natural frequencies of vibration predicted from the consideration of the mathematical models developed to represent the motor vehicle spring-mass-damper system and the natural frequencies actually recorded on the test vehicle. The experimental investigations have revealed the limitations of the mathematical models evolved.

The natural frequencies, calculated for the coupled mathematical model, are assumed to be more accurate than the frequencies predicted using the decoupled, single degree of freedom theory. This is shown to be true when the results are compared with the natural frequencies measured on the test vehicle (see table 5.1.).

The coupled mathematical model does not predict the natural frequencies which are measured between 18 and 20 Hz. and between 15 and 16 Hz. on the test vehicle. The resonance between 18 and 20 Hz. is the frequency associated with the vehicle 'shake' mode and the frequency between 15 and 16 Hz. is associated with the dominant mode of vibration of the engine/transmission mass on its mounting rubbers.

The former resonance is not predicted from the mathematical model investigations, because the vehicle body structure bending is not accounted for in the analysis.

The discrepancy between the theoretically predicted dominant resonance, for the engine/transmission mass in coupled bounce/pitch on its mounts (11.5 Hz.) and the experimental result (between 15 and 16 Hz.) is the result of not including the non-rigidity of the vehicle body structure in the coupled, six degree of freedom model. Calculations carried out in Appendix A.2.6. show that the effective mass of the non-rigid body structure which supports the engine/transmission mass is equivalent to 606 lbf. For the mathematical model the foundation is assumed rigid, with a mass m_2 = 1240 lbf. Hartog (reference 12) shows that this non-rigidity will account for the two different natural frequencies predicted.

Results show that the dominant mode of vibration, of the front 'unsprung' mass, occurs at 12 Hz. The dominant mode of vibration, of the rear 'unsprung' mass, occurs at 9.6 Hz. The dominant mode of vibration, of the vehicle on its tyres, occurs at 3 Hz. and on the suspension springs at 1.5 to 1.7 Hz. The dominant engine/transmission vibration mode occurs between 15 and 16 Hz. The vehicle 'shake' mode occurs between 19 and 20 Hz.

5.3. The 'transfer mobility' characteristics.

The theoretical 'transfer mobility' characteristics show

that the levels of system damping considered produce little shifting of the resonant frequencies. To compare theoretical and experimental 'transfer mobility' results it is best to compare the theoretical characteristics (1) and (2) (figs. 3.5. to 3.10.) with the experimental characteristics (1) and (2) (figs. 4.29. to 4.32) respectively. The engine/transmission damper end fitting bushes, as employed in the experimental tests (2), are of 65 degrees 'Shore' hardness rubber. This is nearest to the theoretical assumption that the engine/transmission dampers have no compliance in their end bushes.

Comparing the theoretical and experimental characteristics shows that the method of equivalent linearisation used to linearise the non-linear suspension damping characteristics, for the mathematical model, gives reasonable agreement, in terms of the 'transfer mobility' amplitudes, though it would appear that the front 'unsprung' mass is more heavily damped, at its natural frequency, in practice, than predicted in theory (compare figs. 3.7. and 4.32.).

Table 5.2. gives a direct comparison of the % decrease in the 'transfer mobilities' that are theoretically predicted and experimentally measured on the vehicle 'body' mass when the engine/transmission damping factor is increased from .05 to .43. At all resonances above the frequency of the fundamental 'body' mode, which is unaffected by the engine/transmission damping,

the reductions in the 'ride transfer' characteristic amplitudes are significant, varying from 30% to 70%.

This improvement to the riding comfort of the vehicle, with increased engine/transmission damping, is confirmed as the result of subjective ride tests, carried out by an experienced 'ride engineer' in the 'field'.

Table 5.1.

A summary of the natural frequencies predicted from the theoretical and experimental investigations.

DOMINANT MODE OF VIBRATION.	NATURAL FREQUENCY. (Hz.)			
	Experimentally determined (see figs.4.29. to 4.32.)	Theoretically calculated.		
		Undamped decoupled model(see A.2.2.)	Undamped coupled model(see A.1.4.)	Damped coupled model(see fig.3.1.)
Vehicle body 'shake' resonance.	18/20	-	-	-
Engine/transmission mass resonance.				
Pure bounce or coupled bounce/pitch.	15/16	9	11.7 & 7.75	11.5 & 8.75
Front axle mass in pure bounce resonance.	12	12.03	12.1	12
Rear axle mass in pure bounce resonance.	-	9.6	9.6	-
Total vehicle mass in pure bounce resonance on the tyre springs.	3	4.33	-	2.5/3.0
Sprung mass in pure bounce or coupled bounce/ pitch resonance on the suspension springs.	1.5/1.4 & 1.1	1.7	1.66 & 1.32	1.75 & .95

Table 5.2.

A summary of the percentage improvements in the 'riding' characteristics measured on the test vehicle and predicted from the six degree of freedom mathematical model, as a result of increasing the engine/transmission damping factor from .05 to .43. (Made with reference to figs. 3.6. and 4.30.)

Mode of vibration.	Percentage decrease in the 'transfer mobility' referred to the vehicle body mass.	
	Theoretical	Experimental
Fundamental body mode (sprung mass resonance or primary ride resonance). (Resonant frequency 1.4/1.5 Hz.)	0	0
Vehicle in bounce on the tyre springs. (Resonant frequency 3 Hz.)	30%	0
Front axle mass in bounce. (Resonant frequency 12 Hz.)	60%	50%
Dominant mode of the engine/transmission mass. (Resonant frequency 15/16 Hz.)	70%	70%
Rear axle in bounce. (Resonant frequency 9.6 Hz.)	Negligible amplitude at resonance with the excitation in the plane of the front axle.	
'Shake' mode. (Resonant frequency 18 to 20 Hz.)	Not accounted for in the theoretical study.	30%

6. GENERAL CONCLUSIONS.

6. GENERAL CONCLUSIONS.

By increasing the damping factor of the engine/transmission mass suspension (referring to the pure bounce mode) from .05 (the inherent value for its suspension) to .43 by mounting hydraulic dampers in parallel with the mounting rubbers, the amplitudes of the 'vehicle ride transfer' characteristics, at the resonances associated with 'secondary' ride (10 to 20 Hz.),are reduced by some 30% to 70%. This result is valid for the particular passenger car which has been studied.

The same result can be achieved for any passenger car, if the engine/transmission mass suspension spring and damping rates are designed to dynamically absorb the 'shake' resonance associated with the longitudinal body bending mode of the vehicle.

The riding quality of a vehicle is a direct function of the 'vehicle ride transfer' characteristic. Therefore, the percentage decrease in the amplitude of the function will give a corresponding increase in the riding comfort of the vehicle.

Because it is not possible to manufacture engine/transmission mounts with a damping factor as high as .43, the use of auxiliary hydraulic dampers, in parallel with rubber mounts, is the only alternative.

Rubber with high inherent, internal damping is not suitable for engine/transmission mounts, because excessive heat would be generated by the internal friction of the material. This heat build-up would result in increased strain in the material and eventually destruction of the mounts.

The transient excitation and subsequent Fourier Analysis technique used to yield the 'transfer mobilities' for the vehicle, in the frequency domain, from recordings made in the time domain, is a valuable addition to experimental vehicle vibration testing techniques used at present in the motor industry. This is an inexpensive method for obtaining vibration results in the frequency domain.

A comparison of the theoretical and experimental 'transfer mobility' characteristics shows that for a study of vehicle 'riding' quality, the theoretical model with six degrees of freedom is not sufficient. The longitudinal bending of the body structure must be included in the model, so that the effect of vehicle 'shake' can be assessed.

The method of equivalent linearisation of the practical non-linear damping rates, for substitution into the mathematical model, by equating the work done by a non-linear damper to the work done by an equivalent linear damper, is a valid method for handling differential damping and damping non-linearities.

Obviously any sudden rate discontinuities should be accounted for by substituting the best approximation to the

practical rate into the mathematical model. For this particular vehicle such a rate change is obvious at about 10"/sec. damper piston velocity, for the suspension dampers. Below this velocity the rate substituted into the model is the practical value, read from the experimental damper characteristics. Above this velocity the calculated equivalent linear rate is used.

The experimental transient impulse, force input, testing and subsequent Fourier Transform Analysis technique employed, to obtain the vehicle 'transfer mobilities' in this research, shows certain advantages over the more usual harmonic testing techniques.

The capital cost of the instrumentation is significantly less. By virtue of the testing technique and use of readily available instrumentation, tests can be carried out 'on site' in any laboratory.

Transient excitation of the test vehicle results in all the system resonances being excited simultaneously. This occurs, in practice, on the road, when a vehicle is continually subjected to random inputs. Random inputs can be considered to be a series of impulse inputs. Harmonic excitation produces only one resonance at the discrete frequency of excitation.

Impulse testing enables the effect of system non-linearities to be studied when all system resonances are excited together.

7. RECOMMENDATIONS.

7. RECOMMENDATIONS.

Analysis of the six degree of freedom model, in the frequency domain, is suitable for the theoretical study of the effect which changes to a vehicle's main suspension and engine/transmission suspension spring and damping rates and vehicle mass parameters, have upon the riding quality of the motor vehicle.

If the effect of a range of engine/transmission mass damping factors or spring rates upon the 'shake' characteristics is required, then the model must be extended to include the longitudinal bending of the vehicle body structure.

The experimental transient excitation, in the time domain, and the subsequent Fourier Transformation analysis techniques used to yield the 'transfer mobility' characteristics, in the frequency domain, for a vehicle in the laboratory, is a recommended method of assessing the effect of the change to any vehicle parameter upon its 'riding quality'.

For any front engined passenger car, of similar sprung weight to unsprung weight ratio (1:10) to the vehicle tested, a suspension damping factor of .35 is suggested, as a compromise to satisfy the optimum damping factor requirement of .22, for the best 'riding comfort', and the requirement of .52, for the best road holding.

For the best 'riding comfort', the damping factor associated with the engine/transmission mass suspension should be .43. This level can only be achieved with hydraulic damping. Because of the small amplitudes of the engine/transmission mass displacements, it is recommended that responsive, pressurised Girling 'Monitube' hydraulic dampers are used. For small displacements these dampers do not exhibit the 'dead' zone, produced as a result of damper fluid aeration, which is characteristic of conventional 'twin tube' dampers. To prevent excessive engine/transmission noise transmission to the vehicle body and passenger compartment by the dampers, they should be attached to the vehicle with rubber bushes. To ensure that the damper movement is responsive to these small displacements, the rubbers should be of 65 degrees 'Shore' hardness rubber.

It is suggested that the transient excitation technique described in this thesis could be employed in the service garage to assess whether the suspension dampers on a vehicle need replacing, after the vehicle has been in service for some time. Damping can be assessed by the inspection of a record of the vehicle body displacement response. By recording the body displacement as opposed to the acceleration response instrumentation would be cheaper and easier to operate.

This method would dispense with the necessity of taking the dampers off the vehicle to check their performance.

A rig is now being designed in line with the above suggestion, for service garage use.

8. FURTHER WORK.

8. FURTHER WORK.

8.1. Theoretical Investigations.

At the time when the original theoretical investigations were carried out, and as reported in this thesis, it was not understood that the beam like bending of the vehicle body structure about a transverse axis was responsible for the 'shake' resonant condition in the motor vehicle. This body bending is not included in the mathematical model of the vehicle (fig. 3.1.). A more accurate representation of the vibrating vehicle will result if this bending mode is included in the mathematical model. The body mass (m_2) can be replaced by a finite number of concentrated masses, each with an associated moment of inertia and second moment of area, at discrete points along the longitudinal axis of the vehicle. Analysis of this model will yield, in addition to the natural frequencies obtained by analysing the mathematical model in fig. 3.1., the natural frequency of the body in bending, or the 'shake' frequency.

A comparison of the 'transfer mobilities' for the vehicle mathematical model with the above suggested modification, and tyre and damping non-linearities included, with the results for the linear model considered in this thesis will be a useful exercise.

The 'Runge Kutta' analysis technique can be employed to solve the equations of motion for the mathematical model, in the time domain, to yield the transient response for the different

parts of the mathematical model. These theoretical results can then be compared with the transient records, in the time domain, such as the ones made in the experimental investigations in this thesis. The passage of the vehicle over a certain road irregularity can be represented by introducing the time dependent forcing function for the mathematical model, first at the front tyre/road interface, and then at the rear tyre/road interface, with an arbitrary time delay, depending upon the forward speed of the vehicle.

To study the effect of the forward speed of the vehicle upon its vibration characteristics the variation of the tyre damping co-efficients v_5 and v_6 with speed, from fig. 4.16., should be included in the mathematical model.

8.2. Experimental Investigations.

The experimental excitation, in the time domain, and subsequent Fourier Transformation techniques developed in this thesis to obtain vehicle 'transfer mobilities', in the frequency domain, are used specifically to study the effect of engine/transmission mass damping on the vehicle vibration characteristics. However, the technique can be applied equally well to study the effects of making changes to any of the motor vehicle parameters upon the vehicle vibration characteristics. Further work to correlate the results of subjective ride tests, in a test vehicle in the 'field', with results obtained using this experimental

transient excitation technique should make it possible to predict the riding 'quality' of a motor vehicle in the laboratory using the 'transient excitation' technique.

The dynamics of the motor vehicle vibration model, with the bending of the body included, may be simulated on an analogue computer. The main reasons for doing this would be so that the non-linearities of the suspension damping characteristics and spring rates can be represented, using suitably designed 'diode function generators'. The 'transfer mobilities' for the model can be generated directly by stepping the frequency of the force input.

By using the analogue computer to represent the vibrating automobile, the time taken to generate a series of 'transfer mobility' characteristics would be much shorter than either the theoretical digital or experimental transient excitation techniques described in this thesis (reference 18). (Preparation time to evolve the model may be much longer for the analogue simulation.)

It is shown, in the theoretical and experimental work in this project, that the theoretical dominant natural frequency of the engine/transmission mass on its mounting rubbers is approximately three Hz. lower than the 15 Hz. measured in the experimental investigations. Further work will be necessary if it is to be shown conclusively that it is the effect of the non-rigidity of the structure of the body which accounts for this

frequency difference. This theory of a mass suspended on non-rigid foundations, having a different natural frequency to that predicted for the same mass suspended on a rigid foundation, is postulated by Hartog (reference 12). Also see Appendix A.4. To check the theory it will be required to mount the engine/transmission mass and its suspension on a solid foundation and determine its resonant frequencies using a vibrator or the transient excitation technique. The results can then be compared with the natural frequencies measured in this project.

The 'transfer mobility' characteristics for the vehicle model can be computed, not only with reference to an input forcing function, but also with reference to a given input displacement. This form of 'transfer mobility' will be of use if results for a given road profile input are required for a comparison with a theoretical prediction of 'transfer mobility' for the given input displacements to the model, at the tyre/road interfaces.

In this thesis hydraulic damping non-linearities are accounted for in the theory by approximating an equivalent linear damper. This is achieved by equating work done and considering any obvious rate discontinuities. (See Chapter 3.2.1.)

It is suggested that further research should be carried out to understand what effect the differential damping rates and the 'velocity-damping power' (see reference 16) have upon the response of a vibrating system.

A study of the various analyses available to account for damping non-linearities should be made, with the aim of recommending the most accurate and useful theory.

APPENDICES.

APPENDIX A.1.

A.1.1. The solution of the equations of motion for the six degree of freedom mathematical model.

Equations 3.1.1.(1) to 3.1.1.(6) are the equations of motion for the mathematical model. These equations can be solved by assuming solutions of the form

$$z_n \text{ or } \theta_n = x_{2n-1} \sin wt + x_{2n} \cos wt = \sqrt{(x_{2n-1} + x_{2n})} \sin(wt + \phi_n) \quad \ldots\ldots A.1.1(1)$$

Differentiating equation A.1.1.(1)

$$\dot{z}_n \text{ or } \dot{\theta}_n = x_{(2n-1)} w \cos wt + x_{2n} w \sin wt \quad \ldots\ldots A.1.1(2)$$

Differentiating equation A.1.1.(2)

$$\ddot{z}_n \text{ or } \ddot{\theta}_n = -x_{2n-1} w^2 \sin wt - x_{2n} w^2 \cos wt = -w^2 z_n \text{ or } -w^2 \theta_n \quad \ldots A.1.1(3)$$

n will take the values 1 to 4 for the terms involving z and the values 5 and 6 for the terms involving θ in the equations which result from the above substitutions. Using the above substitutions in equations 3.1.1.(1) to 3.1.1.(6) and equating the sin. terms and then the cos. terms to zero, in turn, will yield the following equations.

Substituting into equation 3.1.1.(1) and putting the cos. terms equal to zero:

$$x_1 (k_1 + k_2 - m_1 w^2) - x_2 (v_1 w - v_2 w) - x_3 (k_1 + k_2) + x_4 (v_2 w + v_1 w) + x_9 (k_1 a - k_2 b) - x_{10} (v_1 aw - v_2 bw) - x_{11} (k_1 c + k_2 l) + x_{12} (v_1 wc + v_2 wl) = 0 \quad \ldots A.1.1.(4)$$

Substituting into equation 3.1.1.(1) and putting the sin. terms equal to zero:

$$x_1 (v_1w + v_2w) - x_2 (m_1w^2 - k_1 - k_2) - x_3 (v_1w \quad v_2w)$$
$$- x_4 (k_1 + k_2) + x_9 (v_1wa - v_2wb) + x_{10} (k_1a - k_2b)$$
$$- x_{11} (v_1wc + v_2wl) - x_{12} (k_1c + k_2l) = P_1 \qquad \text{... A.1.1.(5)}$$

Substituting into equation 3.1.1.(2) and putting the cos. terms equal to zero:

$$- x_1 (k_1 + k_2) + x_2 (v_2w + v_1w) - x_3 (m_2w^2 - k_3 - k_4 - k_2 - k_1)$$
$$- x_4 (v_3w + v_4w + v_2w + v_1w) - x_5k_3 + x_6 v_3w - x_7k_4 + x_8v_4w$$
$$+ x_9 (k_2b - k_1a) - x_{10} (v_2bw - v_1aw) + x_{11} (k_3c - k_4d + k_2l + k_1c)$$
$$- x_{12} (v_3cw - v_4dw + v_2lw + v_1cw) = 0 \qquad \text{... A.1.1.(6)}$$

Substituting in equation 3.1.1.(2) and putting the sin. terms equal to zero:

$$- x_1 (v_2w + v_1w) - x_2 (k_1 + k_2) + x_3 (v_3w + v_2w + v_1w + v_4w)$$
$$- x_4 (m_2w^2 - k_3 - k_4 - k_2 - k_1) - x_5v_3w - x_6k_3 - x_7v_4w$$
$$- x_8k_4 + x_9 (v_2bw - v_1aw) + x_{10} (k_2b - k_1a) - x_{11} (v_4dw - v_2lw$$
$$- v_1cw - v_3cw) + x_{12} (k_3c - k_4d + k_2l + k_1c) = P_2 \qquad \text{... A.1.1.(7)}$$

Substituting in equation 3.1.1.(3) and putting the cos. terms equal to zero:

$$- x_3k_3 + x_4v_3w + x_5 (k_5 + k_3 - m_3w^2) - x_6 (v_5w + v_3w)$$
$$- x_{11}k_3c + x_{12}v_3cw = 0 \qquad \text{... A.1.1.(8)}$$

Substituting in equation 3.1.1.(3) and putting the sin. terms equal to zero:

$$- x_3v_3w - x_4k_3 + x_5 (v_5w + v_3w) - x_6 (m_3w^2 - k_5 - k_3)$$
$$- x_{11}v_3cw - x_{12}k_3c = P_3 \qquad \text{... A.1.1.(9)}$$

Substituting in equation 3.1.1.(4) and putting the cos. terms equal to zero:

$$x_4 v_4 w - x_3 k_4 + x_7 (k_4 + k_6 - m_4 w^2) - x_8 (v_4 w + v_6 w) + x_{11} k_4 d - x_{12} v_4 dw = 0 \quad \text{... A.1.1.(10)}$$

Substituting in equation 3.1.1.(4) and putting the sin. terms equal to zero:

$$- x_3 v_4 w - x_4 k_4 + x_7 (v_6 w + v_4 w) + x_8 (k_4 + k_6 - m_4 w^2) x_{11} v_4 dw + x_{12} k_4 d = P_4 \quad \text{... A.1.1.(11)}$$

Substituting in equation 3.1.1.(5) and putting the cos. terms equal to zero:

$$- x_1 (k_1 a - k_2 b) + x_2 (v_1 aw - v_2 bw) - x_3 (k_2 b - k_1 a) - x_4 (v_1 aw - v_2 bw) + x_9 (j_1 w^2 - k_1 a^2 - k_2 b^2) + x_{10} (v_1 a^2 w + v_2 b^2 w) + x_{11} (k_1 ac - k_2 lb) - x_{12} (v_1 caw - v_2 blw) = 0 \quad \text{... A.1.1.(12)}$$

Substituting in equation 3.1.1.(5) and putting the sin. terms equal to zero:

$$- x_1 (v_1 aw - v_2 bw) - x_2 (k_1 a - k_2 b) + x_3 (v_1 aw - v_2 bw) - x_4 (k_2 b - k_1 a) - x_9 (v_1 a^2 w + v_2 b^2 w) + x_{10} (j_1 w^2 - k_1 a^2 - k_2 b^2) + x_{11} (v_1 caw - v_2 blw) + x_{12} (k_1 ac - k_2 lb) = P_5 \quad \text{... A.1.1.(13)}$$

Substituting in equation 3.1.1.(6) and putting the cos. terms equal to zero:

$$x_1 (k_1 c + k_2 l) - x_2 (v_1 cw + v_2 lw) - x_3 (k_3 c + k_1 c + k_2 l - k_4 d) + x_4 (v_3 cw + v_1 cw + v_2 lw - v_4 dw) + x_5 k_3 c - x_6 v_3 cw - x_7 k_4 d + x_8 v_4 dw + x_9 (k_1 ac - k_2 lb) - x_{10} (v_1 acw - v_2 lbw) + x_{11} (j_2 w^2 - k_3 c^2 - k_1 c^2 - k_2 l^2 - k_4 d^2) + x_{12} (v_3 wc^2 + v_1 wc^2 + v_2 wl^2 + v_4 wd^2) = 0 \quad \text{... A.1.1.(14)}$$

Substituting in equation 3.1.1.(6) and putting the sin. terms equal to zero:

$$x_1 (v_1cw + v_2lw) + x_2 (k_1c + k_2l) - x_3 (v_3cw + v_1cw + v_2lw - v_4dw) - x_4 (k_3c + k_1a + k_2l - k_4d) + x_5v_3cw + x_6k_3c - x_7v_4dw - x_8k_4d + x_9 (v_1caw - v_2blw) + x_{10} (k_1ac - k_2lb) - x_{11} (v_3c^2w + v_1c^2w + v_2l^2w + v_4d^2w) + x_{12} (j_2w^2 - k_1c^2 - k_3c^2 - k_2l^2 - k_4d^2) = P_6$$

... A.1.1.(15)

Equations A.1.1.(4) to A.1.1.(15) are simultaneous in terms of x_1, x_2, x_3 ... x_{12}. A matrix method, evolved by Choleski (reference 26) - see Appendix A.1.2. - is used to solve the equations for x_1 to x_{12}. The frequency response is obtained by plotting $\ddot{z}_n$ or $\ddot{\theta}_n$ against w for each mass. $\ddot{z}_n$ and $\ddot{\theta}_n$ are arrived at directly from equation A.1.1.(3). The theoretical 'transfer mobilities' for the mathematical model are obtained by ratioing the amplitude of the acceleration response to the amplitude of the force input to the system (P_3).

A.1.2. <u>The matrix method used to solve the simultaneous equations A.1.1.(4) to A.1.1.(15)</u>.

This matrix method is due to Choleski (see 'Mechanical Vibrations - An Introduction to Matrix Methods' - reference 26). Consider n simultaneous equations with solutions x_1, x_2, x_3, x_4 to x_n (e.g. equations A.1.1.(4) to A.1.1.(15)). These equations can be written in the following matrix form:

$$\begin{pmatrix} a_{1,1} & a_{1,2} & a_{1,3} & \cdots & a_{1,n} \\ a_{2,1} & a_{2,2} & a_{2,3} & \cdots & a_{2,n} \\ . & . & . & \cdots & . \\ . & . & . & \cdots & . \\ a_{n,1} & a_{n,2} & a_{n,3} & \cdots & a_{n,n} \end{pmatrix} \begin{pmatrix} x_1 \\ x_2 \\ . \\ . \\ x_n \end{pmatrix} = \begin{pmatrix} y_1 \\ y_2 \\ . \\ . \\ y_n \end{pmatrix} \quad \text{or} \quad Ax = y$$

$$x = A^{-1}y \quad \ldots \quad \text{A.1.2.(1)}$$

The problem is the evaluation of A^{-1}.

To illustrate the method used to obtain A^{-1} consider the 3 x 3 matrix:

$$A = \begin{pmatrix} a_{11} & a_{12} & a_{13} \\ a_{21} & a_{22} & a_{23} \\ a_{31} & a_{32} & a_{33} \end{pmatrix}$$

This can be written as

$$A = B \times D \quad \ldots \quad \text{A.1.2.(2)}$$

where $B = \begin{pmatrix} 1 & 0 & 0 \\ b_{21} & 1 & 0 \\ b_{31} & b_{32} & 1 \end{pmatrix}$ and $D = \begin{pmatrix} d_{11} & d_{12} & d_{13} \\ 0 & d_{22} & d_{23} \\ 0 & 0 & d_{33} \end{pmatrix}$

Now $a_{11} = d_{11}$; $a_{12} = d_{12}$; $a_{13} = d_{13}$; $a_{21} = d_{11}b_{21}$; $a_{22} = b_{21}d_{12} + d_{22}$; $a_{23} = b_{21}d_{13} + d_{23}$; $a_{31} = b_{31}d_{11}$; $a_{32} = b_{31}d_{12} + b_{32}d_{22}$; $a_{33} = b_{31}d_{13} + b_{32}d_{23} + d_{33}$.

More generally for a matrix with r rows and s columns:

$$s < r \quad b_{rs} = (a_{rs} - \sum_{k=1}^{s-1} b_{rk}d_{ks})/d_{ss} \quad \ldots\ldots\ldots \text{A.1.2(3)}$$

$$s \geq r \quad d_{rs} = (a_{rs} - \sum_{k=1}^{r-1} b_{rk}d_{ks}) \quad \ldots\ldots\ldots \text{A.1.2(4)}$$

Inversion of A.

$$A^{-1} = D^{-1} \times B^{-1} \quad \ldots \quad \text{A.1.2.(5)}$$

i.e. $$\begin{pmatrix} a_{11} & a_{12} & a_{13} \\ a_{21} & a_{22} & a_{23} \\ a_{31} & a_{32} & a_{33} \end{pmatrix}^{-1} = \begin{pmatrix} D_{11} & D_{12} & D_{13} \\ 0 & D_{22} & D_{23} \\ 0 & 0 & D_{33} \end{pmatrix} \times \begin{pmatrix} 1 & 0 & 0 \\ B_{21} & 1 & 0 \\ B_{31} & B_{32} & 1 \end{pmatrix}$$

$s < r$ $$\begin{pmatrix} 1 & 0 & 0 \\ b_{21} & 1 & 0 \\ b_{31} & b_{32} & 1 \end{pmatrix} \times \begin{pmatrix} 1 & 0 & 0 \\ B_{21} & 1 & 0 \\ B_{31} & B_{32} & 1 \end{pmatrix} = \begin{pmatrix} 1 & 0 & 0 \\ 0 & 1 & 0 \\ 0 & 0 & 1 \end{pmatrix}$$

where:

$$b_{21} + B_{21} = 0; \quad b_{31} + b_{32} B_{21} + B_{31} = 0;$$

$$b_{32} + B_{32} = 0; \quad b_{41} + b_{42}B_{21} + b_{43}B_{31} = 0;$$

$$b_{42} + b_{43}B_{32} + B_{42} = 0; \quad b_{43} + B_{43} = 0.$$

Or generally for an r x s matrix

$$B_{rs} = -b_{rs} - \sum_{k=s+1}^{r-1} b_{rk}B_{ks} \qquad \text{.....A.1.2(6)}$$

$s \geqslant r$ $$\begin{pmatrix} D & D_{12} & D_{13} \\ 0 & D_{22} & D_{23} \\ 0 & 0 & D_{33} \end{pmatrix} \times \begin{pmatrix} d_{11} & d_{12} & d_{13} \\ 0 & d_{22} & d_{23} \\ 0 & 0 & d_{33} \end{pmatrix} = \begin{pmatrix} 1 & 0 & 0 \\ 0 & 1 & 0 \\ 0 & 0 & 1 \end{pmatrix}$$

where:

$$D_{11}d_{11} = 1; \quad D_{11}d_{12} + D_{12}d_{22} = 0;$$

$$D_{11}d_{13} + d_{12}d_{23} + D_{13}d_{33} = 0$$

$$D_{22}d_{22} = 1; \quad D_{22}d_{23} + D_{23}d_{33} = 0;$$

$$D_{33}d_{33} = 1.$$

Or generally for an r x s matrix

$$D_{ss} = 1/d_{ss} \qquad \text{... A.1.2.(7)}$$

$$D_{rs} = -D_{ss} \sum_{k=r}^{s-1} D_{rk}d_{ks} \qquad \text{... A.1.2(8)}$$

The computer programme 'Damper 14' is written in 'Algol 60' to solve the equations A.1.1.(3) to A.1.1.(15), using the 'Choleski' matrix method. The solutions yield the acceleration amplitudes for each mass in the mathematical model for a range of forcing frequencies.

The 'transfer mobility' is obtained simply by ratioing the acceleration amplitudes by the amplitude of the forcing function (P_3) = 1000 lbf.

A.1.4. <u>The matrix method used to obtain the coupled natural frequencies of the undamped automobile spring-mass system. (Reference fig. 3.1.)</u>

This iterative method of natural frequency determination is well known (reference 35). The method has the drawback that it can only be applied to undamped systems. The values that this method of solution gives for w_n, the natural frequencies of the system, will provide a useful check on the natural frequencies indicated by the 'transfer mobility' characteristics and the decoupled frequencies calculated in Appendix A.2.2.

The equations of motion for the steady state vibration of the mathematical model will be as equations 3.1.1.(1) to 3.1.1.(6) with the damping and forcing terms omitted.

If $\ddot{z}_1$, $\ddot{z}_2$, $\ddot{z}_3$, $\ddot{z}_4$, $\ddot{z}_5$ and $\ddot{z}_6$ are written as $-w^2z_1$, $-w^2z_2$, $-w^2z_3$, $-w^2z_4$, $-w^2z_5$ and $-w^2z_6$ respectively the equations can be rewritten in the following matrix form:

$$1/w^2 \begin{bmatrix} a_{11} & a_{12} & a_{13} & a_{14} & a_{15} & a_{16} \\ a_{21} & a_{22} & a_{23} & a_{24} & a_{25} & a_{26} \\ a_{31} & a_{32} & a_{33} & a_{34} & a_{35} & a_{36} \\ a_{41} & a_{42} & a_{43} & a_{44} & a_{45} & a_{46} \\ a_{51} & a_{52} & a_{53} & a_{54} & a_{55} & a_{56} \\ a_{61} & a_{62} & a_{63} & a_{64} & a_{65} & a_{66} \end{bmatrix} \begin{bmatrix} z_1 \\ z_2 \\ z_3 \\ z_4 \\ z_5 \\ z_6 \end{bmatrix} = \begin{bmatrix} z_1 \\ z_2 \\ z_3 \\ z_4 \\ z_5 \\ z_6 \end{bmatrix}$$

or $1/\lambda A\underline{z} = \underline{z}$ where $\lambda = w^2$ ... A.1.4.(1)

Let the eigenvalues of A be $\lambda_1 \ \lambda_2 \cdots \lambda_6$ in order of descending modulus.

Evaluation of the dominant root.

Take an arbitrary vector $\underline{y}_o$ of six components for the six equations. Generate a sequence of vectors $\underline{y}_i$ and $\underline{z}_i$ using the relations. $\underline{z}_{i+1} = A\underline{y}_i$ ..... A.1.4(2)

$\underline{y}_{i+1} = \underline{z}_{i+1}$ /the numerically largest element of $\underline{z}_{i+1}$

..... A.1.4(3)

The vectors $\underline{y}_i$ form a sequence, each number of which has its largest element equal to unity. If it is assumed that the $\underline{x}_i$ elements are normalised, so that their largest elements equal unity, then $\underline{y}_i$ tends towards the vector $\underline{x}_i$, the eigenvector corresponding to λ_1

$\underline{y}_o$ may be expressed as follows:

$$\underline{y}_o = \sum_1^n \alpha_i x_i \qquad \cdots\cdots\cdots \text{A.1.4(4)}$$

If C_k is the division constant, the k^{th} iteration corresponds to:

$$C_k y_k = \sum_{k=1}^{n} \alpha_i \lambda_i{}^k x_i \qquad \cdots\cdots\cdots \text{A.1.4(5)}$$

The vector $\underline{y}_k$ therefore tends to the largest vector $\underline{x}_1$

The division constant tends to the largest eigenvalue $\lambda_1 = w_1^2$

Example:

$$\begin{pmatrix} x_1 \\ x_2 \\ x_3 \end{pmatrix} = 1/(w)^2 \begin{pmatrix} 4 & 2 & 1 \\ 4 & 8 & 4 \\ 4 & 8 & 7 \end{pmatrix} \begin{pmatrix} x_1 \\ x_2 \\ x_3 \end{pmatrix}$$

For the first iteration let $x_1 = 1$, $x_2 = 2$, $x_3 = 4$.

After the first three iterations

$$\begin{pmatrix} 1 \\ 2 \\ 4 \end{pmatrix} = 12/(w)^2 \begin{pmatrix} 1 \\ 3 \\ 4 \end{pmatrix}$$

Finally

$$\begin{pmatrix} 1 \\ 3.2 \\ 4 \end{pmatrix} = 14.4/3(w)^2 \begin{pmatrix} 1 \\ 3.18 \\ 4 \end{pmatrix}$$

which gives

$w^2 = 14.4/3$ and a value for the eigenvector of:

$$\begin{pmatrix} 1 \\ 3.18 \\ 4 \end{pmatrix}$$

Evaluation of the subdominant roots.

To find the subdominant roots, the highest root must first be removed from the matrix. For asymmetrical matrices the highest root λ_1 and the vector $\underline{x}_1$ can be removed by 'partitioning' the matrix.

A is written in the form $A = \begin{pmatrix} p_1^1 \\ B \end{pmatrix}$ ... A.1.4.(6)

where p_1^1 is the first row of A. The known vector x_1 is normalised so that its first component is unity. The matrix A_1 is then computed using the relationship:

$$A_1 = a - x_1 p_1^1 \quad \ldots \quad \text{A.1.4.(7)}$$

The latent roots of A_1 are the same as those of A, except that the dominant root λ_1 has become zero.

The first row of A_1 is zero throughout, and since each of the latent vectors $\underline{x}_1$ to $\underline{x}_i$ of A_1 has a zero component in the first position, it is only necessary to work with the matrix of order (n - 1) in the bottom right hand corner of A_1. Hence the order of the matrix is reduced by unity as each root is computed. For the computation of the required vector it is necessary to find the latent vector of $\underline{y}_2$ of the $(n - 1) \times (n - 1)^{th}$ matrix obtained from A_1 and extend it to order n by giving it a zero first component. The latent vector $\underline{x}_2$ of A corresponding to $\underline{y}_2$ is then given by the equation

$$\underline{x}_2 = \underline{x}_1 + k\underline{y}_2 \qquad \ldots \qquad \text{A.1.4.(8)}$$

The latent root λ_2 is given by the equation:

$$\lambda_2 = \lambda_1 + k p_1^1 \underline{y}_2 \qquad \ldots\ldots\ldots \qquad \text{A.1.4(9)}$$

Example: Consider the matrix

$$A = \begin{pmatrix} 2 & 3 & 2 \\ 10 & 3 & 4 \\ 3 & 6 & 1 \end{pmatrix}$$

A root and vector of this matrix are

$$\lambda = -2 \quad \text{and} \quad \underline{x} = \begin{pmatrix} 1 \\ 2 \\ -5 \end{pmatrix} \quad \text{respectively.}$$

Normalising $\underline{x}$ so that its largest component is unity, $\underline{x}$ becomes

$$\underline{x} = \begin{pmatrix} -.2 \\ -.4 \\ 1.0 \end{pmatrix}$$

The last row of A is therefore used in the root removal process and

$$A_1 = \begin{pmatrix} 2.6 & 4.2 & 2.2 \\ 11.3 & 5.4 & 4.4 \\ 0 & 0 & 0 \end{pmatrix}$$

since the latent vectors of A_1 all have zero in their last row, it is necessary to work only with vectors of order two and the matrix:

$$\begin{pmatrix} 2.6 & 4.2 \\ 11.3 & 5.4 \end{pmatrix}$$

A latent vector of this matrix is the vector $\begin{pmatrix} -3 \\ 4 \end{pmatrix}$. Its corresponding latent root is equal to -3.

Normalising the vector gives $\begin{pmatrix} -.75 \\ 1.0 \end{pmatrix}$ and using the last row root removal process yields the following matrix

$$\begin{pmatrix} 11 & 8.25 \\ 0 & 0 \end{pmatrix}$$

The last latent root is clearly 11.

Therefore the roots are -2, -3 and 11. The corresponding latent vectors are

$$\begin{pmatrix} -.2 \\ -.4 \\ 1.0 \end{pmatrix} \; ; \; \begin{pmatrix} -.75 \\ 1.0 \end{pmatrix} \; : \; \begin{pmatrix} 1.0 \end{pmatrix} \quad \text{respectively.}$$

The above technique is used to calculate the natural frequencies of the undamped coupled vibration model of the motor vehicle in fig. 3.1. The calculations are performed on a digital computer using the programme 'Damper 01' (Appendix A.1.5.).

COMPUTOR PROGRAMME IN ALGOL 60 USED TO SOLVE EQUATIONS A. 1.4 to A .1.1.15 TO GIVE THE THEORETCIAL FREQUENCY RESPONSE CURVES FOR THE DAMPED MATHEMATICAL MODEL. (FIG. 3.1)

```
DAMP14;                                                    [K5,K6,
"BEGIN" "REAL" A1,A2,B,C,D,L,M1,M2,M3,M4,J1,J2,K1,K2,K3,K4,
          V1,V2,V3,V4,V5,V6,K,W;
"INTEGER" I,J;    "INTEGER" "ARRAY" BB[1:20];
"ARRAY" A,B1[1:12,1:12],X,P[1:12],T,Y,Z[1:6];

"REAL" "PROCEDURE" SUM(A,B,C,D,E,F,G);
"VALUE" A,B,C,D,E,F;  "INTEGER" A,B,C,D,E,F;  "ARRAY" G;
"BEGIN"  "REAL" X;  "INTEGER" K;  X:=0;
"IF" A "NE" B  "THEN"
"BEGIN"  "FOR" K:=C "STEP" 1 "UNTIL" D "DO"
   X:=X + G[E,K]*G[K,F];
"END";  SUM:=X;
"END";

J:=1;  INSTRING(BB,J);
J:=1;  "PRINT" ``L2'',OUTSTRING(BB,J);
"READ" A1,B,C,D,L,M1,M2,M3,M4,J1,J2,K1,K2,K3,K4,K5,K6,
       V1,V2,V3,V4,V5,V6,P[6];
"FOR" K:=.25 "STEP" .25 "UNTIL" 4.1,5 "STEP" 1 "UNTIL"
         30.1,40,60,80,100 "DO"
"BEGIN"  W:=K*3.1416;
"PRINT" SAMELINE,``L2'SOLUTION CORRESPONDING  TO W =',
        FREEPOINT(4),W,``L'';
A[1,1]:=(K1+K2-M1*W*W);  A[1,2]:=-W*(V1+V2);
A[1,3]:=-(K1+K2);  A[1,4]:=W*(V1+V2);
A[1,5]:=A[1,6]:=A[1,7]:=A[1,8]:=0;
A[1,9]:=K1*A1-K2*B;  A[1,10]:=-W*(V1*A1-V2*B);
A[1,11]:=-(K1*C+K2*L);  A[1,12]:=W*(V1*C+V2*L);
A[2,1]:=W*(V1+V2);  A[2,2]:=(K1+K2-M1*W*W);
A[2,3]:=-W*(V1+V2);  A[2,4]:=-(K1+K2);
A[2,5]:=A[2,6]:=A[2,7]:=A[2,8]:=0;
A[2,9]:=W*(V1*A1-V2*B);  A[2,10]:=(K1*A1-K2*B);
A[2,11]:=-W*(V1*C+V2*L);  A[2,12]:=-K1*C-K2*L;
A[3,1]:=-(K1+K2);  A[3,2]:=W*(V1+V2);
A[3,3]:=K1+K2+K3+K4-M2*W*W;  A[3,4]:=-W*(V1+V2+V3+V4);
A[3,5]:=-K3;  A[3,6]:=W*V3;
A[3,7]:=-K4;  A[3,8]:=W*V4;
A[3,9]:=(K2*B-K1*A1);  A[3,10]:=W*(V1*A1-V2*B);          [-V3*C);
A[3,11]:=(K1+K3)*C+K2*L-K4*D;  A[3,12]:=W*(V4*D-V1*C-V2*L
A[4,1]:=-W*(V1+V2);  A[4,2]:=-(K1+K2);
A[4,3]:=(V1+V2+V3+V4)*W;  A[4,4]:=K1+K2+K3+K4-M2*W*W;
A[4,5]:=-W*V3;  A[4,6]:=-K3;
A[4,7]:=-W*V4;  A[4,8]:=-K4;
A[4,9]:=W*(V2*B-V1*A1);  A[4,10]:=K2*B-K1*A1;            [-K4*D;
A[4,11]:=W*((V1+V3)*C+V2*L-V4*D);  A[4,12]:=(K1+K3)*C+K2*L
A[5,1]:=A[5,2]:=A[5,7]:=A[5,8]:=A[5,9]:=A[5,10]:=0;
```

CONTINUED.

```
A[5,3]:=-K3;   A[5,4]:=W*V3;
A[5,5]:=K3+K5-M3*W*W;    A[5,6]:=-W*(V3+V5);
A[5,11]:=-K3*C;    A[5,12]:=W*C*V3;
A[6,1]:=A[6,2]:=A[6,7]:=A[6,8]:=A[6,9]:=A[6,10]:=0;
A[6,3]:=-W*V3;     A[6,4]:=-K3;
A[6,5]:=W*(V3+V5);    A[6,6]:=K3+K5-M3*W*W;
A[6,11]:=-V3*C*W;    A[6,12]:=-K3*C;
A[7,1]:=A[7,4]:=A[7,5]:=A[7,6]:=A[7,2]:=A[7,9]:=A[7,10]:=0;
A[7,4]:=W*V4;     A[7,3]:=-K4;
A[7,7]:=K4+K6-M4*W*W;   A[7,8]:=-W*(V4+V6);
A[7,11]:=K4*D;   A[7,12]:=-V4*D*W;
A[8,2]:=A[8,1]:=A[8,5]:=A[8,6]:=A[8,9]:=A[8,10]:=0;
A[8,11]:=V4*D*W;    A[8,12]:=K4*D;
A[8,3]:=-W*V4;     A[8,4]:=-K4;
A[8,7]:=W*(V4+V6);   A[8,8]:=K4+K6-M4*W*W;
A[9,1]:=K2*B-K2*A1;   A[9,2]:=W*(V1*A1-V2*B);
A[9,3]:=K1*A1-K2*B;   A[9,4]:=W*(V2*B-V1*A1);
A[9,5]:=A[9,6]:=A[9,7]:=A[9,8]:=0;
A[9,9]:=J1*W*W-K1*A1*A1-K2*B*B;   A[9,10]:=W*(V1*A1*A1+V2*B*B);
A[9,11]:=K1*A1*C-K2*L*B;   A[9,12]:=W*(V2*L*B-V1*A1*C);
A[10,1]:=W*(V2*B-V1*A1);   A[10,2]:=K2*B-K1*A1;
A[10,3]:=W*(V1*A1-V2*B);   A[10,4]:=K1*A1-K2*B;
A[10,5]:=A[10,6]:=A[10,7]:=A[10,8]:=0;                    [-K2*B*B;
A[10,9]:=-W*(V2*B*B+V1*A1*A1);   A[10,10]:=J1*W*W-K1*A1*A1
A[10,11]:=W*(V1*A1*C-V2*B*L);   A[10,12]:=K1*A1*C-K2*L*B;
A[11,1]:=K1*C+K2*L;     A[11,2]:=-W*(V1*C+V2*L);          [-V4*D);
A[11,3]:=K4*D-K2*L-C*(K1+K3);   A[11,4]:=W*((V3+V1)*C+V2*L
A[11,5]:=K3*C;     A[11,6]:=-V3*C*W;
A[11,7]:=-K4*D;   A[11,8]:=V4*D*W;
A[11,9]:=K1*A1*C-K2*L*B;   A[11,10]:=-W*(V1*A1*C-V2*L*B);
A[11,11]:=J2*W*W-C*C*(K1+K3)-K2*L*L-K4*D*D;
A[11,12]:=W*((V1+V3)*C*C+V2*L*L+V4*D*D);
A[12,1]:=W*(V1*C+V2*L);   A[12,2]:=K1*C+K2*L;          [-K2*L-K3*C;
A[12,3]:=W*(V4*D-C*(V1+V3)-V2*L);   A[12,4]:=K4*D-K1*A1
A[12,5]:=V3*C*W;     A[12,6]:=K3*C;
A[12,7]:=-V4*D*W;   A[12,8]:=-K4*D;
A[12,9]:=W*(V1*A1*C-V2*B*L);   A[12,10]:=K1*A1*C-K2*L*B;
A[12,11]:=-W*(C*C*(V1+V3)+V2*L*L+V4*D*D);
A[12,12]:=J2*W*W-C*C*(K1+K3)-K2*L*L-K4*D*D;

"FOR" J:=1,2,3,4,5,7,8,9,10,11,12 "DO" P[J]:=0;
  "FOR" I:=1 "STEP" 1 "UNTIL" 12 "DO"
  "FOR" J:=1 "STEP" 1 "UNTIL" 12 "DO"
  "BEGIN"
    "IF" J<I "THEN"
     B1[I,J]:=(A[I,J]-SUM(J-1,0,1,J-1,I,J,B1))/B1[J,J] "ELSE"
     B1[I,J]:= A[I,J]-SUM(I-1,0,1,I-1,I,J,B1);
    "IF" I=J "AND" B1[I,J]=0 "THEN"
    "BEGIN" "PRINT" ``L`INDETERMINATE`; STOP;
    "END"
  "END";
```

CONTINUED.

```
    "FOR" J:=1 "STEP" 1 "UNTIL" 12 "DO"
    "BEGIN"  B1[J,J]:=1/B1[J,J];
    "END";
    "FOR" I:=1 "STEP" 1 "UNTIL" 12 "DO"
    "FOR" J:=1 "STEP" 1 "UNTIL" 12 "DO"
    "BEGIN"
      "IF" J<I "THEN" B1[I,J]:=-B1[I,J]-SUM(I,J+1,J+1,I-1,I,J,B1)
      "ELSE" "IF" I"NE"J "THEN" B1[I,J]:=-B1[J,J]*SUM(I,I+1,I,
    "END";                                                    J-1,I,
    "FOR" I:=1 "STEP" 1 "UNTIL" 12 "DO"                       J,B1);
  "BEGIN"  A2:=0;
      "FOR" J:=1 "STEP" 1 "UNTIL" 12 "DO"
      "BEGIN"
        "IF" J<I "THEN" B1[I,J]:=SUM(I,I+1,I,12,I,J,B1)
        "ELSE" B1[I,J]:=B1[I,J] +SUM(J,12,J+1,12,I,J,B1);
        A2:=A2+B1[I,J]*P[J];
      "END";
      "PRINT" ``L`X`,SAMELINE,DIGITS(2),I,` =`,SCALED(4),A2;
      X[I]:=A2;
    "END";
  "PRINT" ``L2`     Z                Y                T`;
  "FOR" J:=1 "STEP" 1 "UNTIL" 6 "DO"
  "BEGIN"
      Z[J]:=SQRT(X[2*J-1]↑2 + X[2*J]↑2);
      T[J]:=ARCTAN(X[2*J]/X[2*J-1]);
      Y[J]:=Z[J]*W*W;
      "PRINT" SCALED(4),Z[J],``S4``,SAMELINE,Y[J],``S4``,T[J];
  "END"

"END"

"END";
```

A. 1.5.

COMPUTOR PROGRAMME IN ALGOL 60 TO EVALUATE THE COUPLED UNDAMPED NATURAL FREQUENCIES OF THE THEORETICAL MODEL.(FIG.3.1)

```
DAMP01:
"BEGIN" "REAL" C1,C2,A1,B,C,D,L,M1,M2,M3,M4,J1,J2,K1,K2,K3,K4,
"INTEGER" I,J,M,N;   "INTEGER" "ARRAY" BB[1:30];          K5,K6;
"ARRAY" A,AA,B1[1:6,1:6],P,W,Y,Z[1:6];
"SWITCH" SS:=AGAIN,LOOP;

"REAL" "PROCEDURE" SUM(A,B,C,D,E,F,G);
"VALUE" A,B,C,D,E,F;  "INTEGER" A,B,C,D,E,F;  "ARRAY" G;
"BEGIN"  "REAL" X;  "INTEGER" K;  X:=0;
"IF" A "NE" B  "THEN"
"BEGIN"  "FOR" K:=C "STEP" 1 "UNTIL" D "DO"
   X:=X + G[E,K]*G[K,F];
"END";  SUM:=X;
"END";

J:=1;  INSTRING(BB,J);  J:=1;  "PRINT" ``L2``,OUTSTRING(BB,J),
"READ" A1,B,C,D,L,M1,M2,M3,M4,J1,J2,K1,K2,K3,K4,K5,K6;    ``L``;
N:=6;
A[1,1]:=(K1+K2)/M1;   A[1,2]:=-A[1,1];   A[1,3]:=0;
A[1,4]:=0;   A[1,5]:=(K1*A1-K2*B)/M1;   A[1,6]:=-(K1*C+K2*L)/M1;
A[2,1]:=-(K1+K2)/M2;  A[2,2]:=(K1+K2+K3+K4)/M2;  A[2,3]:=-K3/M2;
A[2,4]:=-K4/M2;  A[2,5]:=(K2*B-K1*A1)/M2;
A[2,6]:=(C*(K1+K3)+K2*L-K4*D)/M2;
A[3,1]:=0;   A[3,2]:=-K3/M3;   A[3,3]:=(K3+K5)/M3;
A[3,4]:=0;   A[3,5]:=0;   A[3,6]:=-K3*C/M3;
A[4,1]:=0;   A[4,2]:=-K4/M4;   A[4,3]:=0;
A[4,4]:=(K4+K6)/M4;   A[4,5]:=0;   A[4,6]:=K4*D/M4;
A[5,1]:=(K1*A1-K2*B)/J1;   A[5,2]:=-(K1*A1-K2*B)/J1;
A[5,3]:=0;   A[5,4]:=0;
A[5,5]:=(K1*A1*A1+K2*B*B)/J1;  A[5,6]:=(K2*L*B-K1*A1*C)/J1;
A[6,1]:=-(K1*C+K2*L)/J2;  A[6,2]:=(C*(K1+K3)+L*K2-D*K4)/J2;
A[6,3]:=-K3*C/J2;   A[6,4]:=K4*D/J2;   A[6,5]:=
A[6,6]:=(C*C*(K1+K3)+L*L*K2+D*D*K4)/J2;   -(K1*A1*C-K2*L*B)/J2;
"FOR" I:=1 "STEP" 1 "UNTIL" 6 "DO"
"FOR" J:=1 "STEP" 1 "UNTIL" 6 "DO"
  AA[I,J]:=A[I,J];

AGAIN:  M:=0;   C1:=0;
"FOR" I:=1 "STEP" 1 "UNTIL" N "DO" Y[I]:=1/I;
LOOP:
"FOR" I:=1 "STEP" 1 "UNTIL" N "DO"
"BEGIN"  Z[I]:=0;
  "FOR" J:=1 "STEP" 1 "UNTIL" N "DO" Z[I]:=Z[I]+A[I,J]*Y[J];
"END";
C2:=Z[1];   M:=M + 1;
"FOR" I:=1 "STEP" 1 "UNTIL" N "DO" Y[I]:=Z[I]/C2;
"IF" ABS((C2-C1)/C2)>.0001 "AND" M<1000 "THEN"
"BEGIN"
  C1:=C2;  "GOTO" LOOP;
"END";
```

```
"IF" M>999 "THEN" "PRINT" ^^L`NOT CONVERGENT`;
W[7-N]:=SQRT(C2);
"FOR" J:=1 "STEP" 1 "UNTIL" N "DO" P[J]:=A[1,J];
"FOR" I:=2 "STEP" 1 "UNTIL" N "DO"
"FOR" J:=2 "STEP" 1 "UNTIL" N "DO"
A[I-1,J-1]:=A[I,J]-Y[I]*P[J];
N:=N-1;  "IF" N>0 "THEN" "GOTO" AGAIN;

"FOR" N:=1 "STEP" 1 "UNTIL" 6 "DO"
"BEGIN"
  "FOR" I:=2 "STEP" 1 "UNTIL" 6 "DO"
  "FOR" J:=2 "STEP" 1 "UNTIL" 6 "DO"
  "BEGIN"
    "IF" I=J "THEN" A[I-1,J-1]:=CHECKR(AA[I,J]-W[N]*W[N])
            "ELSE" A[I-1,J-1]:=AA[I,J];
  "END";
  "FOR" J:=2 "STEP" 1 "UNTIL" 6 "DO" P[J-1]:=-AA[1,J];
  "FOR" I:=1 "STEP" 1 "UNTIL" 5 "DO"
  "FOR" J:=1 "STEP" 1 "UNTIL" 5 "DO"
  "BEGIN"
    "IF" J<I "THEN"
     B1[I,J]:=CHECKR((A[I,J]-SUM(J-1,0,1,J-1,I,J,B1))/B1[J,J])
     B1[I,J]:=CHECKR( A[I,J]-SUM(I-1,0,1,I-1,I,J,B1)); [ "ELSE"
    "IF" I=J "AND" B1[I,J]=0 "THEN"
    "BEGIN" "PRINT" ^^L`INDETERMINATE`; STOP;
    "END"
  "END";
  "FOR" J:=1 "STEP" 1 "UNTIL" 5 "DO"
  "BEGIN"  B1[J,J]:=1/B1[J,J];
  "END";
  "FOR" I:=1 "STEP" 1 "UNTIL" 5 "DO"
  "FOR" J:=1 "STEP" 1 "UNTIL" 5 "DO"
  "BEGIN"
    "IF" J<I "THEN" B1[I,J]:=-B1[I,J]-SUM(I,J+1,J+1,I-1,I,J,B1)
    "ELSE" "IF" I"NE"J "THEN" B1[I,J]:=-B1[J,J]*SUM(I,I+1,I,J-1,
  "END";                                                  [I,J,B1).
  "PRINT" ^^L2`SOLUTION CORRESPONDING TO W`,SAMELINE,DIGITS(1),
          N,` =`,ALIGNED(3,2),W[N],^^L2`X 1 = K`;
  "FOR" I:=1 "STEP" 1 "UNTIL" 5 "DO"
"BEGIN"  A1:=0;
    "FOR" J:=1 "STEP" 1 "UNTIL" 5 "DO"
    "BEGIN"
      "IF" J<I "THEN" B1[I,J]:=SUM(I,I+1,I,6,I,J,B1)
      "ELSE" B1[I,J]:=B1[I,J] +SUM(J,6,J+1,6,I,J,B1);
      A1:=A1+B1[I,J]*P[J];
    "END";
    "PRINT" ^^L`X`,SAMELINE,DIGITS(1),I+1,` =`,SCALED(4),A1,` * K`;
  "END"
"END"
"END";
```

APPENDIX A.2. - CALCULATIONS.

A.2.1. The equivalent linear velocity conscious damping rates for the test vehicle.

The theory (Chapter 3.2.) shows how non-linear velocity conscious damping rates and Coulomb damping constants may be transformed to linearly velocity-conscious rates.

1. The equivalent linear viscous damper (v_1) in parallel with the front engine/transmission spring (k_1).

(i) The hydraulic component. (v_{h1}).

The characteristic of the hydraulic damper (No. 64054600 AA X 016) is shown in fig. 4.12. This particular rate was chosen after the theoretical study of the damping requirement to make the engine/transmission mass most effective as a dynamic absorber in reducing vehicle 'shake' (reference Appendix A.4.) and also as a result of the work reported in references 7 and 17. On the test vehicle hydraulic dampers of rate 20 lbf./in./sec. are installed across the near-side and off-side front engine mounts (see figs. 4.4. and 4.5.). Extension and compression rates are the same and approximately linear. Therefore v_{h1} = 40 lbf./in./sec.

(ii) The hysteretic component. (v_{i1}).

For natural rubber the damping factor = .05 (reference Chapter 3.5.). If the engine/transmission mass is considered as a single degree of freedom system constrained to move only in the

'z' direction then

$$v_{il} = \cdot 05.2\sqrt{k_1 m_8} \text{ lbf/in/sec (ref. eq. 3.4(2)).}$$

$$v_{il} = \cdot 05.2.\sqrt{2720. \cdot 855}$$

$$v_{il} = 4 \cdot 8 \text{ lbf/in/sec.}$$

(iii) Total equivalent linear viscous damping rate. (v_1).

The total damping rate is given by equation 3.2.2.(2).

Therefore $v_1 = 40 + 4.8$

$= 44.8$ lbf./in./sec.

2. The equivalent linear viscous damper (v_2) in parallel with the rear transmission mount spring. (k_2).

(i) The hydraulic component. (V_{h2}).

The characteristic of the hydraulic damper (No. 64054600) chosen for the rear engine/transmission mount installation (see fig. 4.3.) is shown in fig. 4.12. This rate was arrived at from the theoretical study of the damping requirement, to make the engine/transmission mass most effective as a 'dynamic absorber', to reduce vehicle 'shake', and also as a result of the findings reported in references 7 and 17. For the experimental tests on the vehicle a damper of rate equal to 4 lbf./in./sec. is installed. Since the damper is inclined at 17 degrees to the vertical, so that adequate road clearance is ensured, the damping rate, in the 'z' direction, is 3.83 lbf./in./sec. Extension and compression rates are the same and approximately linear.

Therefore v_{h2} = 3.83 lbf./in./sec.

(ii) The hysteretic component. (v_{i2}).

Natural rubber is used in the rear mount. Its damping factor = .05 (reference Chapter 3.5.). If m_1 is constrained to move in the z direction only, then

$$v_{i2} = \cdot 05.2\sqrt{k_2 m_9} \text{ lbf/in/sec.}$$

$$v_{i2} = \cdot 05.2\sqrt{534. \cdot 155}$$

$$v_{i2} = \cdot 91 \text{ lbf/in/sec.}$$

(iii) Total equivalent linear viscous damping rate. (v_2).

The total damping rate is given by equation 3.2.2.(2).

Therefore v_2 = 3.83 + .91

v_2 = 4.74 lbf./in./sec.

3. The equivalent linear viscous damper (v_3) in parallel with the front suspension spring. (k_3).

(i) The hydraulic component. (v_{h3}).

The characteristic of the hydraulic damper, as fitted to the front suspension of the test vehicle, is shown in fig. 4.13. Both the compression rate and extension rates are non-linear and they are not equal. The equivalent linear rate is given by equation 3.2.1.(6).

Considering the experimentally obtained characteristic of the damper, the work done on the extension and compression strokes is calculated by measuring the areas under the rate curves using Simpson's Rule. It is considered that sufficient accuracy

will result if the area is calculated up to 34 in./sec. damper piston velocity (this assumption is made for suspension dampers, front, v_{h3} and rear, v_{h4}).

Applying Simpson's Rule, the work done on the extension stroke, A_E equals

$$4/3\ (10 + 460 + 4\ (25 + 100 + 210 + 333)$$
$$+ 2\ (60 + 150 + 270 + 400)\ )\ \text{lbf. in./sec.}$$

Therefore $A_E = 6550$ lbf. in./sec.

The work done on the compression stroke, A_C

$$A_C = 4/3\ (10 + 140 + 4\ (25 + 72 + 102 + 120)$$
$$+ 2\ (50 + 90 + 112 + 128)\ ) = 2910 \text{ lbf. in./sec.}$$

Therefore $v_{h3} = (6550 + 2910)/34^2$ lbf./in./sec./damper (reference equation 3.2.1.(6)). Now there are two dampers per axle and they are installed on the vehicle at 12 degrees to the vertical.

Therefore $v_{h3} = 2\ (8.2) \cos.78$ degrees lbf./in./sec./axle

$$v_{h3} = 15.9 \text{ lbf./in./sec./axle.}$$

(ii) <u>The hysteretic component</u>. (v_{i3}).

Fig. 4.17. shows the static friction measured in the front suspension of the test vehicle. The average value of the 'stiction' F_3 is $\pm$ 50 lbf. per wheel.

The equivalent linear viscous damping rate is given by equation 3.2.2.(1).

Therefore v_{i3} = 1.27 (50) (2)/34 lbf./in./sec./axle.

v_{i3} = 3.74 lbf./in./sec./axle.

(iii) The total equivalent linear viscous damping rate. (v_3).

This is calculated from equation 3.2.2.(2).

v_3 = 15.9 + 3.74 lbf./in./sec./axle.

v_3 = 19.64 lbf./in./sec./axle.

4. The equivalent linear viscous damper (v_4) in parallel with the rear suspension spring (k_4).

(i) The hydraulic component (v_{h4}).

The characteristic of the hydraulic damper, as fitted to the rear suspension of the test vehicle, is shown in fig. 4.12. Both the compression rate and the extension rate are non-linear and they are not equal. The equivalent linear rate is given by equation 3.2.1.(6).

Using Simpson's Rule, the work done on the extension stroke (A_E) equals:

4/3 (10 + 230 + 4 (30 + 100 + 160 + 190)

+ 2 (75 + 120 + 170 + 210)) lbf. in./sec.

Therefore A_E = 3080 lbf. in./sec.

Using Simpson's Rule, the work done on th e compression stroke (A_C) equals:

4/3 (10 + 15 + 4 (30 + 70 + 80 + 90)

+ 2 (60 + 70 + 85 + 100)) lbf. in./sec.

Therefore A_C = 2450 lbf. in./sec.

Using equation 3.2.1.(6)

$$v_{h4} = (3080 + 2450)/34^2 \text{ lbf./in./sec./wheel.}$$

which gives v_{h4} = 11.32 lbf./in./sec./axle.

(ii) The hysteretic component (v_{i4}).

Fig. 4.18. shows the static friction in the rear suspension. This was measured on the test vehicle using the technique described in Chapter 4.1.2.3.

The average 'stiction' F_4 is $\pm$ 25 lbf./wheel. The equivalent linear viscous damping rate is given by equation 3.2.2.(1).

Using this equation

$$v_{i4} = 1.27\ (25)\ 2/34 \text{ lbf./in./sec./axle.}$$

$$v_{i4} = 1.87 \text{ lbf./in./sec./axle.}$$

(iii) The total equivalent linear viscous damping rate (v_4).

This is calculated from equation 3.2.2.(2).

$$v_4 = 11.32 + 1.87 = 13.19 \text{ lbf./in./sec./axle.}$$

A.2.2. Calculation of the decoupled natural frequencies for the undamped mathematical model of the vehicle (fig. 3.1.).

1. The undamped, decoupled natural frequency (w_3) of the front axle mass (m_3).

This natural frequency is the wheel 'hop' frequency of the front axle, the axle restrained to vibrate only in the z direction.

w_3 is given by equation 3.3.(2). Substituting the relevant system constants from table 3.1. into the equation

$$w_3 = 1/2\pi\sqrt{\frac{1800 + 180}{\cdot 347}} = 12\cdot 03 \text{ Hz.}$$

2. The undamped, decoupled natural frequency (w_4) of the rear axle mass (m_4).

This natural frequency is the wheel 'hop' frequency of the rear axle, the axle restrained to vibrate only in the z direction.

w_4 is given by equation 3.3.(3). Substituting the relevant system constants from table 3.1. into the equation

$$w_4 = 1/2\pi\sqrt{\frac{1800 + 190}{\cdot 55}} = 9\cdot 6 \text{ Hz.}$$

3. The undamped, decoupled natural frequency (w_1) of the engine mass (m_1) in pure bounce on its mounts.

From equation 3.3.(4), substituting the relevant data from table 3.1.

$$w_1 = 1/2\pi\sqrt{\frac{2720 + 534}{1\cdot 01}} = 9 \text{ Hz.}$$

4. The undamped, decoupled natural frequency (w_2) of the body mass (m_2) in pure bounce on the suspension springs.

Substituting the relevant data from table 3.1. into equation 3.3.(5)

$$w_2 = 1/2\pi\sqrt{\frac{180 + 190}{3{\cdot}22}} = 1{\cdot}7 \text{ Hz.}$$

5. The undamped, decoupled natural frequency (w_5) of the body/engine/transmission masses in pure, in phase bounce on the suspension springs.

Substituting the relevant data from table 3.1. into equation 3.3.(6)

$$w_5 = 1/2\pi\sqrt{\frac{180 + 190}{3{\cdot}22 + 1{\cdot}01}} = 1{\cdot}49 \text{ Hz.}$$

6. The undamped, decoupled natural frequency (w_{10}) of the body/engine/transmission/axle masses in pure, in phase bounce on the tyre springs.

Using equation 3.3.(7) and the relevant data from table 3.1.

$$w_{10} = 1/2\pi\sqrt{\frac{1800 + 1800}{3{\cdot}22 + 1{\cdot}01 + {\cdot}347 + {\cdot}55}} = 4{\cdot}33 \text{ Hz.}$$

A.2.3. Calculation of the coupled bounce/pitch natural frequencies of the engine/transmission mass on its mounting springs.

If the engine/transmission mass is constrained so that it can only vibrate vertically, in the z direction, and in rotation about transverse axes, parallel with the y axis (reference fig. 1.1.a), then theory, due to Mather (reference 20), can be used to determine the two coupled natural frequencies for the system and also the position of the transverse pitch axes, relative to a transverse axis through the c. of g.

Using Mather's notation:

Substituting the relevant data from table 3.1.

$p = k_1 + k_2 = 39000$ lbf./ft.

$q = k_1 a - k_2 b = -850$ lbf.

$r = k_1 a^2 + k_2 b^2 = 26290$ lbf. ft.

$q/p = -.0218$ ft.

$r/p = .675$ ft.^{2}

using chart number 6 from reference 20.

$$w_{1,1}/w_1 = 1; \qquad w_{1,2}/w_1 = .6$$

Now $w_1 = 9$ Hz. Therefore $w_{1,1} = 9$ Hz. and $w_{1,2} = 5.4$ Hz.

The position of the pitch axes are determined using chart 7

$$L_{1,1} = -20 \text{ ft.} \qquad L_{1,2} = .05 \text{ ft.}$$

i.e. the transverse pitch axes corresponding to the coupled pitch/bounce frequencies of the engine/transmission mass are located 240 inches behind the c. of g. and .6 inches in front of the c. of g.

A.2.4. Calculation of the coupled bounce/pitch natural frequencies of the body/engine/transmission mass (moving in phase) on the suspension springs.

The masses are considered to move as one 'lumped' body. This will occur on the vehicle, at low excitation frequencies, because of the inherent system damping. The mass is given two degrees of freedom as shown in fig. 1.1.a.

Applying the theory due to Mather, and using the same notation, substituting data from table 3.1.

$p = k_3 + k_4 = 4440$ lbf./ft.

$q = k_3c - k_4d = 600$ lbf.

$r = k_3c^2 + k_4d^2 = 74900$ lbf.ft.

$q/p = .135$ fit.

$r/p = 1.68$ ft.^{2}

using the chart number 6 from reference 20

$w_{5,1}/w_5 = 1.05$; $w_{5,2}/w_5 = .96$;

Now $w_5 = 1.49$ Hz.

Therefore $w_{5,1} = 1.56$ Hz. and $w_{5,2} = 1.43$ Hz.

The position of the coupled mode pitch axes are determined from chart 7 of reference 20.

$L_{51} = -1.56$ ft. $L_{52} = 1.1$ ft.

i.e. the pitch axes are located 18 inches behind the vehicle's c. of g. and 13.2 inches in front of the c. of g.

A.2.5. Calculation of the damping factors associated with the decoupled vibration of the mathematical model.

1. The damping factor (η_3), in the wheel 'hop' mode, for the front axle mass (m_3) in pure bounce on the tyre and suspension springs.

η_3 is defined by equation 3.4.(3). Substituting the relevant data from table 3.1. into the equation and using the calculated value for w_3 from page 157

$$\eta_3 = \frac{2.\pi(12\cdot03)29\cdot64}{2.(1980)} = \cdot566$$

2. The damping factor(η_4), in the wheel 'hop' mode, for the rear axle mass (m_4) in pure bounce on the tyre spring and suspension spring.

η_4 is given by equation 3.4.(4). Substituting the relevant data from table 3.1. into the equation and the value of w_4 from page 157

$$\eta_4 = \frac{2\pi(9\cdot6)23\cdot19}{2.(1990)} = \cdot35$$

3. The damping factor (η_5), in the body 'float' mode, for the engine/transmission/body masses in pure in phase bounce on the suspension springs.

η_5 is defined by equation 3.3.(7) Substituting the relevant data and the calculated value for w_5 from table 3.1. and page 158 respectively into the equation:

$$\eta_5 = \frac{2\pi(1{\cdot}49)(19{\cdot}64 + 13{\cdot}19)}{2(370)} = {\cdot}416$$

4. The damping factor (η_1) for the engine/transmission mass in pure bounce on its mounting rubbers.

η_1 is given by the equation 3.4.(6) Substituting the relevant data and the calculated value for w_1 from table 3.1. and page 157 respectively.

$$\eta_1 = \frac{2\pi.9(44{\cdot}8 + 4{\cdot}74)}{2(2720 + 534)} = {\cdot}43$$

A.2.6. Calculation of the effective mass (m_7) of the non-rigid body structure which supports the vehicle engine/transmission mass.

The dominant theoretical natural frequency of the engine/transmission mass, resonating on its mounting springs, is equal to 11.7 Hz. (see Chapter 3.7.5.). The frequency, in practice, will be somewhat different from that predicted by this theoretical calculation because the engine/transmission mass is not mounted on a rigid 'foundation'. Hartog (reference 12) shows that the natural frequency of the mass m_1, on the springs k_1 and k_2, for a non-rigid foundation, will be modified by a factor

equal to $\{(m_1 + m_7)/(m_7)\}^{\frac{1}{2}}$. m_7 is the effective mass of the vehicle body structure which supports the engine/transmission springs (see fig. A.4.1.). From the experimental 'transfer mobility' characteristics for m_1 (see fig. 4.30) the natural frequency w_1 can be identified at 15 Hz.

Therefore from the above

$$15^2 = (11{\cdot}7)^2.(m_1 + m_7) \ /m_7 \ \text{Hz.}$$

i.e. $$m_7 = \frac{(11.7)^2.\ m_1}{(15^2 - 11.7^2)} \quad \text{lbf./in./sec.}^2$$

substituting $m_1 = 1.01$ lbf./in./sec.^{2} (= 390 lbf.) (see table 3.1.) gives:

$m_7 = 1.575$ lbf./in./sec. (= 606 lbf.)

APPENDIX A.3. - THE OPTIMUM DAMPING FOR A PASSENGER CAR SUSPENSION.

A.3.1. A theoretical analysis, in the steady state, of a two degree of freedom system, which represents one corner of the motor vehicle (fig. A.3.1.), to determine the optimum value of the suspension damping ratio to give:

(a) The best riding comfort;

(b) The best wheel to road adhesion or riding safety.

Theory.

The mathematical analysis is the same as described in Chapter 3.1.1., with the number of degrees of freedom reduced from six to two. The two degree of freedom system in fig. A.3.1. is constrained to move vertically in the 'z' direction only. Analysis is carried out in the frequency domain.

Equations of motion

The equations of motion are evolved by considering each mass, in turn, as a 'free body' and applying Newton's Laws.

Vertical motion of the unsprung mass $(m_3/2)$

$$(m_3/2)\,\ddot{z}_3 + ((v_3 + v_5)/2)\,\dot{z}_3 + ((k_3 + k_5)/2)\,z_3 - (v_3/2)\,\dot{z}_2 - (k_3/2)\,z_2 = (P_3/2)\sin. wt. \quad \ldots \quad A.3.(1)$$

Vertical motion of the sprung mass $(m_5/2)$

$$(m_5/2)\,\ddot{z}_2 + (v_3/2)\,\dot{z}_2 + (k_3/2)\,z_2 - (v_5/2)\,\dot{z}_3 - (k_3/2)\,z_3 = 0 \quad \ldots \quad A.3.(2)$$

Assuming harmonic solutions of the form

$$z_2 = x_3 \text{ sin. } wt. + x_4 \text{ cos. } wt. \quad \ldots \quad A.3.(3)$$

$$z_3 = x_1 \text{ sin. } wt. + x_2 \text{ cos. } wt. \quad \ldots \quad A.3.(4)$$

Equating the sin. and cos. terms to zero, in turn, in the equations which result, yields the following equations:

$$x_1 w (v_3 + v_5) + x_2 (k_3 + k_5 - m_3 w^2 - x_3 v_3 w - x_4 k_3 = 0 \quad \ldots \quad A.3.(5)$$

$$x_1 (k_3 + k_5 - m_3 w^2) - x_2 w (v_3 + v_5) - x_3 k_3 + x_4 v_3 w = P_3 \quad \ldots \quad A.3.(6)$$

$$- x_1 w v_3 - x_2 k_3 + x_3 v_3 w + x_4 (k_3 - m_5 w^2) = 0 \quad \ldots \quad A.3.(7)$$

$$- x_1 k_3 + x_2 v_3 + x_3 (k_3 - m_5 w^2) - x_4 v_3 = 0 \quad \ldots \quad A.3.(8)$$

The computer programme 'Damper 16' (Appendix A.3.2.) is used to solve the simultaneous equations A.3.(5) to A.3.(8). The theory of solution is due to Choleski (see Appendix A.1.2.). Vehicle riding comfort is determined by the level of the sprung mass acceleration ($\ddot{z}_2$), for a given vibration frequency (see 1.3.1.) and the 'riding safety' is determined by the level of dynamic to static wheel loads, which in turn is proportional to the wheel displacement (z_3) (reference 22).

The values of $\ddot{z}_2$ and z_3 for a given vibration frequency are given by the following equations:

$$\ddot{z}_2 = \sqrt{x_3^2 + x_4^2} \cdot w^2 \quad \ldots\ldots\ldots \quad A.3(9)$$

$$z_3 = \sqrt{x_1^2 + x_2^2} \quad \ldots\ldots\ldots \quad A.3(10)$$

Results and Calculations

To enable the assessment of the effect of different values of suspension damping on 'ride' and 'safety', typical fixed values are given to the other parameters of the mathematical model. These are substituted into the equations of motion for the computer analysis.

Values given to the system parameters (typical of a passenger car, of 2000 lb. gross weight):

$k_5/2$	(tyre rate)	= 1000 lbf./in.
$k_3/2$	(suspension rate at wheel plane)	= 100 lbf./in.
$m_3/2$	(unsprung mass)	= .133 lbf./in./sec.^{2}
$m_5/2$	(sprung mass)	= 1.33 lbf./in./sec.^{2}
$v_5/2$	(damping rate of the tyre)	= 5 lbf./in./sec.
$v_3/2$	(suspension damping rate)	= 1,5,10,15,20 lbf./in./sec.

Fig. A.3.2. shows the sprung mass acceleration ($\ddot{z}_2$) over the frequency range 0 to 20 Hz., for the different suspension damping rates.

Fig. A.3.3. shows the unsprung mass displacement amplitude (z_3) over the frequency range 0 to 20 Hz., for increments of suspension damping rate.

Fig. A.3.4. shows the relative velocity of the sprung mass to the unsprung mass ($\dot{z}_2 - \dot{z}_3$) over the frequency range 0 to 20 Hz., for increments of suspension damping.

The natural frequency (w_3) of the unsprung mass is given by equation 3.3.(2) (in modified form to take account of the fact

that only one corner of the vehicle is being considered).

$$w_3 = 1/2\pi \sqrt{\frac{1000 + 100}{\cdot 133}} = 14\cdot 4 \text{ Hz.}$$

The natural frequency (w_2) of the sprung mass is given by the equation 3.3.(6) (again in modified form)

$$w_2 = 1/2\pi \sqrt{\frac{100}{1\cdot 33}} = 1\cdot 38 \text{ Hz.}$$

The critical damping factor ($\eta_{3\ crit.}$) of the wheel 'hop' resonant condition is given by equation 3.4.(3).

$$\eta_{3\ crit.} = w_3(V_{3crit.w.} + V_5)/2(k_3 + k_5)$$

Substitution of the system constants from above gives

$$V_{3\ crit.w.} = 19.2 \quad \text{lbf./in./sec.}$$

The critical damping factor ($\eta_{3\ crit.}$) of the body resonant condition is given by equation 3.4.(5).

$$\eta_{3crit} = w_2 \cdot V_{3crit.b}/2k_3$$

Substitution of the system constants from above gives

$$V_{3crit.b} = 23 \quad \text{lbf/in/sec.}$$

η_3 referred to the wheel 'hop' mode is given by the equation

$$\eta_{3w} = v_3 / v_{3crit._w} \qquad \text{(reference eqn. 3.4(1))}$$

η_3 referred to the body float mode is given by the equation

$$\eta_{3b} = v_3 / v_{3crit._b} \qquad \text{(reference eqn. 3.4(1))}$$

Discussion

Reference to fig. A.3.2. indicates that best 'riding comfort' in the vehicle, over the frequency range considered, is given with a suspension damping rate of 5 lbf./in./sec. This gives a value of $\eta_{3b} = {}^{5}/_{23} = .22$. Inspection of fig. A.3.3. indicates that the best tyre to road adhesion, over the frequency range considered, is given with a suspension damping rate of 10 lbf./in./sec. This gives a value of $\eta_{3w} = {}^{10}/_{19.2} = .52$. Fig. A.3.4. gives an indication of the wheel velocities and body velocities that can be expected for different levels of suspension damping. (This assumes that the body will have zero vertical velocity at the wheel 'hop' frequency and that the wheel will have zero vertical velocity at the body resonant frequency.)

Conclusions

As a compromise for best 'riding comfort' and best

tyre to road adhesion, the suspension damping factor for a passenger car should be of the order of .35. For this condition, a vertical wheel velocity of 40 inches/sec. can be expected, and a vertical body velocity of 10"/sec. at their respective resonant frequencies.

In the study no account is taken of the differential damping. Compression and extension rates are assumed to be equal.

COMPUTOR PROGRAMME IN ALGOL 60 USED TO SOLVE EQUATIONS NOS. A.3.5 to A.3.8.

```
DAMP16;
"BEGIN" "REAL" A1,Z,M1,M2,K1,K2,C1,C2,K,W;
"INTEGER" I,J;   "INTEGER" "ARRAY" BB[1:25];
"ARRAY" A,B1[1:4,1:4],X,P[1:4];

"REAL" "PROCEDURE" SUM(A,B,C,D,E,F,G);
"VALUE" A,B,C,D,E,F;  "INTEGER" A,B,C,D,E,F;  "ARRAY" G;
"BEGIN"  "REAL" X;  "INTEGER" K;  X:=0;
"IF" A "NE" B  "THEN"
"BEGIN"  "FOR" K:=C "STEP" 1 "UNTIL" D "DO"
   X:=X + G[E,K]*G[K,F];
"END";  SUM:=X;
"END";

J:=1;  INSTRING(BB,J);
J:=1;  "PRINT" ``L2``,OUTSTRING(BB,J);
"READ" M1,M2,K1,K2,C1,C2,P[2];
"FOR" K:=.5 "STEP" .5 "UNTIL" 4.1,5 "STEP" 2 "UNTIL" 30.1,40
"BEGIN"  W:=K*3.1416;                                          "DO"
"PRINT" SAMELINE,``L2`SOLUTION CORRESPONDING  TO W =`,
        FREEPOINT(4),W,``L``;
A[1,1]:=W*(C1+C2);      A[1,2]:=(K1+K2-M1*W*W);
A[1,3]:=-C2*W;          A[1,4]:=-K2;
A[2,1]:=K1+K2-M1*W*W;   A[2,2]:=-W*(C1+C2);
A[2,3]:=-K2;            A[2,4]:=C2*W;
A[3,1]:=-W*C2;          A[3,2]:=-K2;
A[3,3]:=W*C2;           A[3,4]:=K2-M2*W*W;
A[4,1]:=-K2;            A[4,2]:=W*C2;
A[4,3]:=K2-M2*W*W;      A[4,4]:=-C2*W;

"FOR" J:=1,3,4 "DO" P[J]:=0;
  "FOR" I:=1 "STEP" 1 "UNTIL" 4 "DO"
  "FOR" J:=1 "STEP" 1 "UNTIL" 4 "DO"
  "BEGIN"
    "IF" J<I "THEN"
     B1[I,J]:=(A[I,J]-SUM(J-1,0,1,J-1,I,J,B1))/B1[J,J] "ELSE"
     B1[I,J]:= A[I,J]-SUM(I-1,0,1,I-1,I,J,B1);
    "IF" I=J "AND" B1[I,J]=0 "THEN"
    "BEGIN" "PRINT" ``L`INDETERMINATE`; STOP;
    "END"
  "END";
  "FOR" J:=1 "STEP" 1 "UNTIL" 4 "DO"
  "BEGIN"  B1[J,J]:=1/B1[J,J];
  "END";
  "FOR" I:=1 "STEP" 1 "UNTIL" 4 "DO"
  "FOR" J:=1 "STEP" 1 "UNTIL" 4 "DO"
  "BEGIN"
    "IF" J<I "THEN" B1[I,J]:=-B1[I,J]-SUM(I,J+1,J+1,I-1,I,J,B1)
    "ELSE" "IF" I"NE"J "THEN" B1[I,J]:=-B1[J,J]*SUM(I,I+1,I,
  "END";                                                  J-1,I,
  "FOR" I:=1 "STEP" 1 "UNTIL" 4 "DO"                      J,B1);
```

'DAMPER 16' CONTINUED.

```
"BEGIN"  A1:=0;
    "FOR" J:=1 "STEP" 1 "UNTIL" 4 "DO"
    "BEGIN"
      "IF" J<I "THEN" B1[I,J]:=SUM(I,I+1,I,4,I,J,B1)
      "ELSE" B1[I,J]:=B1[I,J] +SUM(J,4,J+1,4,I,J,B1);
      A1:=A1+B1[I,J]*P[J];
    "END";
    "PRINT" ``L`X`,SAMELINE,DIGITS(2),I,` =`,SCALED(4),A1;
    X[I]:=A1;
  "END";
Z:=3.1416*C2*W*((X[3]-X[1])↑2+(X[4]-X[2])↑2);
"PRINT" ``L`Z =`,SAMELINE,SCALED(4),Z;
"END"
"END";
```

Fig.A.3.1.

A two degree of freedom system representing either the front or rear corner of the automobile.

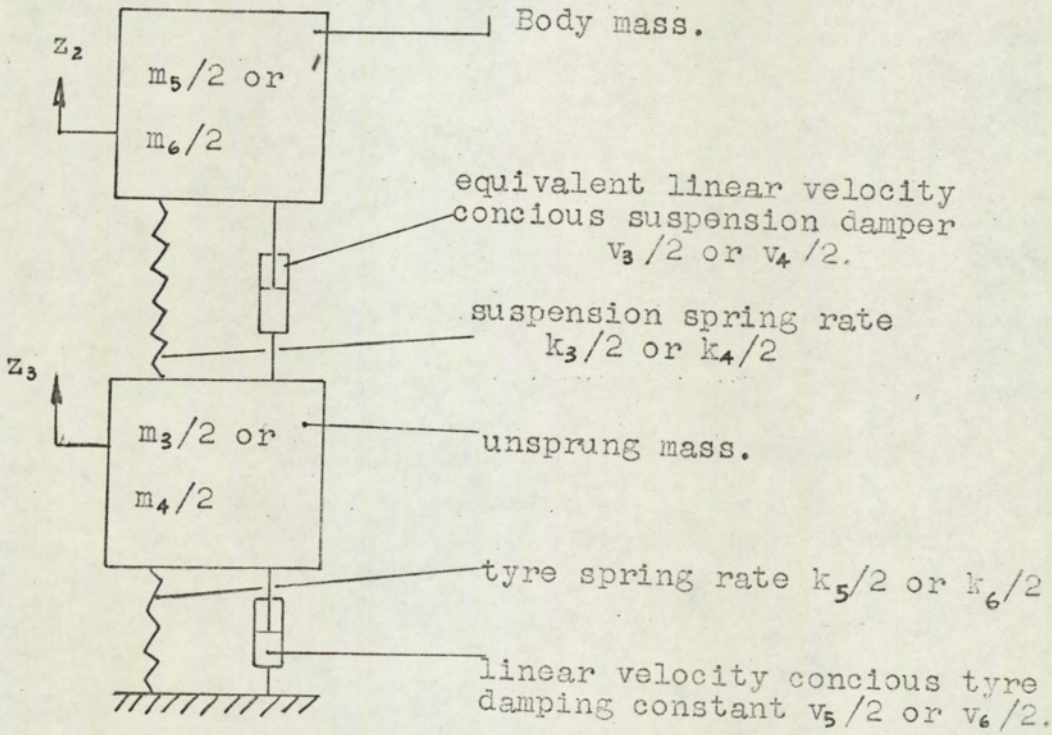

Model constrained to move in the z direction only.

Fig. A.3.2.

Graphs showing the vertical acceleration of the vehicle body mass against forcing frequency for a range of suspension damping constants.

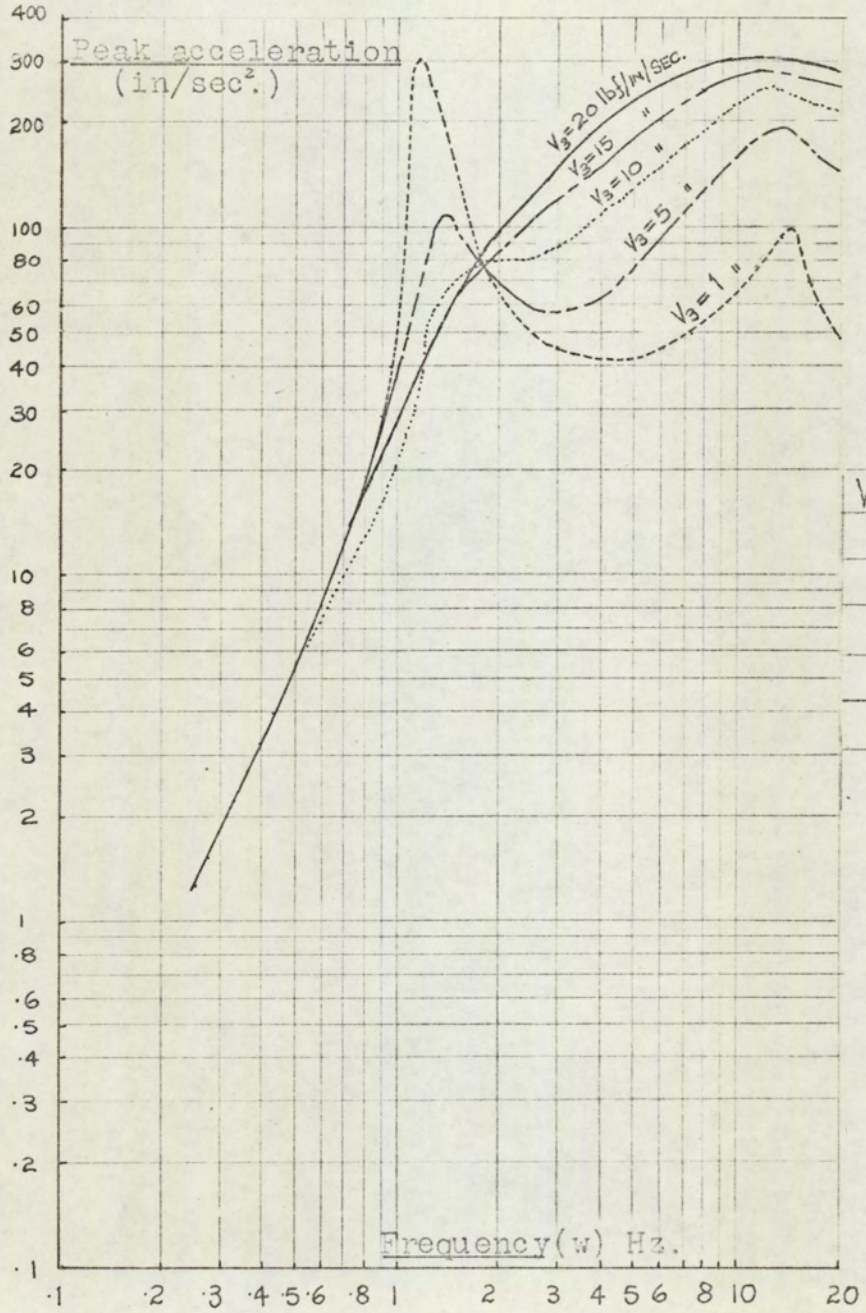

V_3 lbf/in/sec.	η_b	η_w
1	·04	·052
5	·218	·26
10	·434	·52
15	·65	·78
20	·88	1·04

Fig.A.3.3.

Graphs showing the peak absolute displacement of the vehicle unsprung mass against forcing frequency for a range of suspension damping constants.

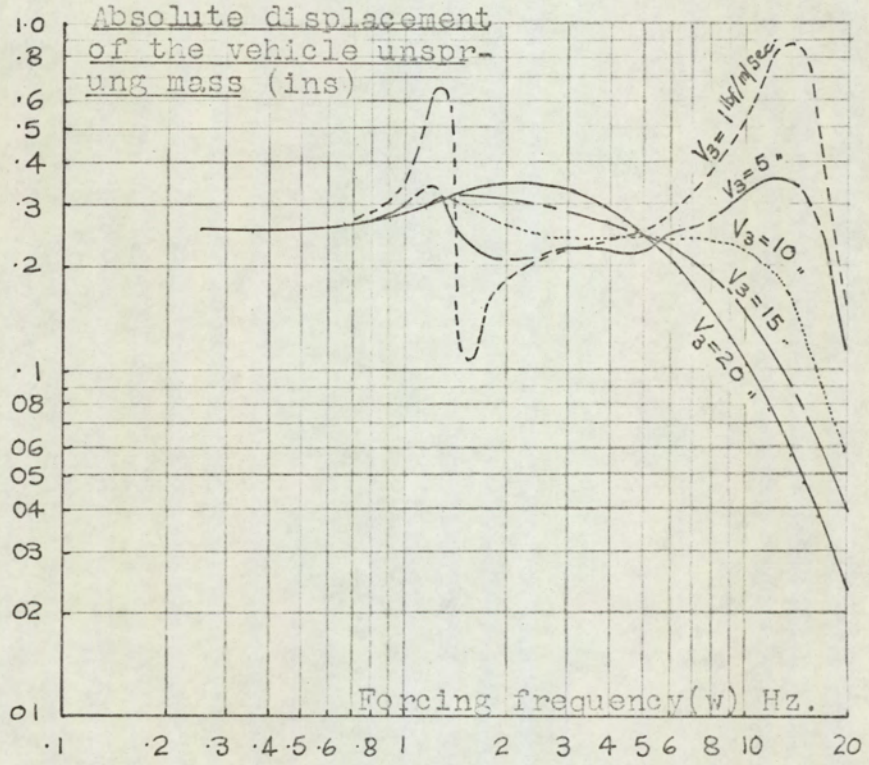

Fig. A.3.4.

Graphs showing the peak suspension damper velocity against forcing frequency for a range ofsuspension damping constants,

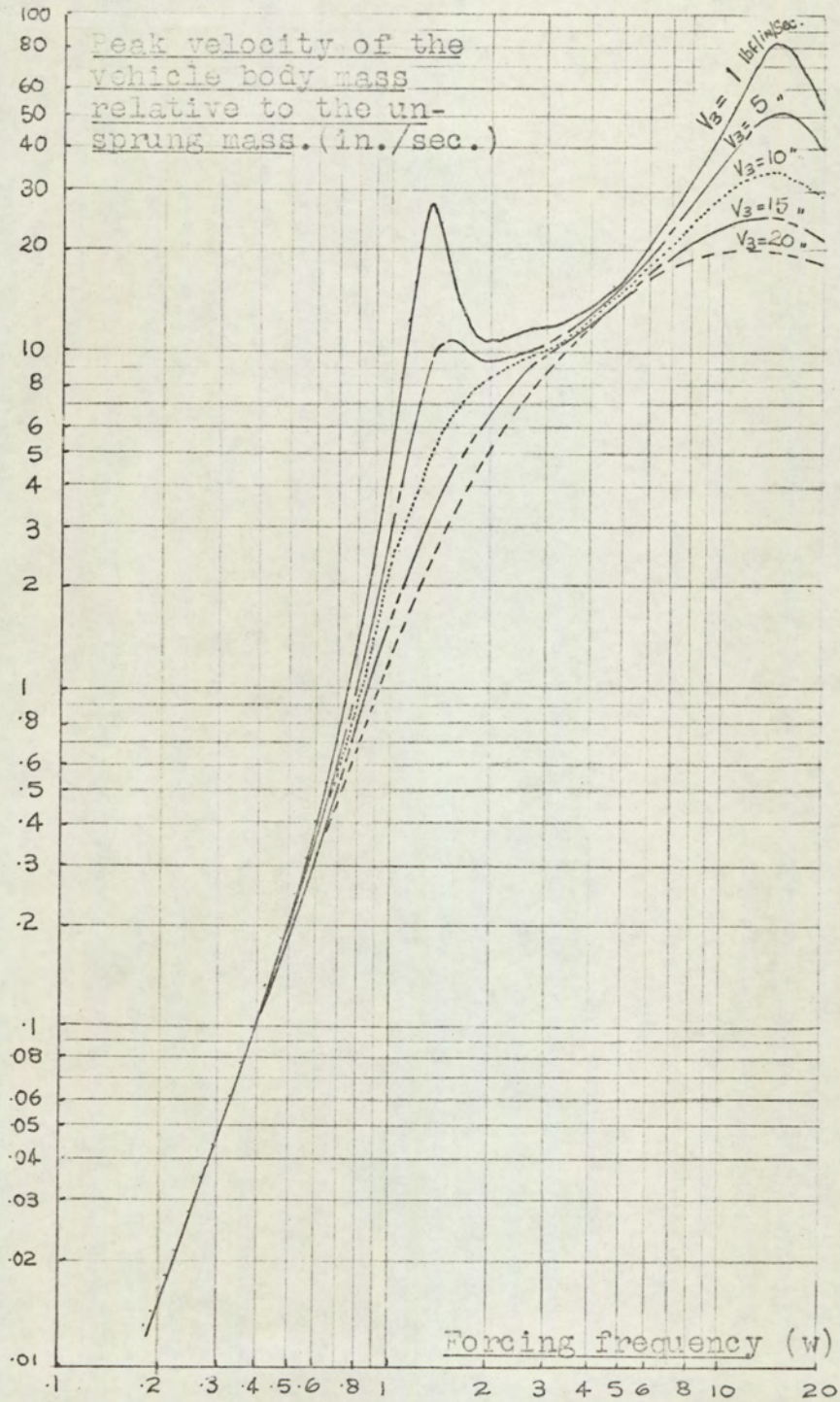

APPENDIX A.4. - CALCULATIONS, USING THE THEORY DUE TO DEN HARTOG (REFERENCE 12), TO ESTABLISH THE OPTIMUM VALUES FOR ENGINE/TRANSMISSION MOUNT SPRING STIFFNESS AND DAMPING RATE, IN THE 'Z' DIRECTION, WHICH MAKE THE ENGINE MASS MOST EFFECTIVE AS A DYNAMIC ABSORBER IN REDUCING VEHICLE 'SHAKE'.

Theory.

For this study a two degree of freedom system, as shown in fig. A.4.1. is considered. m_7 represents the effective mass of the vehicle body structure forward of the centre of gravity of the vehicle. This mass is assumed to have a natural 'shake' frequency of 19 Hz. (This frequency is recorded in the experimental tests and appears as a resonant peak on the graphs figs. 4.30. and 4.31.)

Hartog proves that for a two degree of freedom system which is mathematically identical to fig. A.4.1., the mass m_1 (the engine/transmission mass in this case) is most effective in absorbing the natural frequency of vibration of m_7 when the natural frequency of m_1 on its springs (in the z direction) is equal to $(m_7)/(m_7 + m_1)$ times the natural frequency of m_7 ... A.4.(1)

Hartog, in his theory, goes on to show that the best vibration absorption is achieved with m_1 damped on its springs. Using Hartog's notation, the optimum damping factor($\eta_{(optimum)}$) is calculated using the following equations:

$$z_7 / z_{7(static)} = \sqrt{1 + 2(m_7/m_1)} \quad \text{.....A.4(2)}$$

$$z_7 / z_{7(static)} = \sqrt{\frac{A\eta^2 + B}{C\eta^2 + D}} \quad \text{.....A.4(3)}$$

where $A = 4g^2$; $B = (g^2 - f^2)^2$

$C = 4g^2 (g^2 - 1 + \mu g^2)^2$;

$D = \left(\mu f^2 g^2 - (g^2 - 1)(g^2 - f^2)\right)^2$

$g = {}^{w}/_{w_7}$; $f = {}^{w_1}/_{w_7}$; $\mu = {}^{m_1}/_{m_7}$

and w = forcing frequency (rads./sec.),

w_7 = 'shake' frequency (rads./sec.),

w_1 = the optimum natural frequency of m_1 in pure bounce on its mounts (rads./sec.),

z_7 = the dynamic displacement of m_7 (ins.),

z_7 (static) = the static displacement of m_7 (ins.)

Equations A.4.(2) and A.4.(3) can be equated and rearranged to give a quadratic in g^2.

$$g^4 - 2g^2 \left\{ \frac{1 + f^2 + \mu f^2}{(2 + \mu)} \right\} + \frac{2 f^2}{(2+\mu)} = 0 \quad \text{....A.4(4)}$$

which gives

$$\eta^2(\text{optimum}) = 3\mu/8(1 + \mu)^3 \quad \ldots\ldots \text{A.4(5)}$$

Calculations.

The optimum rate for the engine/transmission mounting springs $(k_1 + k_2)$:

From equation A.4.(1)

$$w_1 \text{ (optimum)} = \frac{19 \times 1.575}{(1.01 + 1.575)} = 11.5 \text{ Hz}$$

where $m_7 = 1.575$ lbf./in./sec.^{2} (reference Appendix A.2.6.)

and $m_1 = 1.01$ lbf./in./sec.^{2} (reference table 3.1.)

The theoretical results from figs. 3.5. and 3.9. show that the dominant frequency of the engine/transmission mass on its mounts (w_1) for the test vehicle equals 11.7 Hz. Therefore in theory the total rate of the engine/transmission mounts, in the z direction, is optimum for the dynamic absorption of the vehicle 'shake' vibration.

The optimum damping factor for the engine suspension system.

From above $\mu = .645$ and $f = .474$.

Substituting the value of μ into equation A.4.(5)

$$\eta^2(\text{optimum}) = (3).645/8 \cdot (1 + .645)^3$$

$$\eta(\text{optimum}) = .223$$

Conclusions.

The value η (optimum) = .223 will not give adequate control of the engine motion, so a value η = .43 has been chosen for the test vehicle,

i.e. v_{1+2} = .43 x 2 x 1.01 x 2 x π x 9.0 lbf./in./sec.

v_{1+2} = 49 lbf./in./sec.

This particular choice of damping was influenced by the work of Kojima, etc. (reference 17) and Engles (reference 7).

Fig. A.4.1.

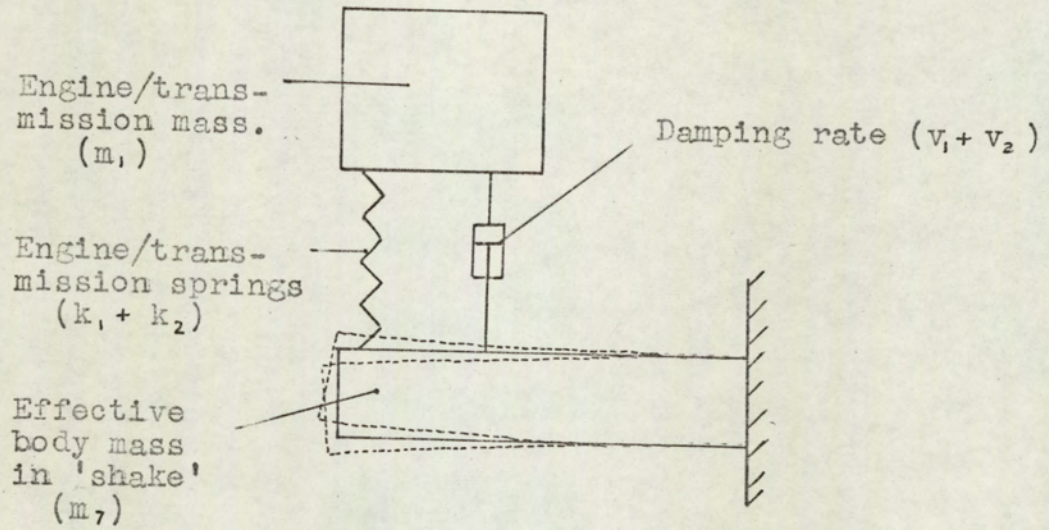

A two degree of freedom system to represent the vehicle engine/transmission mass, its suspension and the 'effective' non rigid body structure support.

APPENDIX A.5. - THE ASSESSMENT OF THE HYDRAULIC PERFORMANCE OF A VELOCITY CONSCIOUS DAMPER, SUBJECTED TO SMALL AMPLITUDE VIBRATIONS, OVER THE FREQUENCY RANGE 1 TO 60 Hz.

Introduction.

During the project it was decided that not enough was known about the low amplitude vibration performance of the Girling 'Monitube' hydraulic damper. Since the 'free' vibrations of the engine are sensibly of low amplitude, it was decided to carry out some low amplitude stroking tests on a damper, using a Dowty electro-hydraulic vibrator made available at Aston University. A damper was subjected to a series of tests using a range of rubber and polyurethane foam end fittings. The experiments conducted gave results showing variation of damper force, for a fixed amplitude of damper piston movement, over the sinusoidal excitation range 0 to 60 Hz.

Equipment and Procedure.

The equipment used for the tests is shown in fig. A.5.1.

The 'Monitube' damper is mounted between the centres of the Dowty vibrator. To prevent the vibrator going unstable, it is necessary to feed back damper piston displacement via a compressor circuit. This circuit keeps the damper piston displacement constant at .01". The force input is measured by means of crystal type load cell. Damper piston displacement is monitored with an inductive displacement transducer. An X-Y

plotter coupled to the transducer amplifier outputs records the log. of the force input against the log. of the forcing frequency, and phase angle between the force input and damper piston displacement, against the log. of the forcing frequency. The equipment is set to sweep through the forcing frequency range 0 to 100 Hz., automatically, for each test. The same damper is used for all tests. Damper'charging pressure' was 400 P.S.I. Tests are carried out using: natural rubber fixing bushes of

(a) 40 degrees 'Shore' hardness and

(b) 65 degrees 'Shore' hardness and

(c) 'Microvon 35' - a polyurethane foam.

Results

Sample X-Y plots of damper 'impedance' and phase shift are shown in fig. A.5.2., for the test using 40 degrees 'Shore' hardness rubber end fittings.

Weight of damper and displacement transducer = 3.7 lb.

Rate of 65 degrees 'Shore' hardness end rubbers (two in series) ... ... = 1380 lb./in.

Rate of 40 degrees 'Shore' hardness and 'Microvon 35' (two in series) ... ... = 900 lb./in.

Calculations

The natural frequency of the damper, resonating vertically on its end fittings as a single degree of freedom system, is 60 Hz. for the 65 degrees 'Shore' hardness end fittings, 49 Hz. for the 40 degrees 'Shore' hardness and 'Microvon 35' end fittings. These

frequencies are arrived at using equation 3.3.(1).

Discussion

A study of the 'impedance' curves shows a sharp reduction in 'impedance' at 60 Hz. for the tests carried out with 65 degrees 'Shore' hardness rubbers, and 50 Hz. for the tests carried out with 40 degrees 'Shore' hardness and 'Microvon 35' rubbers. The phase plots show a phase shift of 180 degrees at these frequencies.

These experimental and calculated results show that if a damper is excited, at its own natural frequency, it becomes ineffective as a damper, at low amplitudes of excitation. This is because the damper acts as a solid strut vibrating on its end rubbers.

Conclusions

If a damper is excited at its own natural frequency, at low excitation amplitudes, when installed on a vehicle, there will be no effective damping from the unit. For suspension dampers weighing in the region of 4 lbs. the frequency at which this phenomenon occurs will be in the range 40 to 60 Hz. This resonance will not be excited by the wheel 'hop' frequency, but may well be excited by the longitudinal tyre resonance, particularly with radial ply tyres. This resonant condition may increase, or be contributory to, passenger compartment 'boom' in the vehicle.

Fig. A.5.1.

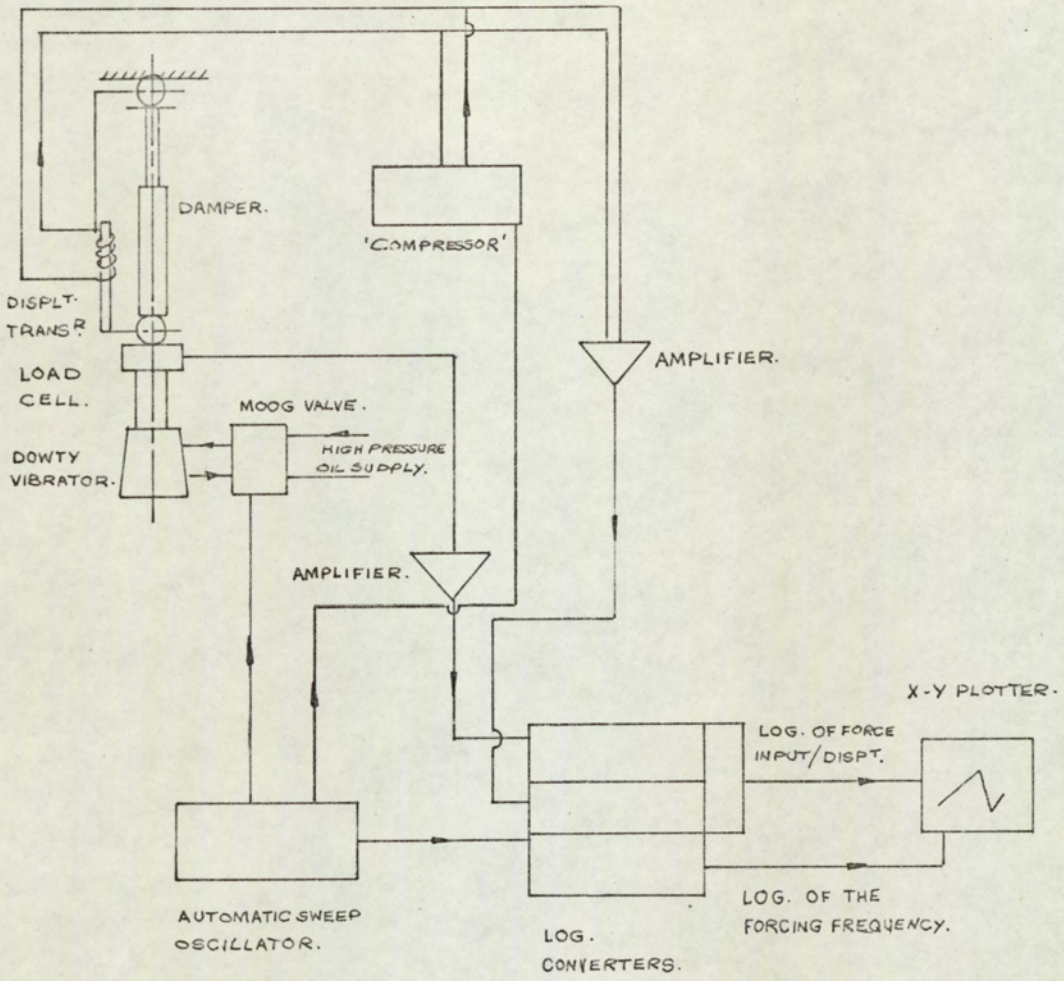

A block diagram of the equipment used to investigate the vibration behaviour of a Girling '28 mm Monitube' hydraulic damper.

Graphs showing the 'impedance' and phase shift for a Girling 28 mm. 'monitube' hydraulic damper, with 40° 'Shore' hardness end fixing bushes.

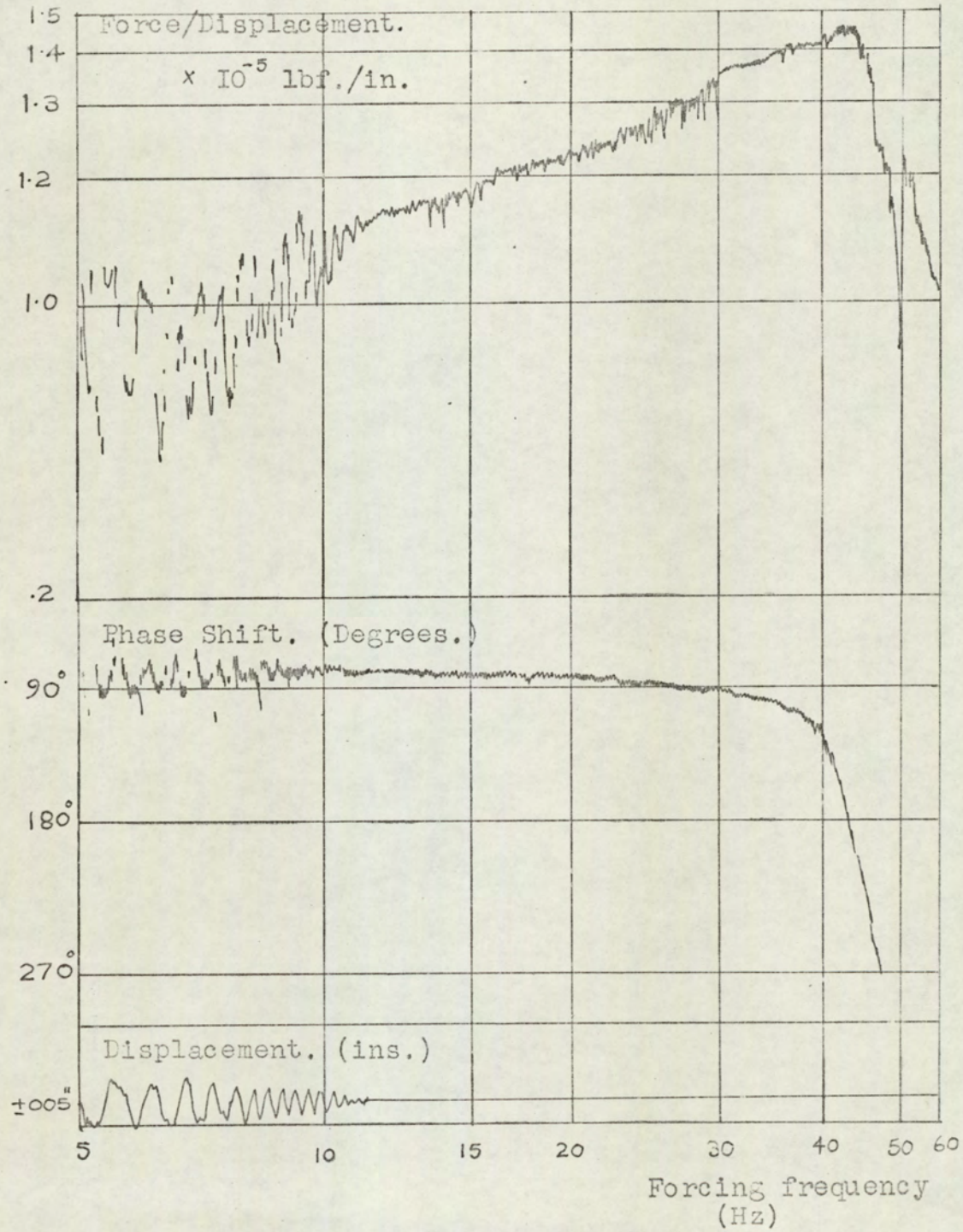

Fig. A.5.2.

APPENDIX A.6. - BIBLIOGRAPHY.

	Author.	Title.	Publication.
1.	B.K. Barrowcliff & R.E. Ehlert.	'Full scale road simulated endurance test'.	S.A.E. Engineering Congress 1968 Paper No. 680148.
2.	P. Van Brommel.	'A simple spring-mass system with dry damping subject to harmonic vibrations'.	V.R.L.D. 1956 Paper No. V.003.
3.	P. Chenchanna.	'Ride, comfort and road holding'.	Automobile Engineer July 1969.
4.	B.D. Van Deusen.	'Human response to vehicle vibrations'.	S.A.E. Engineering Congress 1968 Paper No. 680090.
5.	W.C. Donaghue.	'Instrumentation for truck ride'.	S.A.E. Engineering Congress 1966 Paper No. 660136.
6.	H.C.A. Van Eldik-Thieme.	'Passenger riding comfort criteria and methods of analysing ride and vibration data'.	S.A.E. Paper 295A.
7.	H.R. Engles.	'Influence of oscillation balancing of engine and drive assembly on vertical oscillations of the vehicle'.	F.I.S.I.T.A. Conference Paper B5. 1966.
8.	J. Fenton.	'Ride parameters - the traditional approach'.	Automotive Design Engineering - Sept.1967.
9.	J. Fenton.	'Ride parameters - the recent refinements'.	" Dec.1967.
10.	J.C. Guignard.	'Human response to intense low frequency noise and vibration'.	I.Mech.E. Publication 1967.

	Author.	Title.	Publication.
11.	H. Harrison.	'Engine installation'.	Automobile Engineer October 1965.
12.	J.P. Den Hartog.	'Mechanical vibrations'.	McGraw Hill.
13.	M. Horovitz.	'Suspension of internal combustion engines in vehicles'.	I.Mech.E. Paper 1957.
14.	H. Hsu.	'Outline of Fourier Analysis'.	Unitech Series A.E.S.F. New York 1967.
15.	C. Huss & J. Donegan.	'Tables for the numerical determination of the Fourier Transform of a function of time and the inverse Fourier Transform of a function of frequency, with some applications to operational calculus methods'.	N.A.C.A. Technical note 4073 - 1957.
16.	L.S. Jacobs & R.A. Ayre.	'Engineering vibrations'.	McGraw Hill.
17.	I. Kojima, T. Mizuno, T. Hazemoto, & H. Arita.	'Analysis and control of 'shake' in trucks'.	Mitsubishi Heavy Industries Ltd. Technical Review Jan.1969 (M.I.R.A. ref. 69/6/6).
18.	W.F. Lins, F.B. Hoogterp, & F. Pradko.	'Comparison of time domain and frequency domain analysis of off road vehicles'.	S.A.E. Publication No. 690353.
19.	A. Lloyd-Nedley.	'Effects of wheel non-uniformities on tyre-wheel assembly and the vehicle'.	S.A.E. Congress 1968. Paper No. 680005.
20.	D. Mather.	'Analysis of steady state engine shake'.	I.Mech.E. paper to the Coventry branch 1969.

	Author.	Title.	Publication.
21.	G. Mitchell & A.W. Wildig.	'Ride evaluation in the design office'.	Automotive Design Engineering, March & April 1968.
22.	M. Mitschke.	'The influence of road and vehicle dimensions on the amplitude of body motions and dynamic wheel loads. (Theoretical and experimental investigations)'.	S.A.E. Congress 1961. Paper No. 310C.
23.	R.J. Oliver & D.T. Aspinall.	'Vehicle riding comfort, the correlation between subjective assessments of vehicle ride and physical measurements of vehicle motion'.	M.I.R.A. Report No. 1964/10.
24.	R.J. Oliver.	'The development and use of a meter for the evaluation of vehicle riding comfort'.	M.I.R.A. Report No. 1968/3.
25.	H.R. Pickford.	'Hints on how to reduce truck drive train vibration'.	S.A.E. Journal April 1962.
26.	J.M. Prentis & F.A. Leckie.	'Mechanical vibrations, an introduction to matrix methods'.	Longmans.
27.	J.C. Riedel.	'Accurate measurement of shock phenomena'.	Proc. Institute of Environmental Sciences, 1962.
28.	J.C. Snowdon.	'Dynamic mechanical properties of rubber like materials with reference to the isolation of mechanical vibrations'.	Noise Control, March 1960.

	Author.	Title.	Publication.
29.	J.C. Snowdon.	'The choice of resilient materials for anti-vibration mountings'.	Brit. Journal of Applied Physics Vol.9. Dec. 1958.
30.	G. Stathopoulos.	'Effects of mounting on an accelerometer response'.	Electronic Industries May 1962.
31.	E. Stepp.	'A computer technique for designing engine mounts to control shake'.	S.A.E. Congress 1960.Paper No. 127B.
32.	A.G. Woods.	'Human response to low frequency sinusoidal and random vibration'.	Aircraft Engineering July 1967.
33.	R. Woods.	'An investigation into vibration criteria for rotating machinery'.	Ph.D. Thesis University of Aston in Birmingham 1970
34.	Anon.	'Design analysis of the Hillman Hunter and Minx'.	Automobile Engineer. Feb., March & Apr.1967.
35.	Anon.	'Modern computing methods'.	Notes on applied science No. 16 H.M.S.O.
36.	Symposium	'Instrumentation and test techniques for motor vehicles' Papers 4,5,7,8 & 15.	I.Mech.E. Publication 1967.
37.	Anon.	'Isolation of the engine and transmission system'.	Automobile Engineer. October 1969.